

Bonding in Molecules

Michaelmas Term - Second Year

2019

These 8 lectures build on material presented in "Introduction to Molecular Orbitals" (HT Year 1). They provide a basis for analysing the shapes, properties, spectra and reactivity of a wide range of molecules and transition metal compounds.

The essentials of molecular orbital theory

1. The requirements for a good theory of bonding
2. The orbital approximation
3. The nature of molecular orbitals
4. The linear combination of atomic orbitals (LCAO) approach to molecular orbitals

Diatomic molecules: H_2^+ , H_2 and AH

5. The wave functions for H_2^+ and H_2 using an LCAO approach
6. MO schemes for AH molecules (A = second period atom, Li to F)

Symmetry and molecular orbital diagrams for the first row hydrides AH_n

7. The use of symmetry in polyatomic molecules
8. MO treatment of AH_2 (C_{2v})
9. MO diagrams for AH_3 (C_{3v})
10. MO diagrams for AH_4 (T_d)

Photoelectron spectroscopy and experimental energy levels

11. Photoelectron spectroscopy and "experimental" MO diagrams
12. Photoelectron spectra of AH_n molecules

The use of Walsh diagrams in exploring molecular shapes

13. The shapes of AH_2 molecules
14. The bonding and shapes of H_3^+ and H_3^- : 3c-2e and 3c-4e bonds

Molecular orbital diagrams for hyper-coordinate molecules

15. The bonding in XeF_2 (and CO_2)
16. 12-electron main group octahedral systems: SF_6 as an example
17. Expanding the coordination sphere in carbon: $[C(AuPR_3)_6]^{2+}$ as an analogue of CH_6^{2+}

Fragment approach to bonding in electron deficient clusters

18. Build up of molecules from fragments
19. Bonding in $[B_6H_6]^{2-}$ (from 6 equivalent BH fragments) and Wade's rules, the concept of isolobality

Complexes of the transition metals: octahedral, tetrahedral and square planar.

20. Octahedral transition metal complexes: σ -bonding
21. π -interactions and the spectrochemical series
22. Molecular orbitals for 4-coordinate geometries: ML_4 (T_d and D_{4h})
23. A miscellany of bonds (quadruple, quintuple, sextuple!)

Bibliography

1. Jean, Volatron and Burdett; An Introduction to Molecular Orbitals (OUP)
2. DeKock and Gray: Chemical Structure and Bonding (Benjamin)
3. Burdett: Molecular Shapes (Wiley)
4. Burdett: The Chemical Bond: A Dialog (Wiley).
5. Albright, Burdett and Whangbo: Orbital Interactions in Chemistry (Wiley)
6. Streitweiser: Molecular orbital theory for Organic Chemists (Wiley)
7. Albright and Burdett: Problems in Molecular Orbital Theory (OUP)

Resources

Character tables

<http://global.oup.com/uk/orc/chemistry/qchem2e/student/tables/>

Software:

Python_extended_huckel: <http://course.chem.ox.ac.uk/bonding-in-molecules-year-2-2019.aspx>

and a python (3.x) platform to run it:

Anaconda <https://www.continuum.io/downloads>

Preliminary remarks

Any theory of bonding must be consistent with quantum theory, in particular the Schrödinger wave equation, $\hat{H}\Psi = E\Psi$ that relates the total energy E of a (molecular) system to its wave properties Ψ . For H_2^+ , for example, the Hamiltonian takes the form

$$\hat{H} = -\frac{\hbar^2}{2m}\nabla^2 - \frac{e^2}{4\pi\epsilon_0 r_a} - \frac{e^2}{4\pi\epsilon_0 r_b} + \frac{e^2}{4\pi\epsilon_0 R_{ab}}$$

where the first term relates to the kinetic energy of the electron, the second two to the energy of attraction between the electron and the two nuclei and the last to repulsion between the two nuclei.

The orbital approximation

The wavefunction is in principle a highly complex multi-dimensional entity. The most common simplification is to assume that the wave function Ψ for all the N electrons in a molecule can be written as a product of N one-electron wavefunctions, ϕ_i .

$$\Psi(1,2, \dots, N) = |\phi_1, \phi_2, \dots, \phi_N|$$

(The ϕ_i here refer to a spin orbital and $||$ indicates that the wave-function is anti-symmetrized with respect to exchange of electrons. These are requirements of the Pauli Principle - no two electrons in a system can have the same set of quantum numbers)

The square of the total wavefunction Ψ^2 , gives the total electron density in the molecule.

The one-electron wavefunctions, ϕ_i , are **molecular orbitals**.

Definition: "A molecular orbital is the wavefunction of an electron in a molecule moving under the influence of the nuclear attraction and the average repulsion of all other electrons". It has the same formulation as an atomic orbital does in a many electron atom.

An MO has an energy, ϵ_i (the eigenvalue) and a wavefunction (ϕ), the eigenfunction.

The square of the wavefunction, ϕ_i^2 , or more correctly $\phi_i^* \phi_i$, gives the probability density for the electron.

MOs can be delocalized: an electron wave function extends throughout the molecule, and is not confined to a "bond" between two atoms except in diatomic molecules.

The linear combination of atomic orbitals (LCAO) approximation to molecular orbitals

The **LCAO** approximation expresses each individual molecular orbital as a linear combination of atomic orbitals

$$\phi_i = c_A\chi_A + c_B\chi_B + \dots \dots$$

Note: the number of MOs obtained from LCAO equals the number of AO basis functions.

Justification: when an electron is close to the nucleus of one atom, A, its wave function closely resembles an atomic orbital (AO), χ_A , of that atom. We can therefore make a reasonable first approximation to an MO by superimposing AOs of each atom in the molecule. The LCAO approach is visually satisfying and transparent since one can follow fairly easily how the inclusion of one

atomic orbital or another influences the resultant molecular orbitals and (consequently) the molecular properties.

In the simplest form of LCAO theory, only the valence orbitals of the atoms are used to construct MOs (e.g. just the 1s for hydrogen, only the 2s and 2p for carbon, and so on). In more accurate forms of calculation other orbitals are also included (see below in the treatment of H₂⁺). The atomic orbitals used are known as a **basis set**. In general, the larger the basis set the more accurate are the calculations (e.g. of bond energies and distances). The down-side is that the calculations become very computationally demanding as the size of the basis set increases, and in general only the "simplest" systems can be calculated with a great degree of accuracy.

Linear combinations of atomic orbitals (LCAOs) are used to construct molecular orbitals ϕ_i . If we take two AOs, χ_A and χ_B , of energies $-\epsilon_A$ and $-\epsilon_B$ respectively, we form two molecular orbitals:

$$\phi_1 = N_1(\chi_A + \lambda_1\chi_B)$$

$$\phi_2 = N_2(\chi_A - \lambda_2\chi_B)$$

The MOs form an **orthonormal** set. This comprises two key features, namely:

the normalization condition: $\int \phi_i^2 d\tau = 1$

and the orthogonality condition: $\int \phi_i\phi_j d\tau = 0$

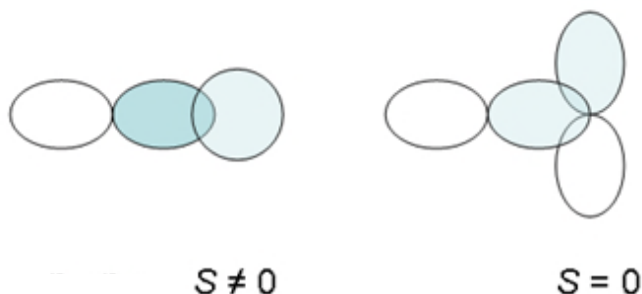
Overlap

Atomic orbitals must overlap in order to combine to form an MO. In other words, the **overlap integral** S_{AB} between two atomic orbitals χ_A and χ_B must be non-zero.

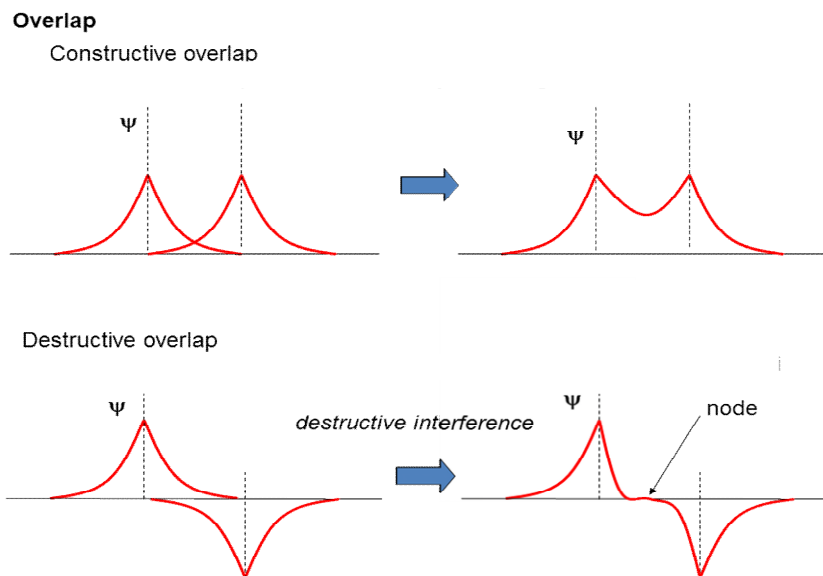
$$S_{AB} = \int \chi_A\chi_B d\tau$$

In diatomics, it is relatively straightforward to see which orbitals overlap and which do not:

In polyatomic molecules (see Section 7 below), it is not so easy to see, and we need to use group theory. The key result from group theory is that only orbitals carrying the same symmetry labels (when analysed in the same point group) can overlap, otherwise S_{AB} is zero.



Orbitals which overlap constructively (*i.e.* "in-phase") are bonding. Orbitals which overlap destructively are antibonding. In general, the greater number of internuclear nodes the higher the energy of an orbital (*c.f.* AOs in the H atom, particle in a box, *etc.*).



(but see Baird, *J Chem Ed* **1986**, 63, 663 for a discussion of the origin of bonding).

The energy of stabilization of a bonding MO, and the energy of destabilization of an anti-bonding MO (with respect to the combining AOs) depends on:

- The **size of overlap**, S_{AB} , between the AOs and
- The **energy separation of the combining AOs**, $\Delta E = |\varepsilon_A - \varepsilon_B|$. The energy of stabilisation of an MO is at a maximum when the two combining AOs have similar energy. Conversely, orbitals with very different energies will interact poorly, irrespective of the size of the overlap.

To ascertain the best possible wave function within the LCAO approximation, we use the variation principle. The variation principle states that for any trial wavefunction $E_{trial} > E_{true}$ (E_{true} is the true energy of the system).

For a trial wavefunction, ψ_{trial} , the associated energy is given by:

$$E_{trial} = \frac{\int \psi_{trial}^* \hat{H} \psi_{trial} d\tau}{\int \psi_{trial}^* \psi_{trial} d\tau}$$

The task is to find the set of coefficients c_i in the molecular orbitals $\phi_i = c_A \chi_A + c_B \chi_B + \dots$ which give the minimum possible energy (*i.e.* we vary them until the change is less than a target criterion). There are a number of well-established computational procedures for doing this.

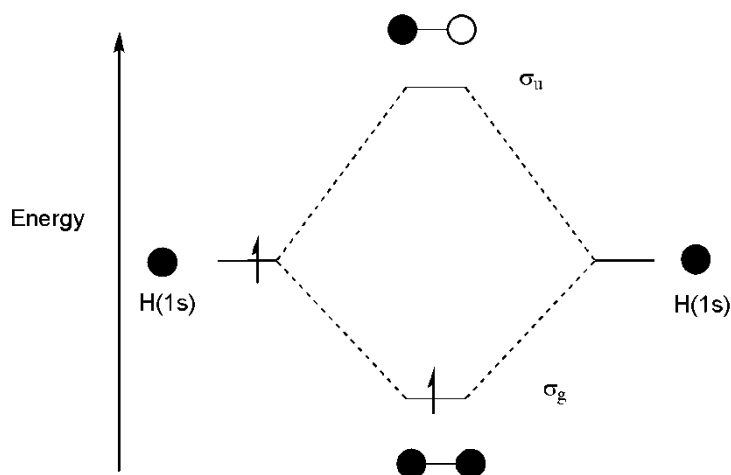
Homonuclear diatomic molecules: H_2^+ , H_2

5. The wave functions for H_2^+ and H_2 using an LCAO approach

An approximation to the wave function of the electron in the one-electron ion H_2^+ may be made by taking a linear combination of the two $1s$ atomic orbitals, $1s_A$ on atom H_A and $1s_B$ on atom H_B . The two atoms (*i.e.* H) in this species are obviously the same so the coefficients c_i introduced above are identical and in this case are represented by N , the normalisation constant.

$$\phi = N(1s_A + 1s_B)$$

N normalizes the wavefunction so that $\int \phi^2 d\tau = 1$. The normalisation constant is chosen so that the probability of finding the electron somewhere in space is unity.



However, such a "first-guess" wave function gives only 64% (!) of the experimental bond dissociation energy of H_2^+ and a bond length that is 0.26 \AA too long. In other words, the form of the wavefunction that we have chosen to start from is pretty inadequate. So what went wrong?

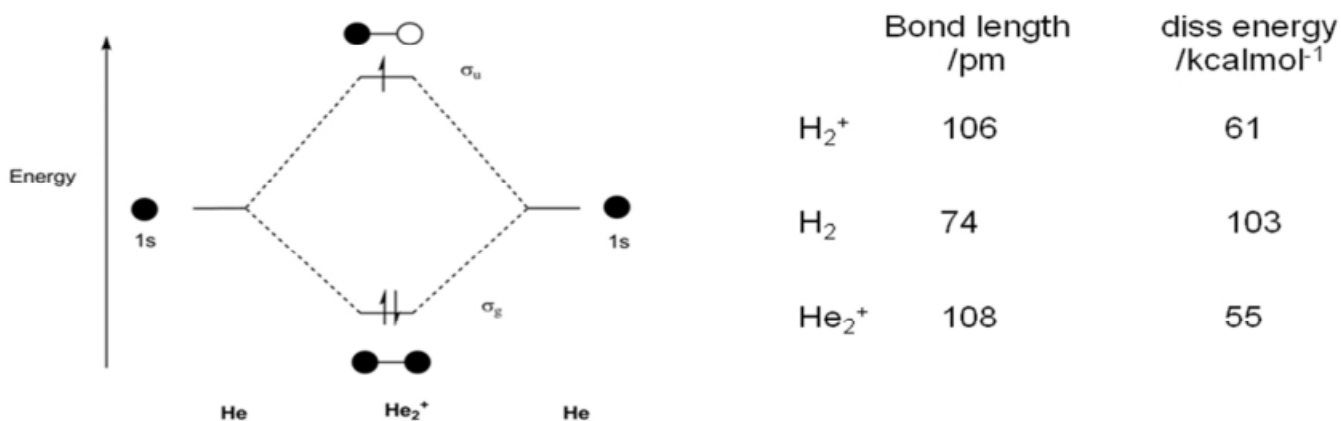
There is no reason to assume that the s orbital in an H atom in H_2^+ should be the same size as an s orbital in H itself. It turns out that the energy can be improved by contracting the $1s$ atomic orbitals. These wavefunctions have the form:

$$\phi(1s) = \frac{1}{\sqrt{\pi}} \left(\frac{Z}{a_0} \right)^{3/2} e^{-Zr/a_0}$$

where Z is the nuclear charge acting on the electron. It is found that a minimum energy for H_2^+ is obtained when $Z = 1.24$ rather than $Z = 1$, and the bond energy is now 84% of the experimental value.

Extensions to H_2 : Wave functions for the **hydrogen molecule** H_2 can be generated by placing two electrons (labelled "1" and "2") with opposite spins in the bonding MO [i.e. $\phi = N(1s_A + 1s_B)$] that we have just derived for H_2^+ . The spatial wavefunction for the molecule is then given by the product of the two one-electron wavefunctions, $\phi(1)$ and $\phi(2)$

$$\Psi = |\phi(1)\phi(2)|$$



6. Heteronuclear diatomics AH molecules (A = second period atom, Li to F)

We shall first consider linear heteronuclear diatomic molecules AH where A is one of the second period atoms, Li to F. These atoms have one $2s$ and three $2p$ valence orbitals. In such systems it is conventional to take z as the molecular axis (as is also the case for homonuclear diatomics A_2).

Symmetry analysis: Pt grp $C_{\infty v}$

From the group theory (character) table for $C_{\infty v}$ (see appendix):

$$\text{For the A atom (4 AOs):} \quad \Gamma(2s) = \sigma \quad \Gamma(2p_z) = \sigma \quad \Gamma(2p_{x,y}) = \pi$$

$$\text{For the H atom (1 AO):} \quad \Gamma(1s) = \sigma$$

$$\text{For the AH molecule (5 MOs):} \quad \Gamma(\text{MOs}) = 3\sigma + 1\pi \quad (\pi \text{ is a doubly degenerate set})$$

The valence $2s$ and $2p_z$ atomic orbitals of the A atom overlap with the H $1s$ orbital (all are σ symmetry). The $2p_{x,y}$ (π) have no symmetry match on H, so will be non-bonding. The three MOs of σ symmetry take the form

$$\phi(n\sigma) = c_1\chi_{1s(H)} + c_2\chi_{2s(A)} + c_3\chi_{2p_z(A)}$$

In all cases, one σ bonding, one σ -non-bonding and one σ anti-bonding orbital are formed, but the distribution of bonding/non-bonding/antibonding character between the three MOs varies.

Perturbation theory tells us that the interaction between two orbitals with different energies depends on the overlap (squared) divided by the energy difference between them ($\propto \frac{S^2}{\Delta E}$).

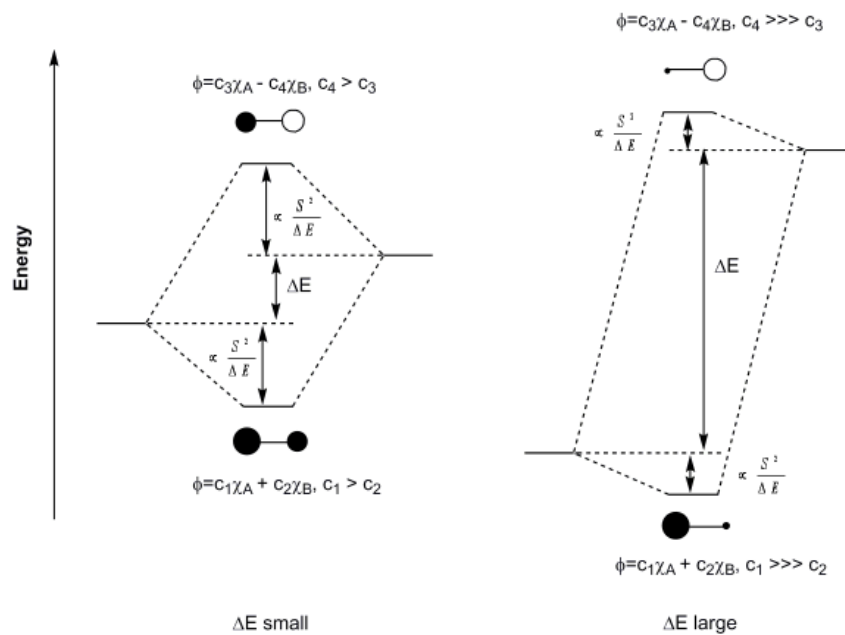


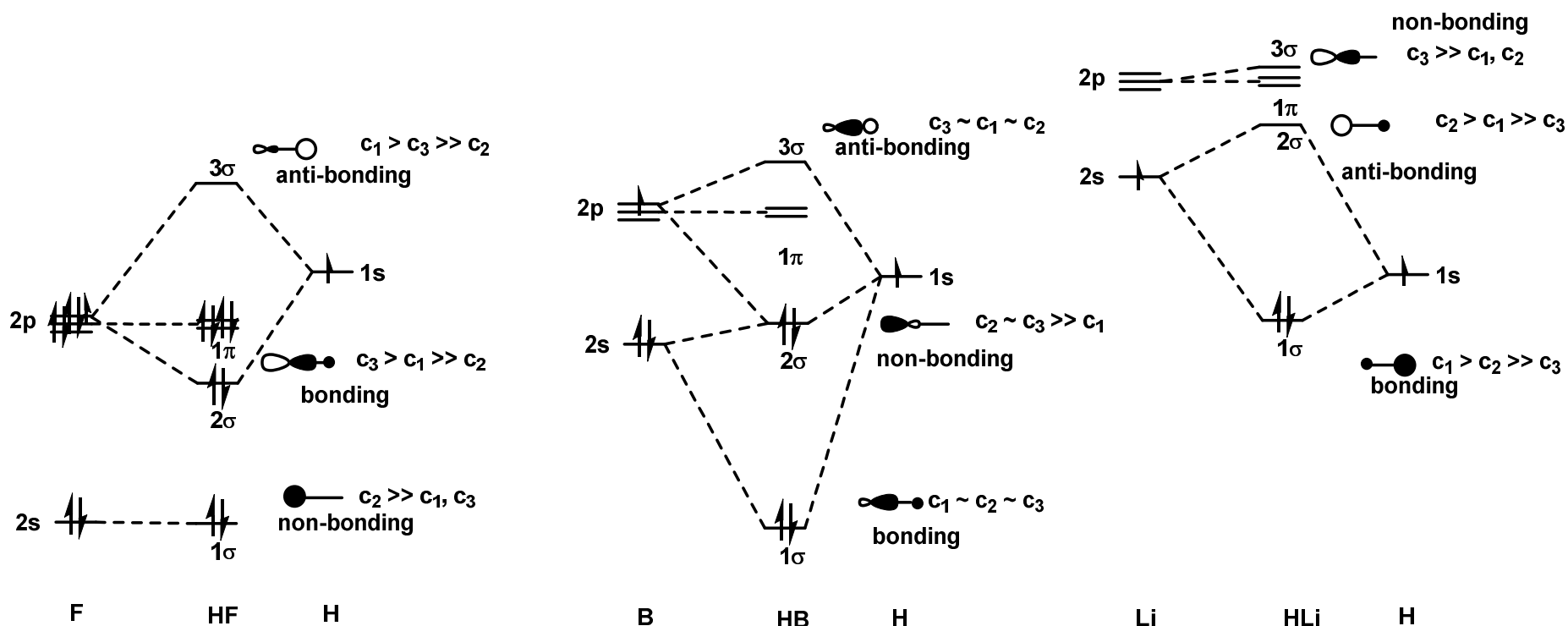
Figure: Interaction energies between two orbitals with different ΔE .

Even if overlap is good, when orbitals have very different energies their interaction will be very weak and they will be effectively non-bonding.

For HA we can distinguish two limiting cases.

- i) A is much *more* electronegative than H (HF), in which case the 2s orbital lies well below 1s of H. In this case the only significant interaction is between A $2p_z$ and H 1s.
- ii) A is much *less* electronegative than H (LiH), in which case $2p_z$ of A is too high to interact with 1s of H, and the bonding is dominated by 2s of A and 1s of H.

In between these two scenarios (HB), interactions with both 2s and $2p_z$ need to be considered.



$$\phi(n\sigma) = c_1 1s(H) + c_2 2s(A) + c_3 2p_z(A)$$

Figure: Limiting cases for HA systems

Note that the MOs are labelled according to their symmetry. For orbitals of the same symmetry, the lowest in energy is labelled 1 (here 1σ), the next 2 (2σ), *etc.*

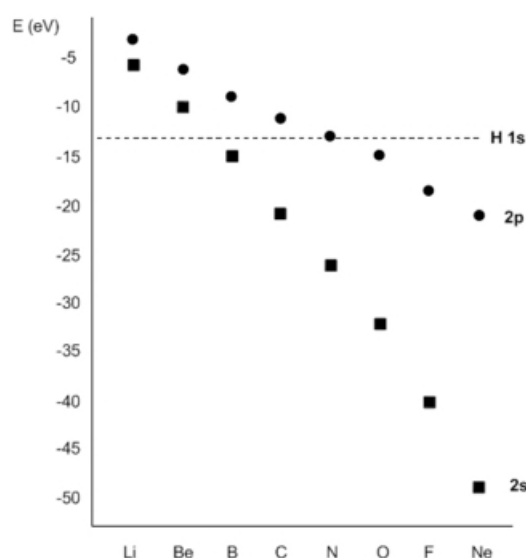
In HB the bonding is maximized in the more stable orbital (i.e. the 1σ level above). The mixing of the s and p orbitals in the MO of a molecule is the equivalent of hybridization in valence bond theory. $2s$ - $2p$ mixing results in a build up (as in 1σ) or diminution (as in 2σ) of orbital overlap and electron density in the internuclear region (similar to N_2 , see Year 1 notes).

In the case of HF the $2s$ orbital on F is too low in energy to interact significantly with the $1s$ orbital, and the $1a_1$ MO is almost entirely made up from the $2s$ atomic orbital of the A atom. In other words, $|c_2| \gg |c_1|, |c_3|$ in the molecular orbital

$$\phi(1\sigma) = c_1 1s(H) + c_2 2s(A) + c_3 2p_z(A)$$

and the lower energy orbital (1σ) now behaves like a core orbital.

If the A atom is very electropositive (Li, Be) the $2s$ and $2p$ valence orbitals lie high in energy and above that of the H $1s$ orbital (note $2s/2p$ separation is due to penetration). If, on the other hand, A is very electronegative (*e.g.* F) its $2s$ and $2p$ orbitals lie lower in energy than H $1s$. For elements of intermediate electronegativity, such as B, C and N, the H $1s$ orbital lies between the A atom's $2s$ and $2p$ levels (the valence shell energy of the H atom $1s$ orbital is normally taken as -13.6 eV). In general we expect much more s - p mixing in B and C than in O and F because the energy difference between $2s$ and $2p$ levels is not yet prohibitively large.



Valence shell energies (in eV) of $2s$ and $2p$ electrons of second period atoms								
	Li	Be	B	C	N	O	F	Ne
$2s$	- 5.4	- 10.0	- 15.2	- 21.4	-26.0	-32.3	- 40.0	- 48.5
$2p$	- 3.5	- 6.0	- 8.5	- 11.4	- 13.4	- 14.8	-18.1	- 21.6
$2p - 2s$	1.9	4.0	6.7	10.0	12.6	17.5	21.9	26.9

Note that it is widespread practice (and generally convenient) to refer to " σ " and " π " type orbitals even though in a strict (group theoretical) sense these Mulliken symbols for irreducible representations only formally apply to the cylindrical point groups $D_{\infty h}$ and $C_{\infty v}$ (even in the latter instance it is also permitted to use the a_1, e_1 etc. symbols). For example, in ethene we like to refer to $H_2C=CH_2$ " σ " and " π " bonds even though the molecular orbitals being referred to actually have the Mulliken symbols a_g and b_{1u} in the D_{2h} symmetry of ethene.

Symmetry and molecular orbital diagrams for the first row hydrides AH_n

We have already seen for the AH molecule how knowledge of the symmetry (irreducible representations) of atomic orbitals helps identify those atomic orbitals that (in principle at least) can overlap to form MOs. Symmetry becomes an indispensable tool when analysing the bonding in polyatomic molecules AH_n with n > 1.

7. The use of symmetry in polyatomic molecules

So far we have a good idea of the MO pattern when 2 or 3 AOs interact. With polyatomic systems we have a potentially very large number of AOs, so expect an equally large number of MOs. However if a molecule is symmetric (or can be approximated as such) we can still deal with their interactions in a semi-qualitative way.

If two or more atoms are chemically identical, they must be associated with equal electron density. In H₂ we have:

$$\phi = (c_A 1s_A + c_B 1s_B)$$

but electron density (given by ϕ^2) must be the same on the two indistinguishable atoms.

Hence:

$$c_A^2 = c_B^2$$

$$c_A = \pm c_B$$

Therefore in any molecule with two equivalent H atoms (H₂O, HC≡CH *etc*) the contribution to any MO in the molecule will be either $c_1(1s_A + 1s_B)$ or $c_1(1s_A - 1s_B)$. Such linear combinations of equivalent atomic orbitals are known as **Symmetry Adapted Linear Combinations** (SALCs).

If we can generate SALCs for equivalent orbitals for molecules just by using symmetry, we pre-determine the ratio of coefficients of the AOs in the MOs and the interaction between the different atoms is then often reduced to that between 2 or 3 orbital sets. Many examples of this will be presented throughout these lectures and later courses.

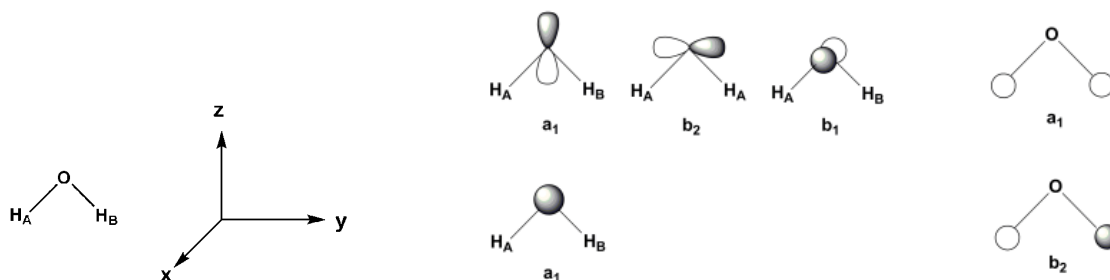
SALCs for various symmetry arrays of equivalent orbitals are given in the appendix, along with relevant character tables. You should now be familiar with these from the "Symmetry 1" 2nd year lectures.

8. MO treatment of AH₂ (C_{2v})

We shall take as our specific example H₂O, but the general scheme developed will be applicable to any C_{2v} symmetric AH₂ main group molecule. We will use group theory to classify the irreducible representation of SALCs of the H atom 1s AOs in the C_{2v} symmetry of bent AH₂. Having then identified the irreducible representations of the O atom 2s and 2p orbitals (in C_{2v} symmetry) we shall then construct an MO diagram for H₂O using the principles of AO overlap and energy separation developed above.

Symmetry analysis

First we choose the coordinate system. Conventionally we assign the z-axis as the C_2 axis, take yz as the molecular plane, and assign the x-axis as being perpendicular to molecular plane.



Now identify the AO basis sets. These are H atom 1s and the O atom 2s and 2p orbitals. Assign these AOs or SALCs to their irreducible representation in the C_{2v} point group of H_2O .

We find these from group theory (character) tables for the central atom (on an invariant point), and either by inspection or using the reduction formula (see "Symmetry 1" lectures) for the SALCs of the peripheral atomic orbitals. Therefore:

For the O (A) atom (4 AOs): $\Gamma(2s) = a_1$ $\Gamma(2p_z) = a_1$ $\Gamma(2p_x) = b_1$ $\Gamma(2p_y) = b_2$

For the H atoms (2 x 1s AO): $\Gamma(2 \times 1s) = a_1 + b_2$

Hence for the resulting H_2O molecule (6 MOs): $\Gamma(\text{MOs}) = 3a_1 + b_1 + 2b_2$

This simple symmetry analysis shows that the in-phase (a_1) SALC of H atom 1s AOs can interact with both the 2s and $2p_z$ AOs of oxygen (but NOT with the $2p_x$ or $2p_y$ AOs). So in general any orbital of a_1 symmetry in a molecule AH_2 will be of the form

$\phi(na_1) = c_1 2s(O) + c_2 2p_z(O) + c_3(1s(A) + 1s(B))$ where the coefficients depend on the relative energies of the orbitals.

The out-of-phase (b_2) SALC of H atom 1s AOs can only interact with the $2p_y$ AO of oxygen, so any orbital of b_2 symmetry will be of the form ($\phi(nb_2) = c_1' 2p_y(O) + c_2'(1s(A) - 1s(B))$)

The $2p_x$ AO of oxygen (b_1) cannot interact at all with either H_A or H_B and so will be strictly non-bonding in H_2O . ($\phi(nb_1) = 2p_x(O)$)

Starting with the 6 AOs (4 from O, 2 from 2 H atoms), to construct an MO diagram we now have reduced the problem to combining a set of three orbitals ($2a_1 + b_2$ on oxygen) and a set of 2 orbitals ($a_1 + b_2$ SALCs). Symmetry has told us the number of each type of MO. We must use calculation or qualitative arguments to get the final ordering of the MOs. These are given below. Note that the ordering of the $2a_1$ and the $1b_2$ orbitals is not obvious. As predicted in **8.2**, The net result is: three MOs of symmetry a_1 , two of symmetry b_2 and one of symmetry b_1 .

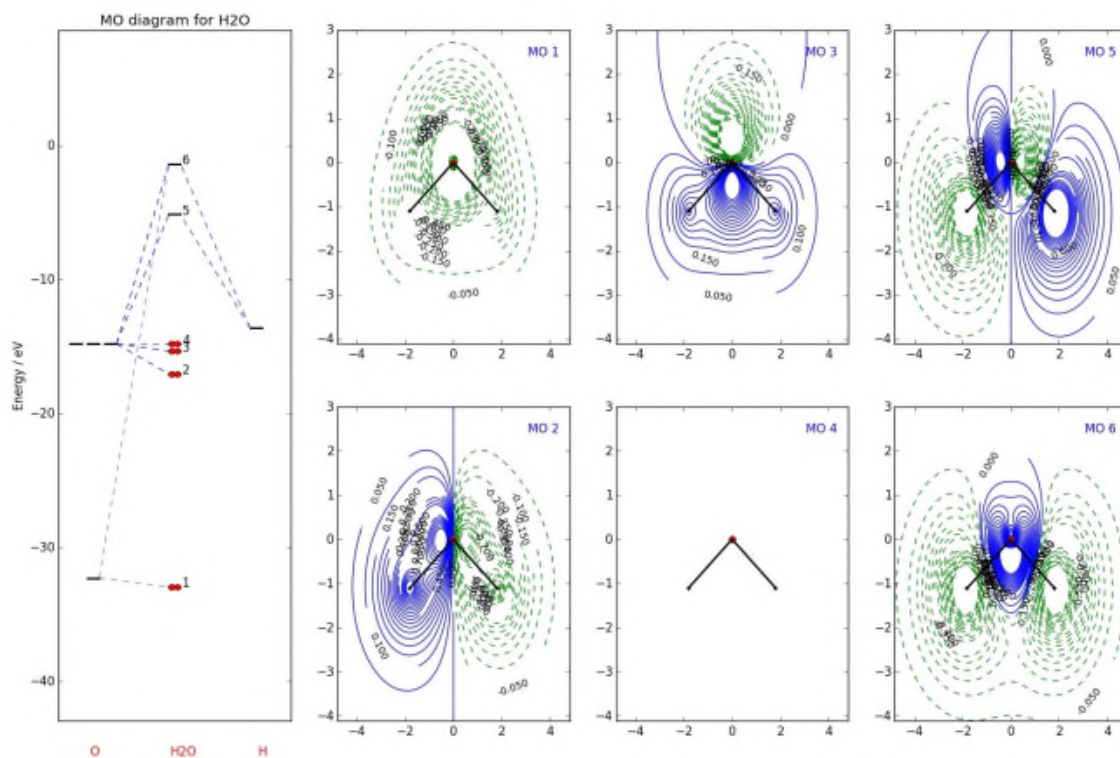
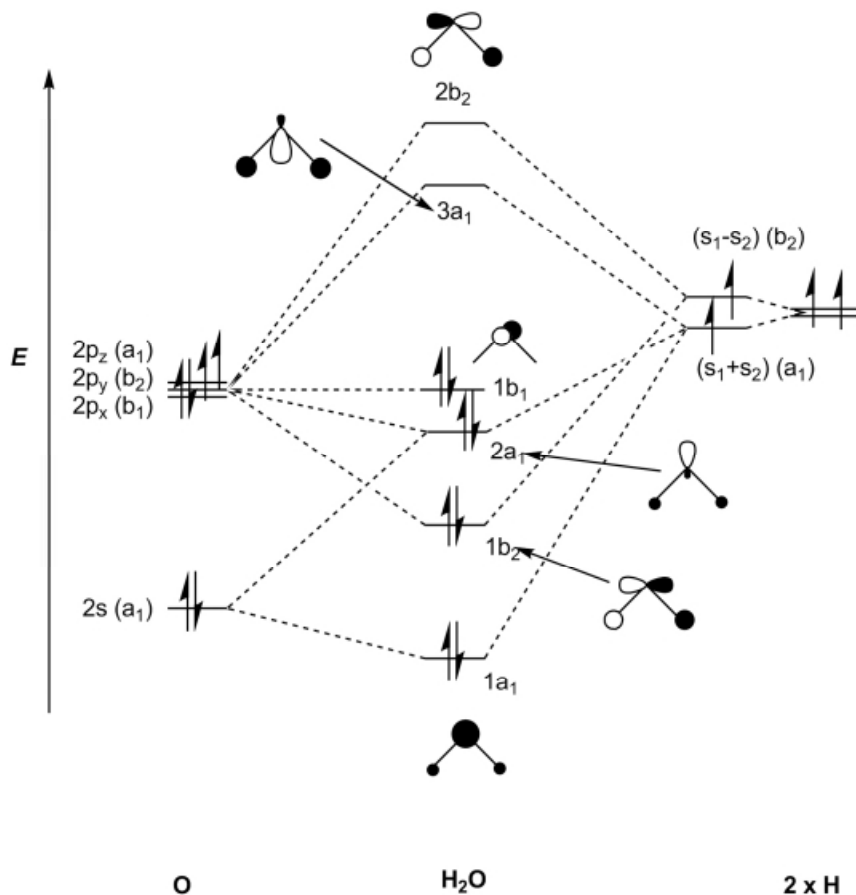


Figure: MO diagrams for H₂O (cartoon and “real” versions). Note different orders of orbitals 5 and 6. In this MO diagram the highest occupied molecular orbital (HOMO) is the non-bonding 1b₁ level and is indicated by the two arrows representing paired electrons. The lowest unoccupied molecular orbital (LUMO) is the 3a₁ level. Note that (as is the usual convention) we have used C_{2v} Mulliken symbols

for the oxygen AOs and (H⋯⋯H) SALCs even though the real symmetry of these fragments is much higher than that of the resultant H₂O molecule.

A variational calculation for water gives the AO coefficients shown in the Table below. The results show that there is very little oxygen 2p_z or H 1s AO contribution in the lowest of the 1a₁ symmetry valence MOs

Table: MO coefficients for extended Hückel calculation on H₂O

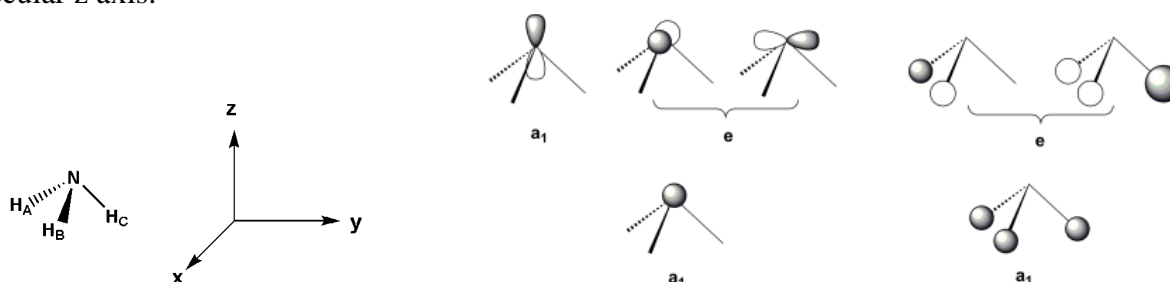
MO	Oxygen				Hydrogen	
	2s	2p _z	2p _y	2p _x	1s ₁	1s ₂
1a ₁	0.91	-0.02	0	0	0.12	0.12
2a ₁	-0.16	0.93	0	0	0.15	0.15
1b ₂	0	0	0.7	0	0.36	-0.36
1b ₁	0	0	0	1	0	0
2b ₂	0	0	0.85	0	-0.75	0.75
3a ₁	0.69	0	0.46	0	-0.77	-0.77

The schematic cartoons given in the MO diagram above emphasise the AO contributions and are helpful to visualise the LCAO origins of the MOs. However, a more accurate picture of an MO function is given by a contour diagram such as those shown in the ‘real’ figure.

9. MO treatment of AH₃ (C_{3v})

We shall take as our specific example NH₃, but again the bonding scheme developed will be broadly applicable to any C_{3v} symmetric AH₃ main group molecule (CH₃, PH₃). As above we will use group theory to classify the irreducible representation of SALCs of the three H atom AOs, along with the 2s and 2p AOs of the central N atom in the C_{3v} symmetry of the molecule.

Symmetry analysis The coordinate system conventionally chosen has the C₃ axis lying along the molecular z axis.



The 2s and 2p AOs of N and the SALCs of C_{3v} (H)₃ span the irreducible representations:

For the N (A) atom (4 AOs):

$$\Gamma(2s) = a_1 \quad \Gamma(2p_z) = a_1 \quad \Gamma(2p_{x,y}) = e$$

For the H atoms (3 x 1s AO):

$$\Gamma(3 \times 1s) = a_1 + e$$

Hence for the resulting NH₃ molecule (7 MOs):

$$\Gamma(\text{MOs}) = 3a_1 + 2e$$

Note that the combinations derived from 2p_{x,y} form a *degenerate pair* because the C₃ operation in C_{3v} mixes the 2p_x and 2p_y AOs so they must have identical energy.

The resultant MO scheme for NH₃ is illustrated below. Note that there is a fair degree of 2s -2p mixing (like the BH molecule above). Therefore in the a₁ orbital manifold N-H bonding is well-developed in the more stable orbital (i.e. the 1a₁ MO) with 2a₁ possessing somewhat more non-bonding character. Indeed, the two electrons in the 2a₁ level are the MO equivalent of the NH₃ "lone pair" obtained in valence bond descriptions of the bonding.

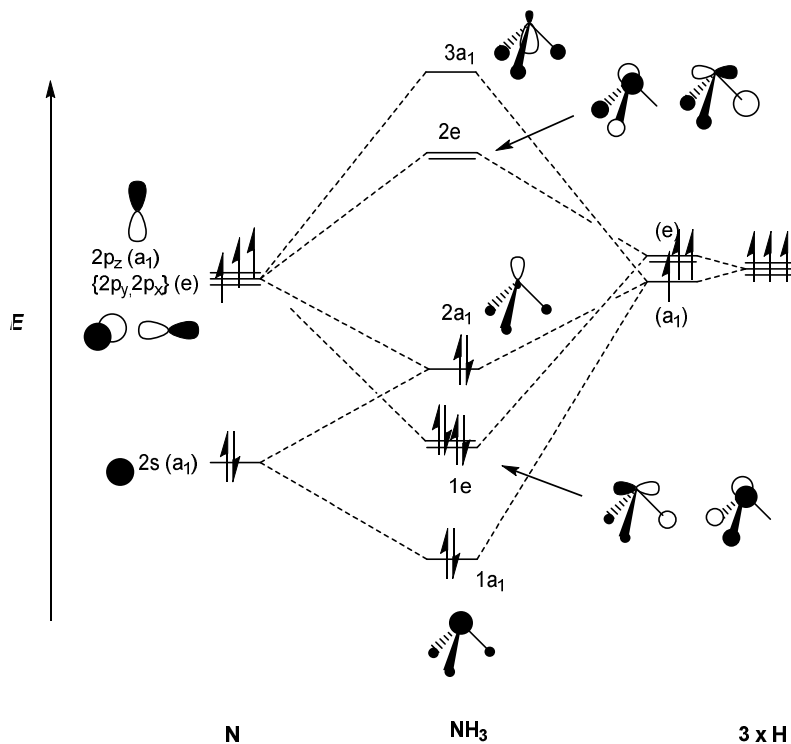
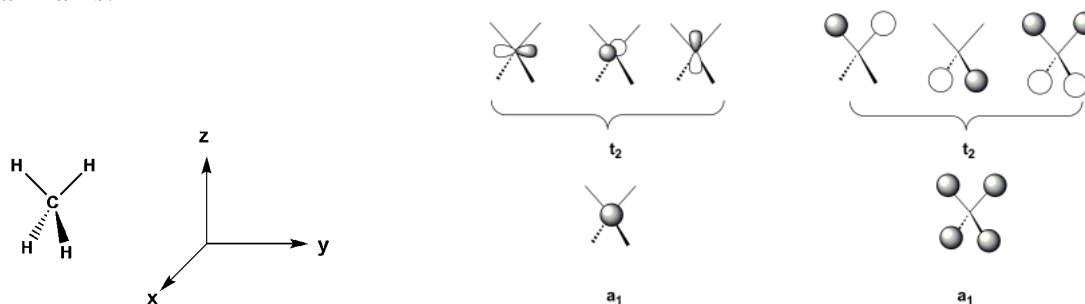


Figure: LCAO MO scheme for NH₃

10. MO treatment of AH₄ (T_d) We shall take as our specific example CH₄, but once again the bonding scheme developed will be applicable to any T_d symmetric AH₄ main group molecule. As above we will use group theory to classify the irreducible representation of SALCs of the four H atom AOs, along with the 2s and 2p AOs of the central C atom in T_d symmetry.

Symmetry analysis We chose a coordinate system with one of the C₂ (S₄) axes lying along the molecular z axis.



The 2s and 2p AOs of C and the SALCs of T_d (H)₄ span the irreducible representations:

For the C (A) atom (4 AOs): $\Gamma(2s) = a_1 \quad \Gamma(2p_{x,y,z}) = t_2$

For the H atoms (4 x 1s AO): $\Gamma(4 \times 1s) = a_1 + t_2$

Hence for the resulting CH₄ molecule (8 MOs): $\Gamma(\text{MOs}) = 2a_1 + 2t_2$

Note that we anticipate no non-bonding MOs in this AH_n compound since all of the carbon atomic orbitals ($a_1 + t_2$) have a symmetry match among the $(H)_n$ SALCs. In the AH_n ($n = 1, 2, 3$) compounds discussed above symmetry analyses predicted three, two or one non-bonding MOs (AH: 1 x a_1 and 1 x e_1 non-bonding MOs; AH_2 : 1 x a_1 and 1 x b_1 ; AH_3 : 1 x a_1 non-bonding MO).

Note that the combinations derived from the $2p_{x,y,z}$ form a **triply degenerate** set of MOs because the C_3 operation in the T_d point group mixes the three $2p$ AOs, so they must have identical energy.

The resultant MO scheme for CH_4 is illustrated below. Note that although there is a favourable $2s - 2p$ AO energy separation, there is no $s-p$ mixing in CH_4 because the $2s$ and $2p_{x,y,z}$ orbitals have different irreducible representations in the T_d point group (the overlap, S , is zero, and therefore so is

$$\frac{S^2}{\Delta E}$$

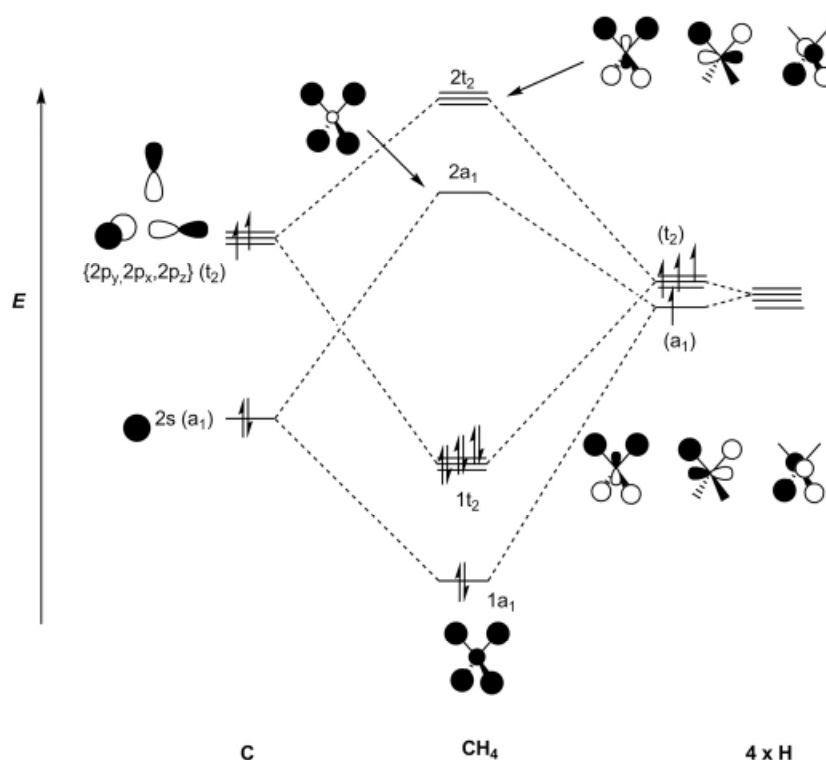
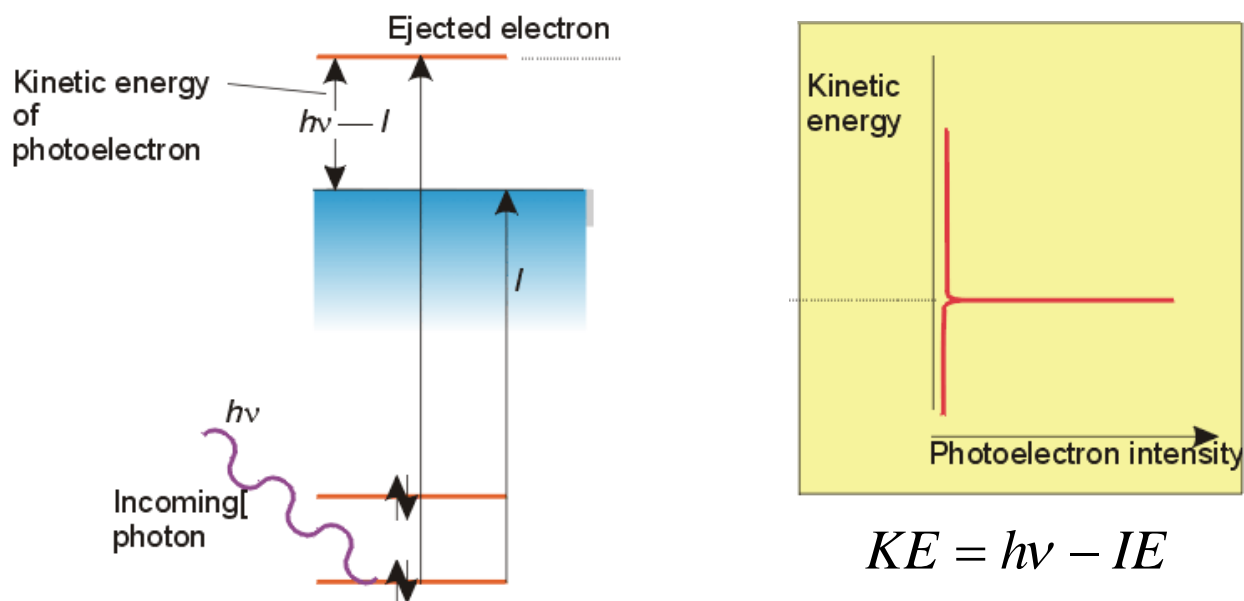


Figure: LCAO MO scheme for CH_4

11. Photoelectron spectroscopy and experimental energy levels

It is helpful to have some experimental tests of the electronic structures proposed and this is where photoelectron spectroscopy (PES) has important applications. Just as atomic spectroscopy can give information on atomic orbitals and their energies, we can obtain information on molecular orbitals by studying ionization of molecules.



In a photoelectron (PE) experiment, monochromatic radiation (single energy photons) $h\nu$, are used to ionize gas phase molecules, and the kinetic energy (KE) of the ejected electrons is measured. Einstein's equation is used to convert the KEs to ionization energies (IEs).

$$IE = h\nu - KE$$

A PE spectrum consists of the number of electrons $N(E)$ of a particular energy plotted against the IEs. The simplest molecular PE spectrum is that of H_2 . Photoejection of an electron leads to the formation of H_2^+ . The PE spectrum of H_2 is very well understood and is reproduced below.

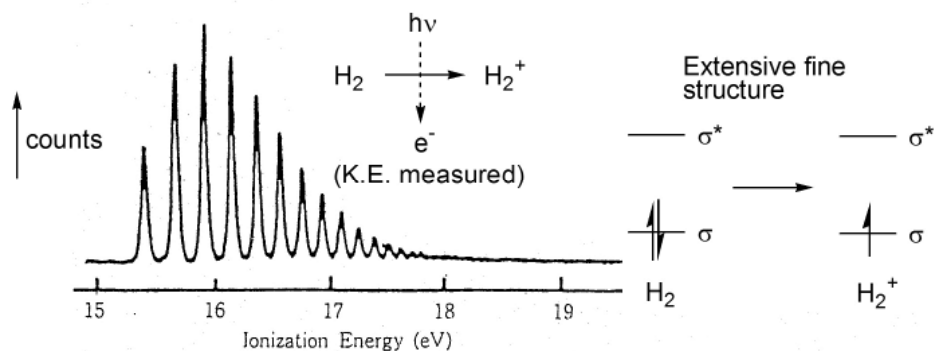


Figure: The photoelectron spectrum of H_2

The process can be interpreted with the aid of an energy diagram.

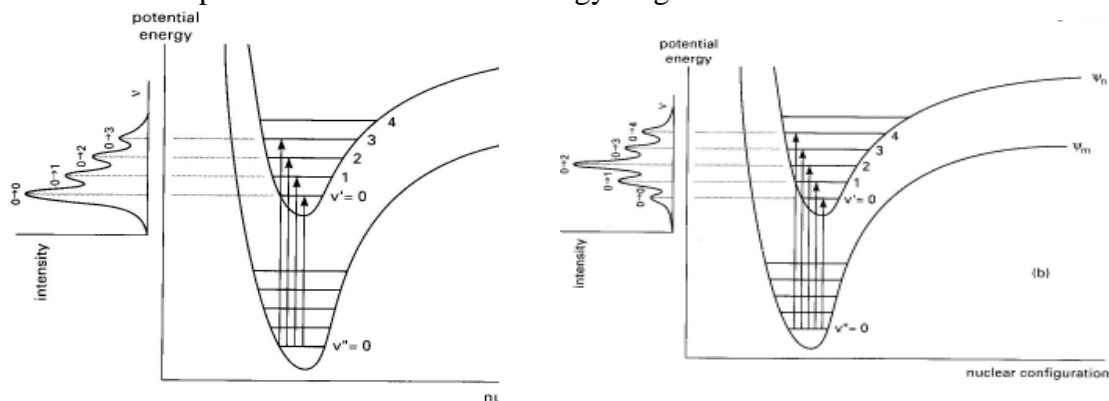


Figure: Potential energy curves for ionisation of a diatomic (a) with minimal change in geometry (b) with large change in geometry.

The depths of the two curves for H_2 and H_2^+ correspond to the bond dissociation energy for each species. The energy difference between the two minima corresponds to the ionization energy (IE) (15.45 eV for H_2). The horizontal straight lines drawn "within" the potential energy for H_2^+ correspond to the vibrational energy states in which H_2^+ can be formed. Under the conditions of the experiment ionization occurs from H_2 in its lowest vibrational state ($v'' = 0$).

The fine structure in the ionization band arises because excitation of the electron happens so fast that the nuclei do not move during the transition. This is known as the **Franck-Condon principle** that you will meet in many branches of spectroscopy.

The molecular ion is formed with the **same geometry as the neutral molecule**. Therefore, given that the photon energy is sufficient, a molecular ion may be formed in a number of **vibrationally excited** states as well as in the ground state. Thus a PE spectrum consists of a number of discrete bands of different IE, even though one is ionizing from a single orbital for each envelope of bands.

In the case of H_2^+ the equilibrium bond length ($r_e = 1.06 \text{ \AA}$) is longer than that of 0.74 \AA for the H_2 molecule (because the bond order of H_2^+ is only 0.5) – case (b) in the figure above. Therefore it is most probable that the molecule is formed in a vibrationally excited state. We can see from the vibrational structure of the PE band that the vibrational state in which H_2^+ is most likely to be formed has $v' = 2$.

Koopmans' approximation equates ionization energy to the negative of an orbital energy.

$$IE = -\varepsilon_i$$

This is an approximation as orbitals tend to be slightly different in molecular ions than in molecules, and as we have seen above MO calculations themselves are not normally very accurate. Nevertheless, Koopmans' approximation gives a good indication of orbital energies in molecules.

PES of HF

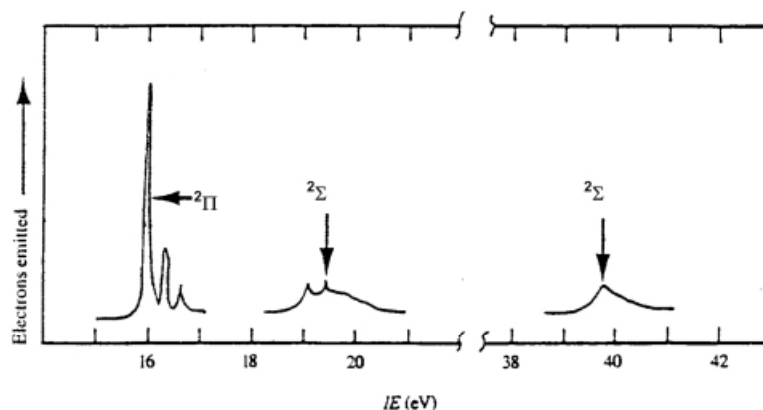


Figure: The photoelectron spectrum of HF

As in the spectrum of H_2 , the fine structure in the bands corresponds to the different vibrational states in which the molecular HF^+ ion can be formed. Note that the lowest energy state ($^2\Pi$) of the ion is most likely to be formed in the lowest vibrational energy level. This suggests that there is little difference between the bond lengths of the ion in this state and the molecule; the electron that has been removed is therefore non-bonding.

The energy levels deduced from the PE spectrum of HF can readily be interpreted in terms of the ground state MO description given on Page 9. Clearly we do not expect to get any direct information about the unoccupied MOs from the PE spectra.

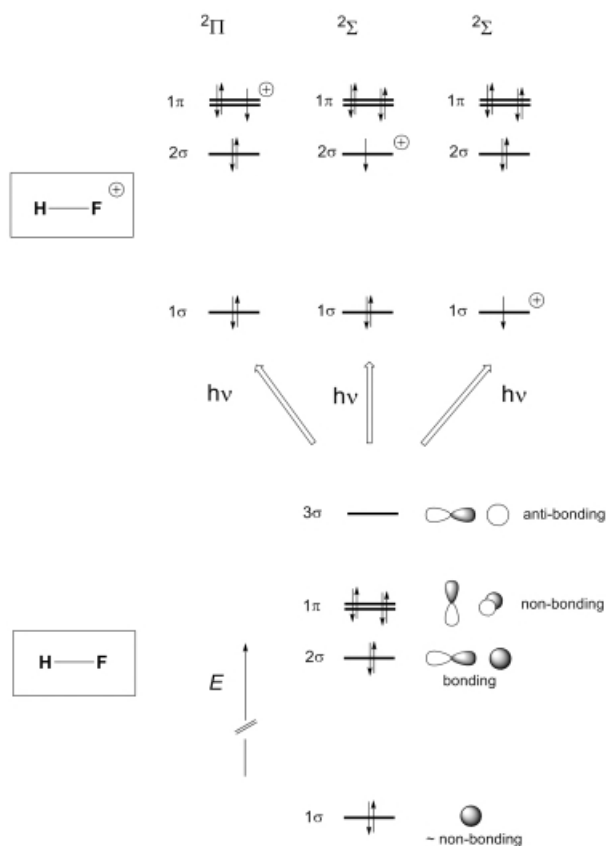


Figure: Interpretation of the PE spectrum of HF in terms of the LCAO MO scheme

12. Photoelectron spectra of AH_n molecules

Schematic representations of the PE spectra of the isoelectronic series of species: CH₄, NH₃, H₂O, HF and Ne are shown in the following Figure. The photon energy used is not sufficient to ionize the 1s core electrons so for each system we are looking at the ionization of the eight valence electrons.

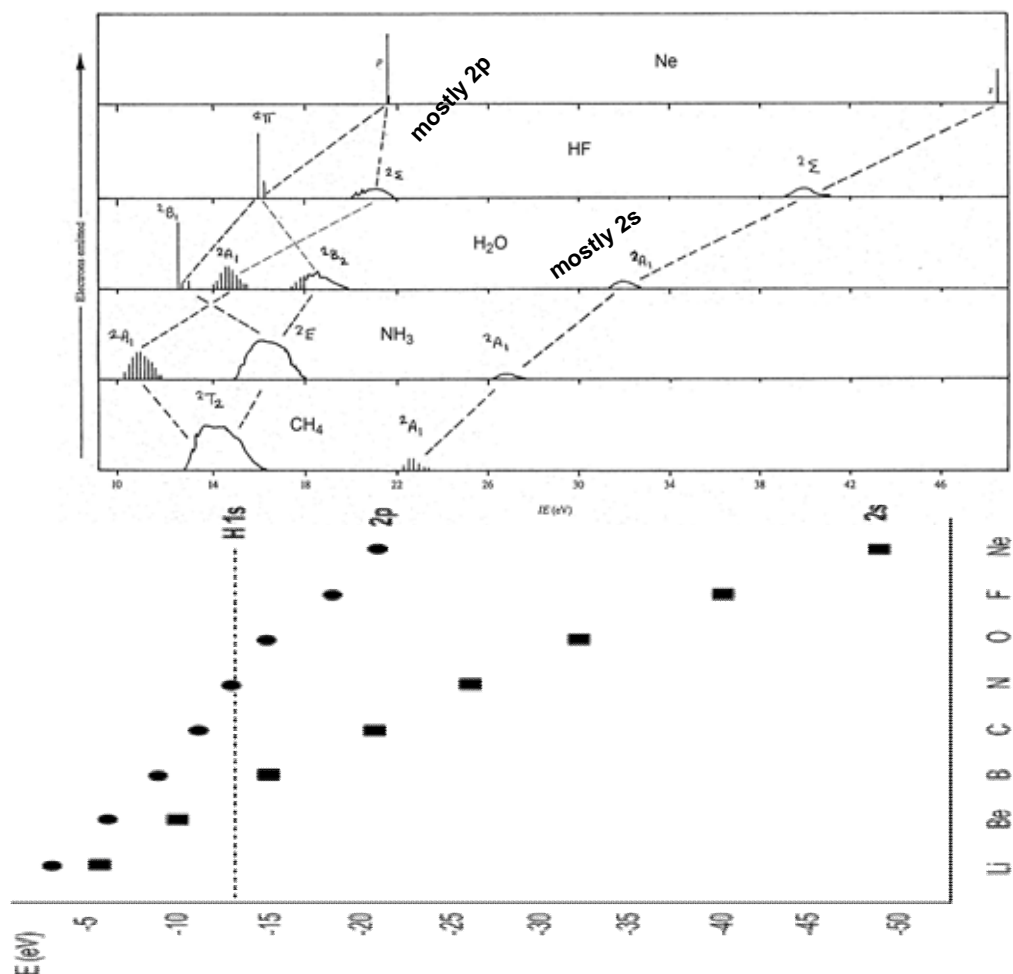


Figure: PE spectra of the isoelectronic series of species: CH₄, NH₃, H₂O, HF and Ne. Energies of the atomic orbitals are plotted below (*c.f* page 10).

The number of bands are related to the symmetry of the species under consideration:

Species	Symmetry	No. of bands	Symmetry labels for orbitals
CH ₄	T_d	2	t_2, a_1
NH ₃	C_{3v}	3	$2a_1, e, 1a_1$
H ₂ O	C_{2v}	4	$b_1, 2a_1, b_2, 1a_1$
HF	$C_{\infty v}$	3	$\pi, 2\sigma, 1\sigma$
Ne	R	2	p, s

The energy of the highest IE band is dominated by the energy of the 2s orbital of the A atom. The binding energy increases across the series in a similar manner to that of the 2s orbital. The other orbitals have an energy variation similar to that of the 2p orbitals.

The use of Walsh diagrams in exploring molecular shapes

A Walsh diagram is a correlation diagram that portrays the variation in the orbital energies of a molecule as its shape is changed. By selecting the geometry that results in the lowest total energy (which is approximated as the sum of the orbital energies) it is possible to predict the likely shape of a molecule from the occupation of its orbitals and also from their relative energies.

Walsh's rule for predicting molecular shapes states: A molecule adopts the structure that best stabilises the HOMO. If the HOMO is unperturbed by the structural change under consideration, then the occupied MO lying closest to it governs the geometric preference. A general "rule of thumb" is that molecules tend to adopt the geometry that maximises the HOMO-LUMO gap.

13. The shapes of AH₂ molecules

Consider the case of a general AH₂ molecule. It can have either a linear ($D_{\infty h}$) or a bent (C_{2v}) structure. We already have an MO scheme for a bent AH₂ molecule such as water (see Section 8). A linear one is readily derived in the same way:

Symmetry analysis: Point group $D_{\infty h}$

For the A atom (4 AOs): $\Gamma(2s) = \sigma_g$ $\Gamma(2p_z) = \sigma_u$ $\Gamma(2p_{x,y}) = \pi_u$

For the H atoms (2 x 1s AO): $\Gamma(2 \times 1s) = \sigma_g + \sigma_u$

Hence for the resulting $D_{\infty h}$ - AH₂ molecule (6 MOs): $\Gamma(\text{MOs}) = 2\sigma_g + 2\sigma_u + \pi_u$

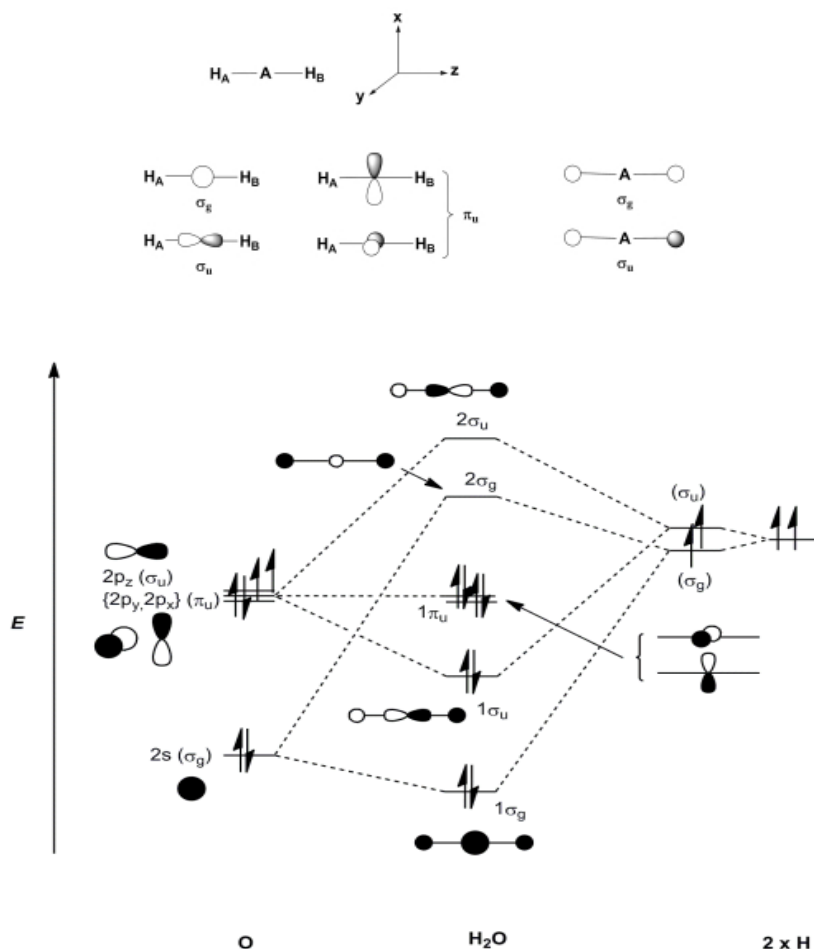


Figure: LCAO MO scheme for linear ($D_{\infty h}$) AH_2

In the Walsh correlation diagram for AH_2 the $1b_2$ (bonding) and $2b_2$ (antibonding) orbitals become less stable and more stable, respectively as the H-A-H angle is decreased from 180° because the $2p_y$ orbital no longer points directly at the H atoms and so overlap decreases.

The $2a_1$ orbital also drops in energy on bending, partly because the originally non-bonding $2p_z$ orbital can now overlap with the H $1s$ orbitals. More importantly, the reduction in symmetry from $D_{\infty h}$ to C_{2v} allows the $2s$ and $2p_z$ orbitals of the central A atom to mix as both now transform as a_1 . This effectively results in the mixing of the $1\sigma_g$ and $2\sigma_g$ MOs of linear AH_2 with the p_z component of the $1\pi_u$ non-bonding set. It is the $2\sigma_g$ MO that mixes best with the $2p_z$ component of the $1\pi_u$ MO because the energy separation (ΔE above) between these two MOs is much smaller than that between $1\pi_u$ and $1\sigma_g$.

Stabilisation due to mixing of HOMO and LUMO induced by a reduction in symmetry is often called a *second-order Jahn-Teller effect*. Recall a first order Jahn-Teller distortion requires a degenerate state (see later)

The deciding factor that determines whether or not an AH_2 molecule is bent is whether the $2a_1$ orbital (orbital 3 in the real plot) is occupied. The $2a_1$ orbital has a much lower energy in the bent geometry than the linear one. Hence, when the $2a_1$ orbital is occupied, a lower energy is achieved if molecule is bent. The shape adopted by an individual AH_2 species depends on:

- Primarily the number of electrons in the valence orbitals (as just stated).
- Secondly (e.g. for 8 electron systems: H_2O , H_2S , etc.) the energy gap ΔE (see Walsh diagram above) between the $2\sigma_g$ and $1\pi_u$ MOs (this governs the extent of $s-p$ mixing and the extent of stabilisation of the $2a_1$ MO on bending).

Known shapes of some AH_2 molecules are summarised in the following table.

Known shape of some AH_2 molecules		
Molecular species	No. of valence electrons	Shape
LiH_2^+	2	Bent
LiH_2 , BeH_2^+	3	Linear
BeH_2 , BH_2^+	4	Linear
BH_2 , AlH_2 , CH_2^+	5	Bent
CH_2 , SiH_2 , BH_2^- , NH_2^+	6	Bent
NH_2 , PH_2 , CH_2^- , OH_2^+	7	Bent
OH_2 , SH_2 , NH_2^- , FH_2^+	8	Bent

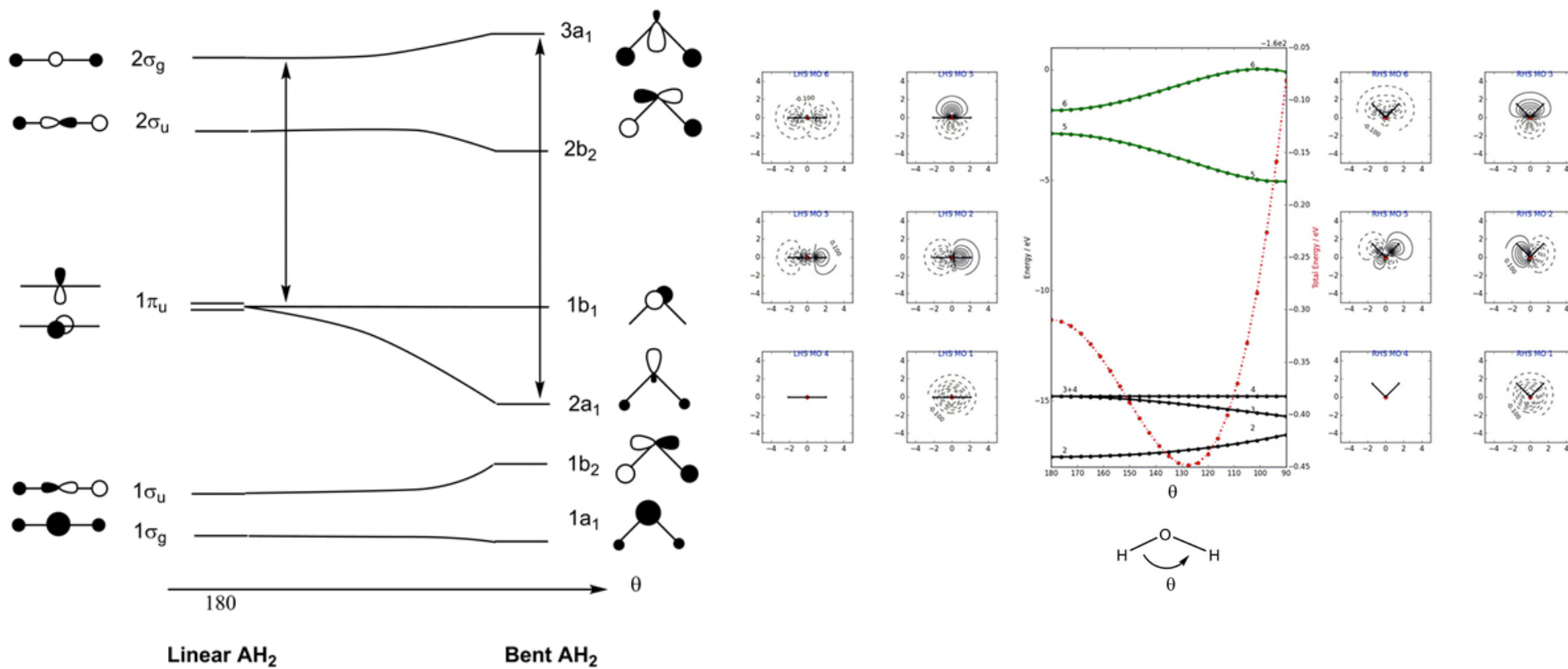


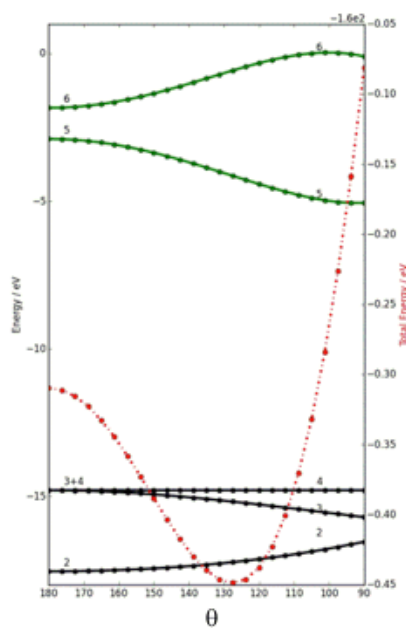
Figure: Walsh correlation diagram between the MO levels of linear and bent AH₂ (cartoon version and ‘real = Extended Hückel theory’ version, with total energy in red)

For three or four electrons the molecules are linear as this gives a more stable $1b_2$ orbital. For more than four electrons the molecules are bent as the $2a_1$ orbital is then occupied and this orbital changes most rapidly with angle (*i.e.* is stabilised).

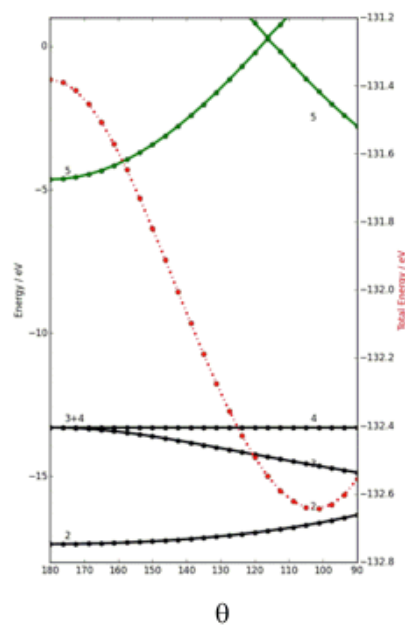
Bond angles (°) in bent 5 - 8 electron AH_2 species								
$1a_1^2 1b_2^2 + \dots$	$2a_1^1$		$2a_1^2$		$2a_1^2 1b_1^1$		$2a_1^2 1b_1^2$	
	BH ₂	131	CH ₂	110	NH ₂	103	OH ₂	104.5
			NH ₂ ⁺	115-120	OH ₂ ⁺	110.5	FH ₂ ⁺	118
			BH ₂ ⁻	102	CH ₂ ⁻	99	NH ₂ ⁻	104
	AlH ₂	119	SiH ₂	93	PH ₂	92	SH ₂	92.1
					AsH ₂	91	SeH ₂	90.6
							TeH ₂	90

Molecules with just one electron in the $2a_1$ orbital have significantly larger H-A-H angles than those with two. Remember that to bend the molecule destabilizes the b_2 electrons. With two electrons in the $2a_1$ orbital there is more stabilization on bending than with just one. Occupation of the b_1 orbital, which is non-bonding in both linear and bent configurations, makes less of a difference to the angle.

The H-A-H valence angles of eight-electron molecules H₂O, H₂S and H₂Se are 104.5, 92.1 and 90.6°, respectively. These molecules have the same MO configuration, namely $1a_1^2 1b_2^2 2a_1^2 1b_1^2$. The difference in H-A-H valence angles comes from the extent of mixing of the $2\sigma_g$ and $1\pi_{u(z)}$ MOs of linear AH_2 on bending. This is heavily influenced by the energy separation ΔE between them (see Walsh diagram below for H₂S and compare to H₂O).

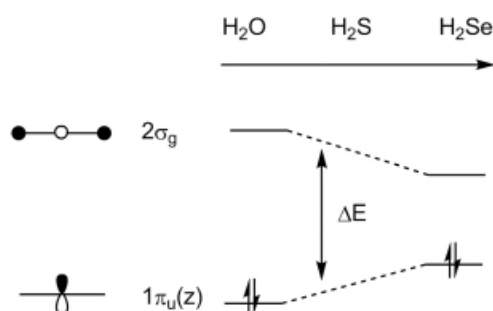


H₂O



H₂S

As the diagram below shows, the energy gap ΔE decreases with decreasing electronegativity of the atom A (e.g. down the group O, S, Se, Te) ($\sim 13\text{eV}$ in the Walsh diagram above for H_2O but only $\sim 7\text{eV}$ for H_2S).



This is because:

- 1) The antibonding $2\sigma_g$ level becomes less antibonding (and so is stabilised) as the ns atomic orbitals of A become more diffuse on descending the group.
- 2) The non-bonding $1\pi_u(z)$ MO becomes less stable as electronegativity decreases and principal quantum number increases.

Therefore as ΔE decreases, the mixing of the $2\sigma_g$ and $1\pi_u(z)$ MOs increases giving a more stable $2a_1$ level and so greater driving force for bending

It is also possible, from the changes in the population of the orbitals, to predict how the shape will change when a molecule is electronically excited. The configuration for CH_2 given above, $1a_1^2 1b_2^2 2a_1^2$, is in fact an excited state. The ground state is a triplet, with configuration $1a_1^2 1b_2^2 2a_1^1 1b_1^1$, and an angle of 136° . The angle is wider because there is only one $2a_1$ electron. SiH_2 has a singlet ground state with a $1a_1^2 1b_2^2 2a_1^2$ configuration and an angle of 93° . The triplet excited states with configurations $1a_1^2 1b_2^2 2a_1^1 1b_1^1$ have a wider angle of 123° .

Photoelectron spectroscopy (again) A great deal of information can also be obtained from the vibrational structure of the bands in a PES.

The PE spectrum for H_2O may be compared with the MO diagram (see page 13 and the Figure below). There are four bands in the valence region, three "p" bands and one "s" band. The first band, arising from the $1b_1$ orbital, has minimal vibrational structure and is characteristic of ionization from a non-bonding orbital. The second ($2a_1$) band shows a vibrational progression associated with bending the water molecule.

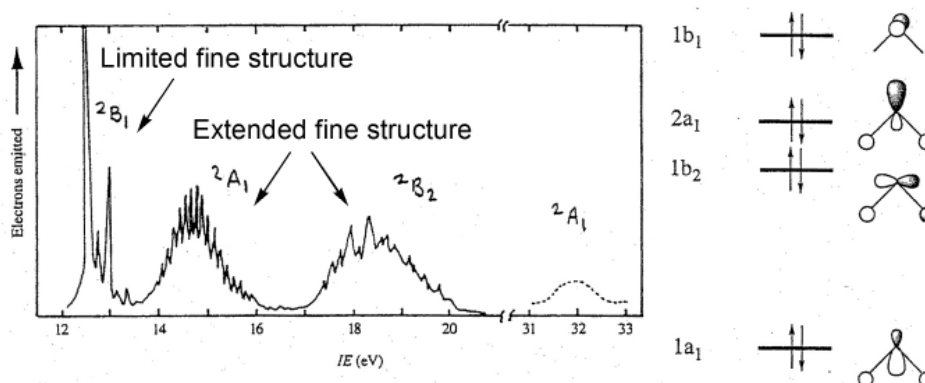
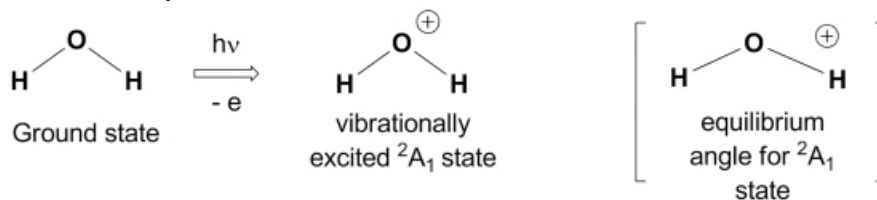


Figure: Comparison of the PE spectrum of H_2O with the LCAO MO scheme

That the band assigned to ionization from the $2a_1$ orbital has considerable fine structure should come as no surprise after the discussions under Section 13 above (shapes of AH_2 molecules). Molecules with just one electron in the $2a_1$ orbital have significantly larger angles than those with two. Remember that bending the molecule destabilizes the b_2 electrons. With two electrons in the $2a_1$ orbital there is more stabilization on bending than with just one. Occupation of the b_1 orbital, which is non-bonding in both linear and bent configurations, makes less difference to the angle.

Therefore the equilibrium H-O-H angle of H_2O^+ in its first 2A_1 ion state should be much larger than in neutral H_2O and so the H_2O^+ ion 2A_1 state will be formed in one of a number of vibrationally excited states in much the same way that H_2^+ is.



The PE spectrum of NH_3 may be also compared with its MO diagram (see Figure below).
Figure below).

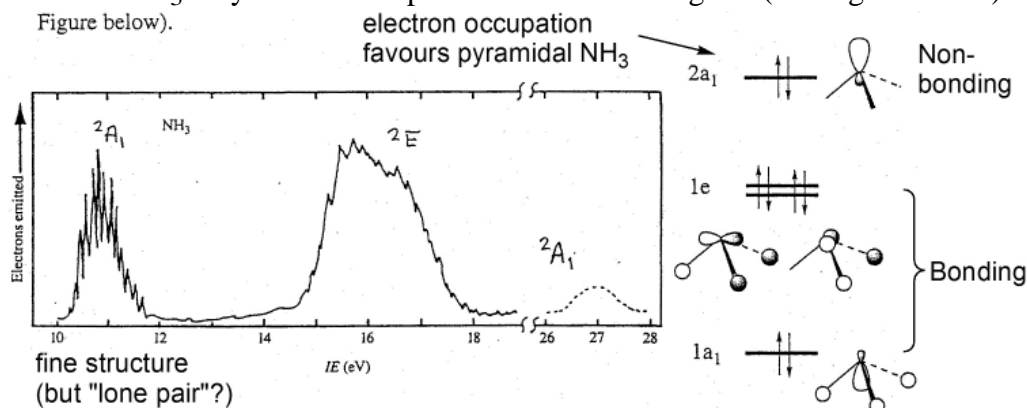
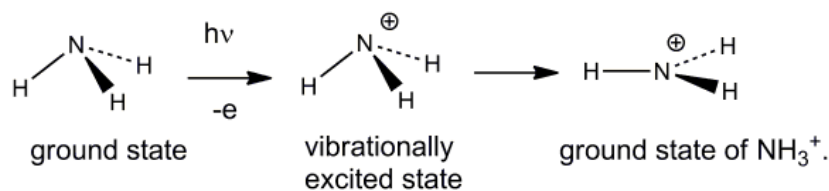
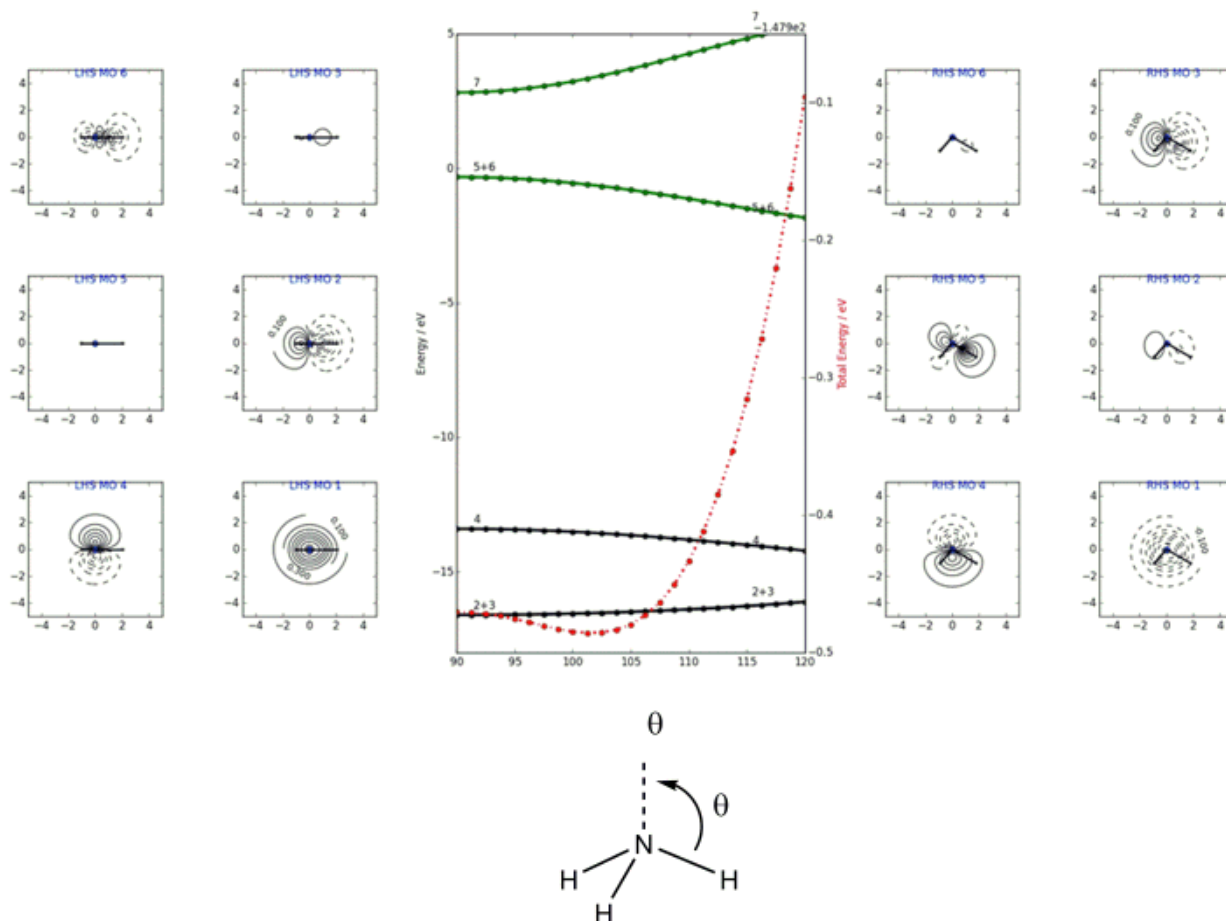


Figure: Comparison of the PE spectrum of NH_3 with the LCAO MO scheme

The PE spectrum of NH_3 shows three main bands exactly as predicted by the LCAO MO scheme. The lowest energy band is for ionization from the $2a_1$ MO (2A_1 state) and exhibits extensive vibrational fine structure. This is at first sight surprising since we have previously described the $2a_1$ MO of NH_3 as partially non-bonding (corresponding formally to the "lone pair" in a valence bond description). But again we have to recognise that we are forming the NH_3^+ ion in a vibrationally excited state. The equilibrium geometry of NH_3^+ (like the CH_3^\bullet radical and BH_3) is **trigonal planar**. The vibrational spacing of 900 cm^{-1} in the first 2A_1 band corresponds to the energy required to bring the NH_3^+ from a trigonal pyramidal (C_{3v}) shape in ground state NH_3 to one that is trigonal planar (D_{3h}) in NH_3^+ .



The trigonal planar (D_{3h}) shape favoured by 7- and 6-electron 1st row compounds AH_3 can readily be explained by reference to the appropriate Walsh diagrams for the process $C_{3v} AH_3 \rightarrow D_{3h} AH_3$ (practise your skills by doing the MO diagram of D_{3h} -symmetric BH_3 !)



In the PE spectrum for CH₄ the presence of two bands corresponds to ionization from the t_2 and a_1 orbitals, and so the PE spectrum is fully consistent with the MO description. The fine structure in each of the PE bands is consistent with significant bonding character in the two MOs from which ionization is occurring.

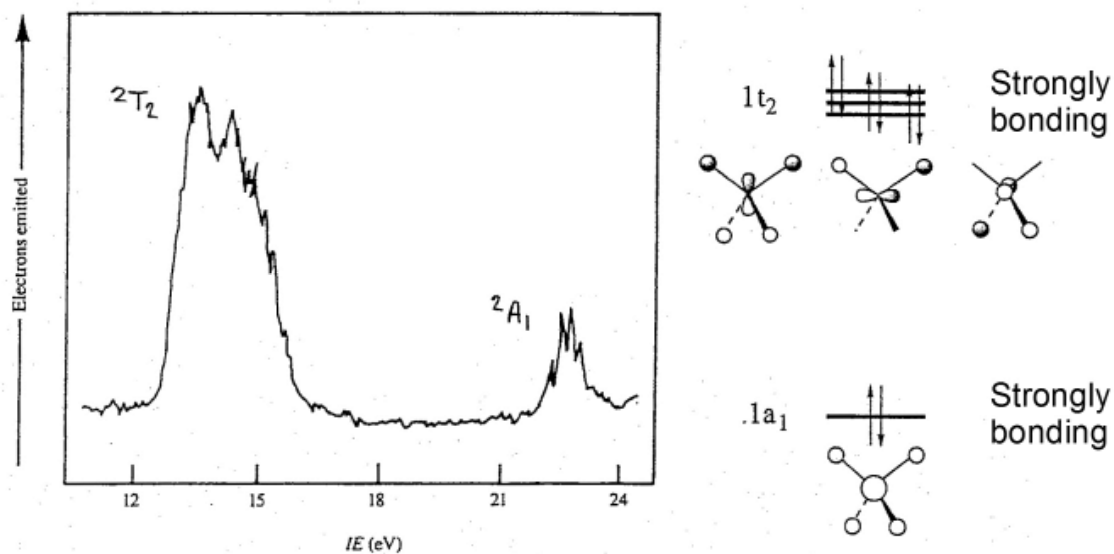


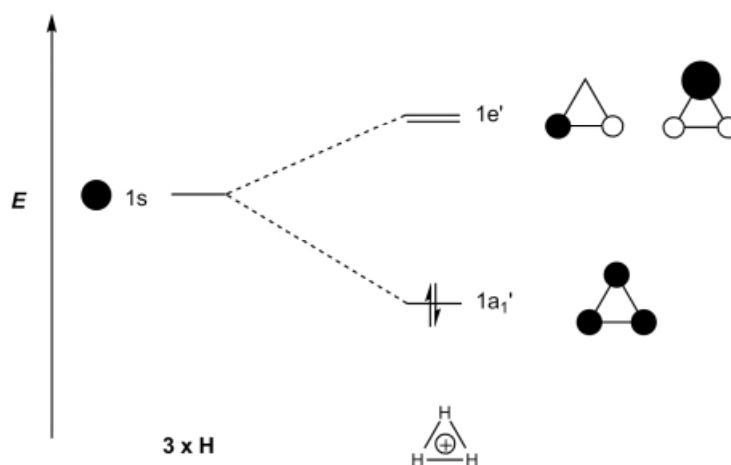
Figure: Comparison of the PE spectrum of CH₄ with the LCAO MO scheme

14. The shapes of H_3^+ and H_3^- : 3c-2e and 3c-4e bonds

The molecules considered so far have obvious ties between the MO descriptions and traditional ideas of electron pair bond formation (*i.e.* molecules with n bonds and $2n$ bonding electrons). But as you know from "electron-deficient" compounds such as diborane, B_2H_6 (containing two 3-centre-2-electron B-H-B bonds), this is certainly not always the case. In this Section we use Walsh diagrams to explore the molecular structures of H_3^+ and H_3^- and discuss their bonding in terms of 3-centre-2-electron (3c-2e) and 3-centre-4-electron (3c-4e) interactions. We return to the topic of 3c-2e and 3c-4e bonds in our discussion of octahedral hypervalent compounds in later Sections.

The principal alternative shapes for H_3^+ and H_3^- are triangular (D_{3h}) and linear ($D_{\infty h}$).

The SALCs of triangular H_3^+ are easily derived from the three H 1s AOs: $\Gamma(3 \times 1s) = a_1' + e'$. These combine to give three MOs of symmetry $a_1' + e'$ as shown below. In H_3^+ , two electrons occupy them.



n.b. bond order = 1/3 per H-H 'bond'

The H_3^+ ion has been observed by mass spectrometry in electrical discharges through H_2 gas. The bonding orbital a_1' accommodates the two electrons and the overall electronic structure can be described as a 3c-2e bond. The H_3^+ ion is thermodynamically stable with respect to $\text{H}^+(\text{g})$ and $\text{H}_2(\text{g})$. Calculations have shown that the enthalpy of dissociation for the process:



is about 400 kJ mol^{-1} which is comparable to that of the H-H bond in H_2 itself. This example shows how important delocalisation of electron pairs is for stabilising molecules.

H_3^- is linear: this immediately presents a problem – do the lines connecting the H atoms in the structure diagram mean normal 2c-2e bonds? If so, we have a problem: there are 2 bonds to the central H, which therefore ‘expands its doublet’. Can we get out of this problem using MO theory?

The SALCs of linear H_3^- can be constructed using a conventional fragment orbital approach as usual. In this case the two outer hydrogens [$\Gamma(1s(A), 1s(C)) = \sigma_g + \sigma_u$] combine with a central H atom [$\Gamma(1s(B)) = \sigma_g$]. This is analogous to the MO diagram in **13** for a $D_{\infty h}$ AH_2 molecule. The rather obvious difference is that the central H atom does not possess valence p orbitals. Four electrons occupy the $1\sigma_g$ and $1\sigma_u$ MOs and the H-H bond order is $\frac{1}{2}$.

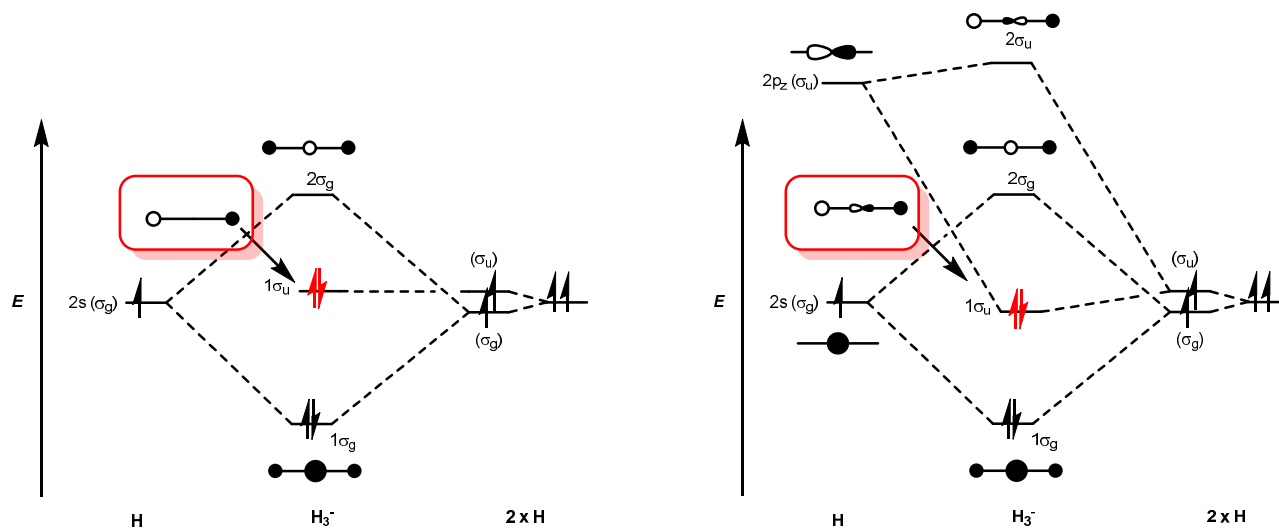
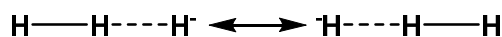


Figure: MO diagrams for H_3^- (a) without and (b) with a p_z orbital on the central hydrogen.

The situation in H_3^- is usually described as 3c-4e bonding. The "surplus" two electrons in H_3^- are accommodated in a $\text{H}\cdots\text{H}$ non-bonding MO ($1\sigma_u$) localised on the terminal $\text{H}_{A,C}$ atoms. Therefore the central H atom does not, in fact, ‘expand its doublet’ at all – the 2 electrons in $1\sigma_u$ have zero amplitude at the central atom. Alternatively, we can think of it in terms of 2 resonance structures, neither of which offends the doublet rule.



Can we use some tricks to recover the picture, where each line in the diagram means a ‘normal’ 2c-2e bond? We can, if we allow the central H to use a p_z orbital in addition to the 1s (right hand figure, above) in which case it would be allowed to accommodate 4 electrons, not just 2.

The $1\sigma_u$ orbital now becomes bonding, so the formal H-H bond order is increased to 1.

But: $1\sigma_u$ is only a little bit bonding, because the $2p$ orbitals are *much* higher in energy than 1s. So the $1\sigma_g$ pair of electrons contributes much more to the net stability than the $1\sigma_u$ pair.

Take home message: on paper, including p orbitals seems to be a good idea because it increases the formal bond order and gets us out of the tricky problem of expanding the doublet at the central H. In reality, the central H doesn’t really ‘expand its doublet’ anyway, so that was never a problem in the first place, and the inclusion of p orbitals makes a very marginal difference to total energy. *We can explain the stability of H_3^- perfectly well without invoking p orbitals!*

Why does H_3^+ have the triangular structure while H_3^- is linear? A Walsh diagram shows how the energies of the D_{3h} and $D_{\infty h}$ H_3 MOs correlate. Clearly for 4 electrons (H_3^-) the linear structure is favoured but for 2 electrons (H_3^+) the triangular one gives the best electronic stabilisation.

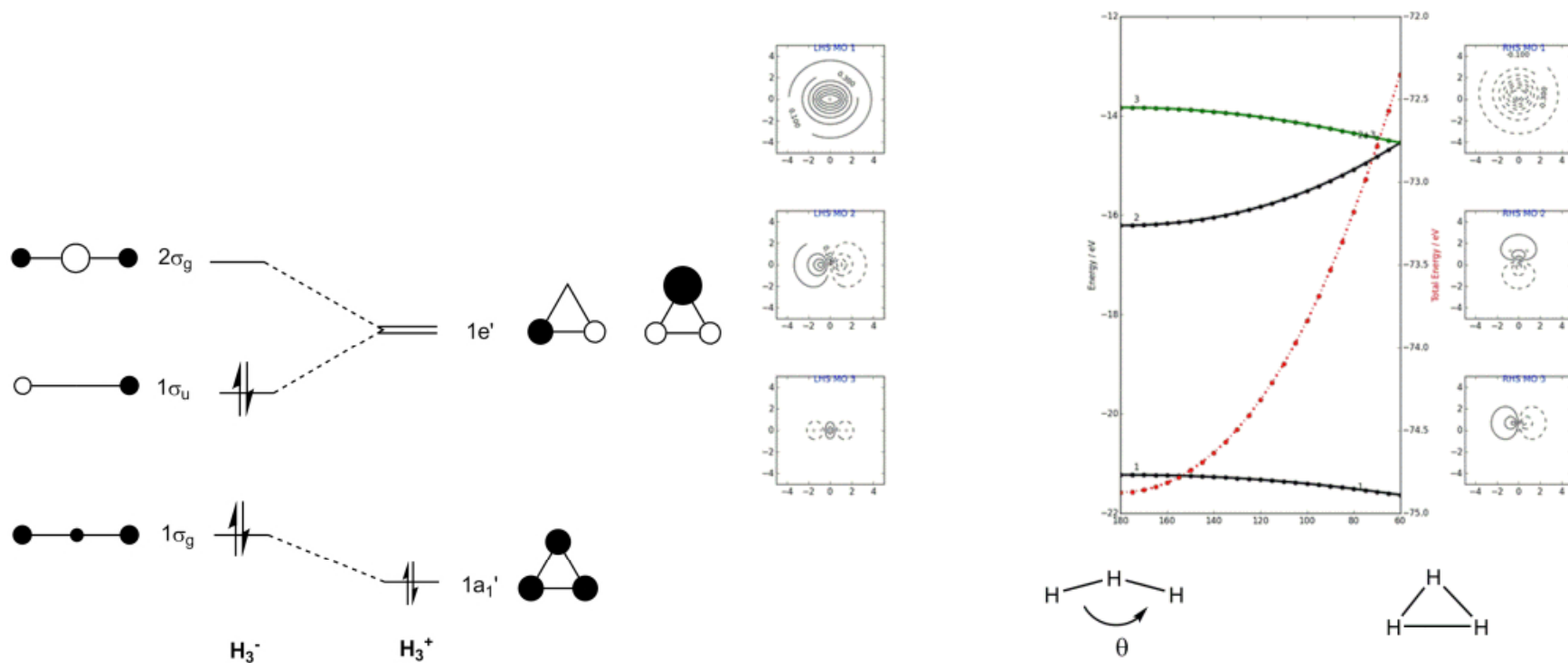


Figure: Walsh correlation diagram between the MO levels of linear and triangular H_3 . (cartoon and 'real'). In the right hand figure the red total energy line corresponds to H_3^- .

Molecular orbital descriptions of hypervalent molecules

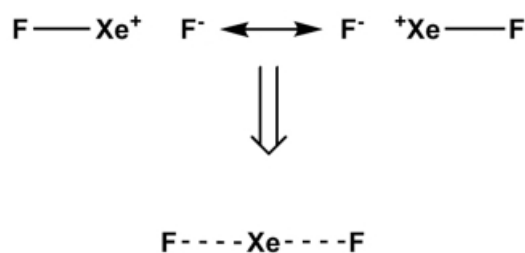
In Section 14 above we discussed the 3c-2e bonding in triangular H_3^+ , as well as the 3c-4e bonding in linear H_3^- . We found that such delocalised σ -bonding is easily accounted for in MO theory.

Nevertheless, we need to revisit now some other important examples of hypervalent molecules, and also address the question of d -orbital participation in the bonding in post-transition metal compounds. It will be shown how the bonding in such compounds can readily be accounted for without the need to include high energy d orbitals (just as we can account for H_3^- without using p 's).

15. The bonding in CO_2 and XeF_2

One of the simplest examples of a post-transition metal hypervalent compound is xenon difluoride. Xe atoms have 8 valence electrons in $5s$ and $5p$ orbitals (and hence a full octet) while each of the terminal F atoms provides (in a Lewis picture) a further electron to the bonding. In a Lewis description of XeF_2 , the Xe atom therefore, apparently, has 10 electrons around it (note the problem is very reminiscent of H_3^-).

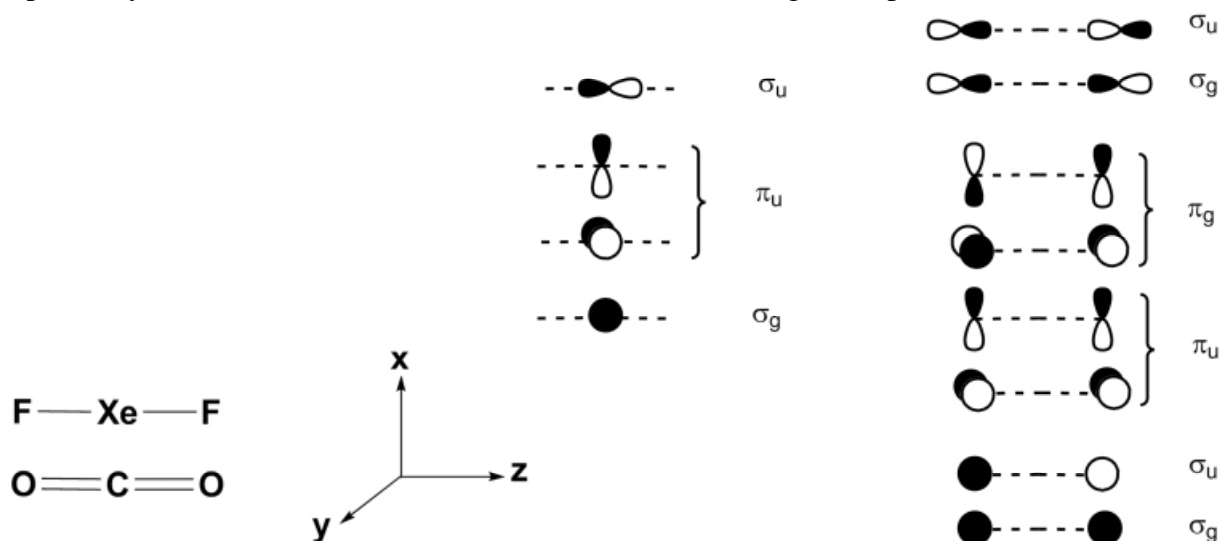
A valid resonance description to achieve an octet description of Xe is:



Here we still maintain the desired octet and overall this suggests delocalised bonding with an average Xe-F bond order of 0.5. Again by analogy to H_3^- , we might expect to recover a normal 2c-2e (single) valence bond description if we allow Xe to use the high energy $5d_{z^2}$ orbital on Xe to produce five sp^3d hybrids. These five hybrid orbitals can accommodate the 10 electrons (3 lone pairs and 2 bonding pairs) and each Xe-F bond can now be described as a 2c-2e localised single bond. The intuitive difficulty with this model is that the $5d_{z^2}$ AO of Xe must be very high in energy and so one should question whether it is reasonable (and indeed necessary) to invoke its use in bonding, just as we would question the use of $2p_z$ in H.

In this section we explore the MO description of XeF_2 with and without the use of the $5d_{z^2}$ AO and see how the photoelectron spectrum helps support the MO picture developed. To do this we first develop an MO description of CO_2 which is related to that of XeF_2 .

Symmetry analysis: In Section 13 above, we developed an MO scheme for linear ($D_{\infty h}$) AH_2 . The symmetry analysis of CO_2 and XeF_2 is similar except that now the terminal atoms bring np ($n = 2$ or 5 , respectively) valence AOs as well as the ns AOs to the bonding description:



Central atom (4 AOs):

$$\Gamma(ns) = \sigma_g \quad \Gamma(np_z) = \sigma_u \quad \Gamma(np_{x,y}) = \pi_u$$

Terminal atoms (2 x 2s; 6 x 2p AOs):

$$\Gamma(2 \times 2s) = \sigma_g + \sigma_u \quad \Gamma(2 \times 2p_z) = \sigma_u + \sigma_g$$

$$\Gamma(2 \times 2p_{x,y}) = \pi_u + \pi_g$$

For the resulting $D_{\infty h}$ molecule (12 MOs): $\Gamma(\text{MOs}) = 3\sigma_g + 3\sigma_u + 2\pi_u + 1\pi_g$

The **symmetries** (i.e. $3\sigma_g + 3\sigma_u + 2\pi_u + 1\pi_g$) of the MOs of CO_2 and XeF_2 are **identical** although the contributions of the various AOs to the bonding (see below) differs, as does their occupation by electrons. We consider first the bonding description of CO_2 which has 16 valence electrons (4 from C and 12 from 2 x O respectively).

The resultant MO diagram for CO_2 is shown in the Figure below. In the σ -bonding manifold there are three σ_g and three σ_u symmetry MOs. These MOs (without $2s$ - $2p$ mixing shown for the terminal atoms) are predominantly bonding, non-bonding and anti-bonding in character. In the π -bonding framework there are two bonding ($1\pi_u$) and two anti-bonding ($2\pi_u$) MOs. The $1\pi_g$ MO is based entirely on the terminal atoms as there is no symmetry match (i.e. no π_g AO) on the central atom. Note that there are 4 occupied orbitals with significant bonding character ($2\sigma_g$, $2\sigma_u$ and $1\pi_u$) and four empty antibonding counterparts. The net bond order is therefore 4, or 2 per bond (i.e. C=O double bonds).

Note also that s - p mixing will accumulate bonding character in the $1\sigma_g$ and $1\sigma_u$ orbitals and make $2\sigma_g$ and $2\sigma_u$ rather more non-bonding, but this does not affect the bond-order analysis.

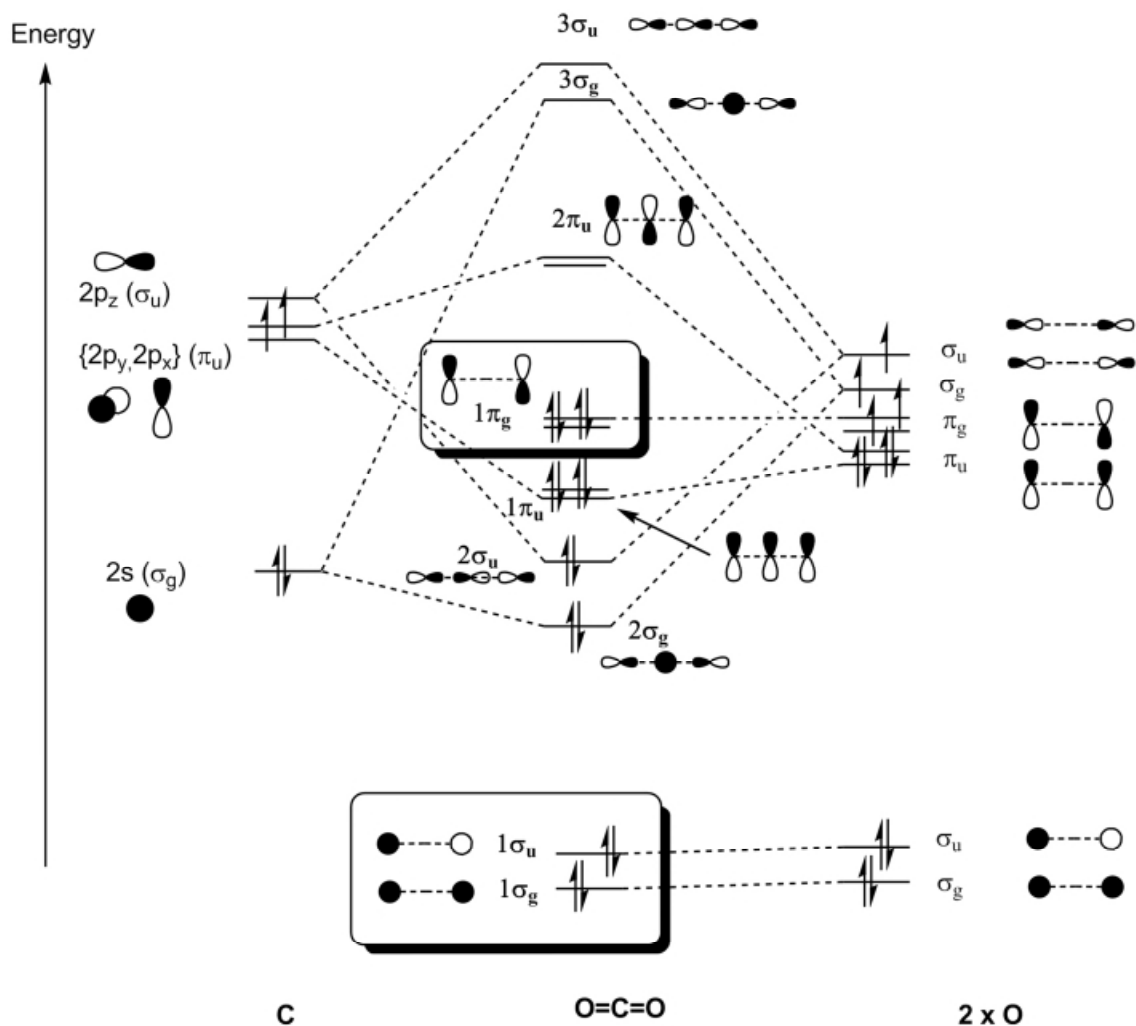


Figure: MO energy level diagram for CO₂.

Approximate MO descriptions of XeF₂ are shown on page 34, first where we assume that the 5d orbitals on Xe are too high in energy to participate, and secondly where we allow some bonding interaction with the SALCs on fluorine. XeF₂ has 22 valence electrons (8 from Xe and 7 each from F) to be accommodated in this MO scheme. In the MO scheme without 5d_{z²} contribution, this requires the MOs to be filled up to and including the 3σ_g level. Therefore there are 11 filled MOs. If we assume that the three s orbitals are too low in energy to participate, we are left with one σ-bonding; two π-bonding; one σ-non-bonding; two π-non-bonding; two π-anti-bonding; and one σ-anti-bonding. Of these, only one anti-bonding MO (the 3σ_u level) is left unoccupied in XeF₂. In XeF₂ therefore the Xe-F bonding can be considered to be based on a net 3c-4e interaction derived from the σ MO manifold: 2σ_u² 3σ_g² 3σ_u⁰, with a net Xe-F bond order of ½, (compare to H₃⁻, 1σ_g² 1σ_u² 2σ_g⁰). This is sometimes called the Pimentel-Rundle model of bonding.

The second XeF₂ MO diagram shows how the high energy 5d_{z²} AO could in principle mix in with the 3σ_g MO to stabilise the two electrons in this orbital. Antibonding character builds up in the new 4σ_g MO. It is clear that mixing of the 5d_{z²} into the 3σ_g level would have a stabilising effect by adding some bonding character. The π_g SALC is also stabilised somewhat by interaction with 5d_{xz/yz}. By doing this, we increase the formal Xe-F bond order from ½ to 1, but in reality the effect is marginal.

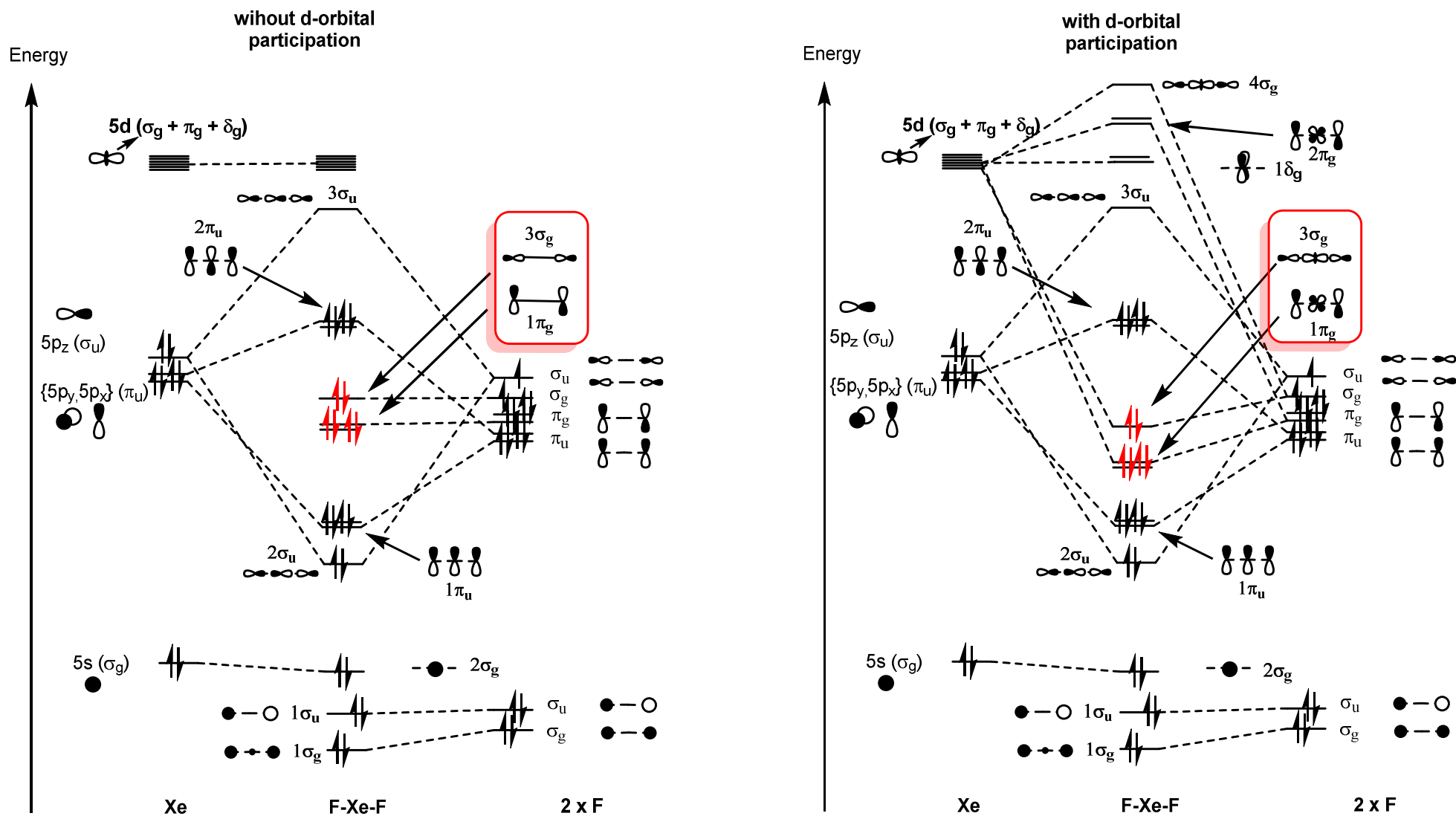


Figure: Qualitative MO energy level diagram for XeF₂ without (left) and with (right) 5d participation.

The photoelectron spectrum of XeF₂ is shown below. It can be assigned assuming Koopmans' approximation ($IE = -\epsilon_i$) and the level ordering on the right hand side MO diagram above in which the $3\sigma_g$ orbital lies below $2\pi_u$

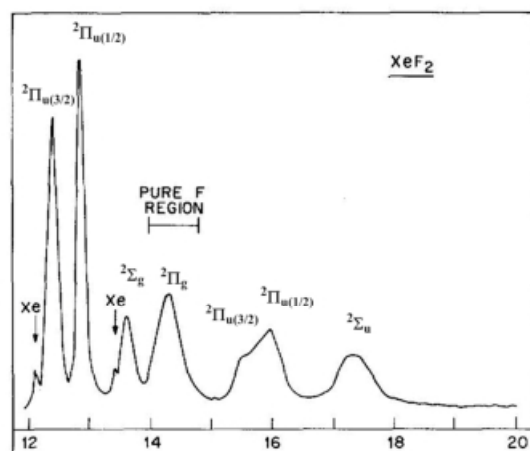


Figure: The photoelectron spectrum of XeF₂

The first **two bands** are both associated with ionization from the $2\pi_u$ MO because of spin-orbit coupling that produces two XeF₂⁺ ion states $^2\Pi_{u(3/2)}$ and $^2\Pi_{u(1/2)}$ on ionizing from just one MO. Spin-orbit coupling is very pronounced in heavy atoms. The separation of the $^2\Pi_{u(3/2)}$ and $^2\Pi_{u(1/2)}$ bands (0.47 eV) can be compared with the spin-orbit coupling constant of 0.87 eV in Xe⁺. This establishes that the $^2\Pi_{u(3/2)}$ and $^2\Pi_{u(1/2)}$ bands arise from orbitals with 54% Xe character, the remaining 46% being localised on the two fluorine atoms. The remaining bands can be assigned as shown in accordance with the MO scheme. Note that the $^2\Pi_g$ band does not show splitting from spin-orbit coupling because (apart from a very small mixing in of $5d_{xz/yz}$) there is no Xe character in the $1\pi_g$ MO and spin-orbit coupling for light atoms is not significant. The angular momentum of a σ orbital is zero so ionization from $\sigma_{g/u}$ MOs has no spin-orbit splitting.

12-electron main group octahedral systems: SF₆ as an example

The next class of hypervalent complex we need to look at are the 12 valence electron (σ -framework) complexes exemplified by SF₆. As for XeF₂, molecules such as SF₆ have more than 8 electron pairs around the central atom and so satisfactory Lewis octet structures require a series of resonance forms of the type shown below.

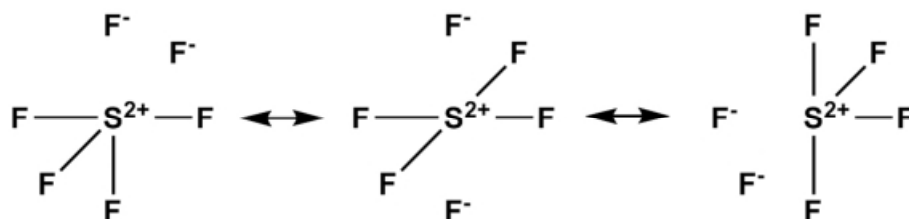


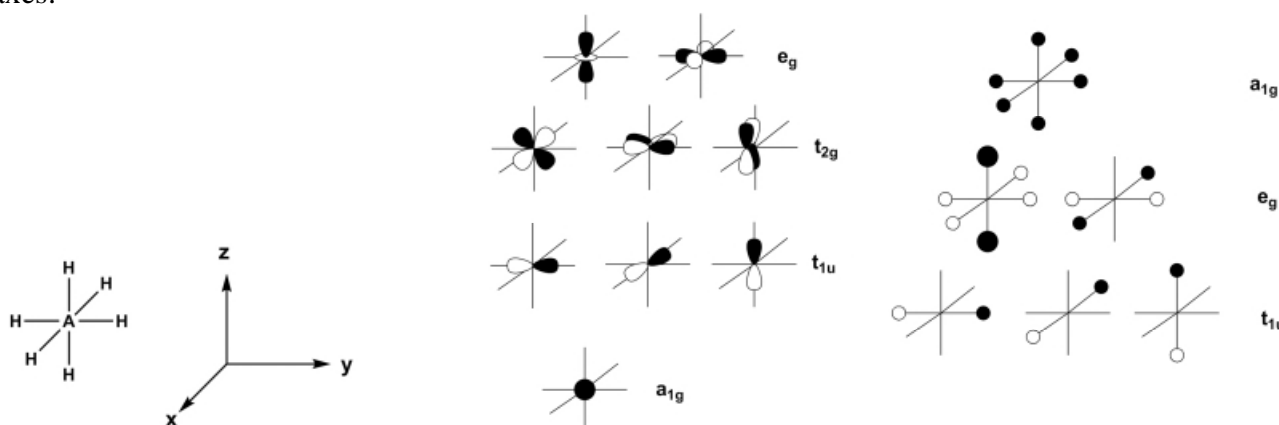
Figure: Some resonance forms for SF₆ that **do** conform to the octet rule

As for XeF₂ such resonance structures imply a delocalised bonding description such as that anticipated by an MO analysis. But as was the case for XeF₂, valence bond 2c-2e models can at first sight be postulated. If we invoke $3d_{z^2}$ and $3d_{x^2-y^2}$ atomic orbitals (not normally employed in an

Aufbau sense until at least Ca has been passed) then a set of sp^3d^2 hybrid orbitals can be produced. Each of these six hybrids then contributes to a 2c-2e S-F bond. Again there is a problem with proposing the extensive use of 3d orbitals on sulfur: the 3d AOs lie 800 kJmol^{-1} higher in energy than the 3p and so the extent to which they can contribute is arguable. Here we will analyse the general σ -bonding in molecules such as SF_6 and show how a satisfactory delocalised multicentre model (without 3d AOs) can account for the bonding.

We shall take as a starting point the hypothetical model hexahydride compound AH_6 . The orbital analysis will be a general one and is applicable to both 12- and 8- σ -electron systems with appropriate electronegativity perturbations as we shall see later

Symmetry analysis: The coordinate system chosen has the H atoms of AH_6 arranged along Cartesian axes:



The ns and np and nd AOs of atom A and the SALCs of $O_h(\text{H})_6$ span the irreducible representations:

For the A atom (1 x ns and 3 x np AOs): $\Gamma(s) = a_{1g}$ $\Gamma(p_x, p_y, p_z) = t_{1u}$

For the A atom (5 x nd AOs): $\Gamma(d_{z^2}, d_{x^2-y^2}) = e_g$ $\Gamma(d_{xy}, d_{xz}, d_{yz}) = t_{2g}$

For the H atoms (6 x $1s$ AO): $\Gamma(6 \times 1s) = a_{1g} + t_{1u} + e_g$

Hence for the resulting AH_6 molecule (15 MOs): $\Gamma(\text{MOs}) = 2a_{1g} + 2t_{1u} + 2e_g + t_{2g}$

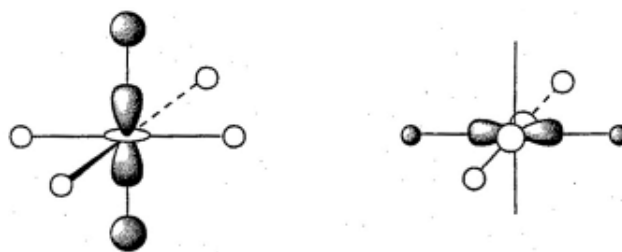
This simple symmetry analysis is a **general result** for any AH_6 σ -only octahedral complex with s , p and d AOs included in the A atom orbital basis set. You will return to this many times in discussions of the bonding in transition metal complexes. In the AH_6 post-transition metal complexes we need to consider two distinct cases, namely **with or without** nd orbital participation.

In the first instance we will assume that the nd AOs are **too high in energy** to contribute to the A-H bonding. The symmetry analyses therefore predicts:

- 4 bonding MOs ($a_{1g} + t_{1u}$) and 4 anti-bonding MOs ($a_{1g} + t_{1u}$).
- 5 A atom-based non-bonding (i.e. the nd) orbitals (e_g and t_{2g})
- 2 H atom-based non-bonding LCAO/SALCs (e_g)

A fragment orbital interaction diagram for AH_6 without d -orbital participation is shown on the left in the figure on the following page. The 12 valence electrons occupy the six lowest energy MOs. Four MOs are A-H bonding ($1a_{1g}$ and $1t_{1u}$). **Thus four highly delocalised electron pairs** are involved in forming six A-H "bonds", and the net bond order for each A-H bond is $2/3$. The two remaining pairs of electrons ($1e_g$) are non-bonding and located entirely on the H atoms. This explains why SH_6 is in fact not known but SF_6 is perfectly stable. The electrons in $1e_g$ rely entirely for their stability on the electronegativity of the atoms upon which they are localised: if the atoms were not highly electronegative, the molecule would be expected to undergo oxidation very easily and be inherently unstable.

Now consider the effect of bringing the five nd ($e_g + t_{2g}$) orbitals into the bonding picture (see Figure below, right). The t_{2g} set (d_{xy}, d_{xz}, d_{yz}) are unable to find a match with any of the $(\text{H})_6$ SALCs, but the e_g ($d_{z^2}, d_{x^2-y^2}$) set have the correct nodal properties and symmetry to interact with the previously non-bonding $(\text{H})_6 e_g$ SALCs.



The previously non-bonding $1e_g$ set is stabilised, all 12 electrons are now in bonding orbitals and so the formal bond order is increased to 1.0 per A-H bond. However, the extent to which d -orbital participation actually contributes to the bonding in post-transition metal compounds is **minimal**; the bonding is best considered in terms of multi-centre bonding with d orbitals making only a **minor contribution**.

Note the parallels between H_3^- , XeF_2 and SF_6 . We can **always** explain the stability of the molecule without the polarisation functions.

	without polarisation	with polarisation (p on H or d on Xe/S)
H_3^-	$1\sigma_u$ is non-bonding H-H bond order = $1/2$	$1\sigma_u$ becomes weakly bonding <i>formal</i> H-H bond order = 1
XeF_2	$3\sigma_g$ is non-bonding Xe-F bond order = $1/2$	$3\sigma_g$ becomes weakly bonding <i>formal</i> Xe-F bond order = 1
SF_6	$1e_g$ is non-bonding S-F bond order = $2/3$	$1e_g$ becomes weakly bonding <i>formal</i> S-F bond order = 1

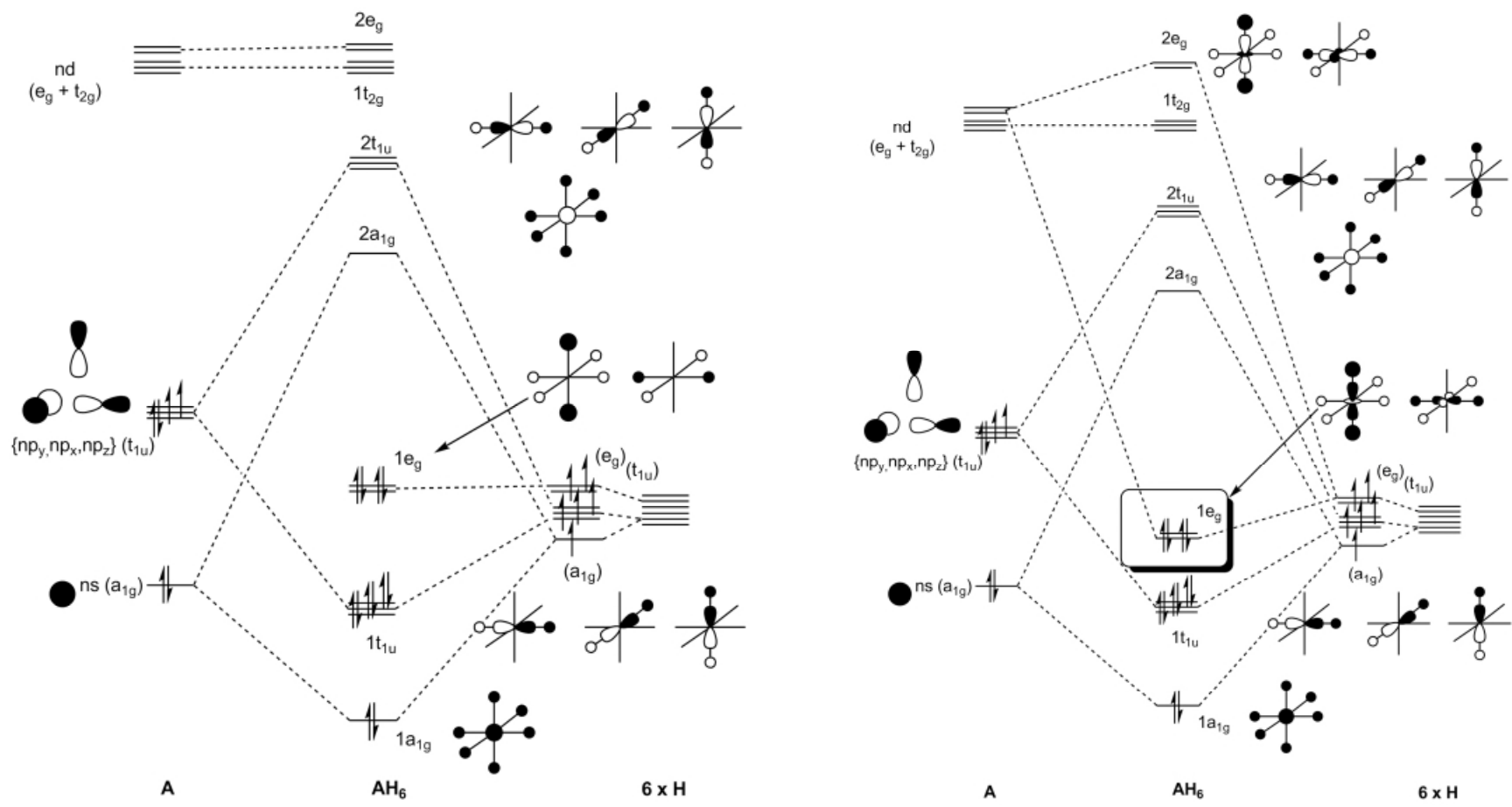
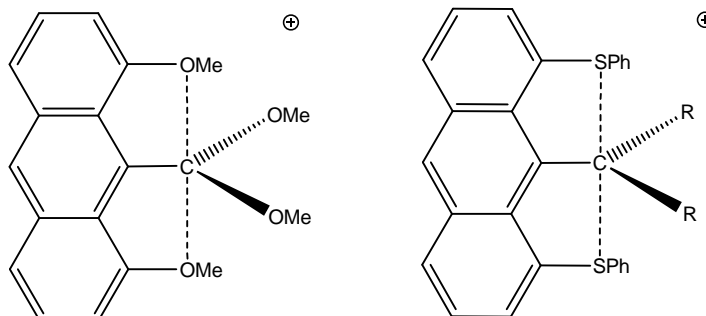


Figure: Qualitative fragment orbital interaction diagram for a 12 valence electron AH₆ Compound without (left) and with (right) participation of the *nd* atomic orbitals on the central atom.

17. Hypervalent carbon? Not as uncommon as you might think.....

Many examples of this type are known:



8-electron main group octahedral systems: $[C(AuPR_3)_6]^{2+}$ as an analogue of CH_6^{2+}

CH_6^{2+} has been observed only in the gas phase but $[C(AuPR_3)_6]^{2+}$ is a crystalline solid. The latter class of complex are stable at room temperature and a number of these have been crystallographically characterised. The $AuPR_3$ ligand is a one-electron, σ -type donor ligand like H ($(PR_3)Au^+$ is sometimes referred to as a ‘fat proton’) and so $[C(AuPR_3)_6]^{2+}$ complexes are isolobal to CH_6^{2+} .

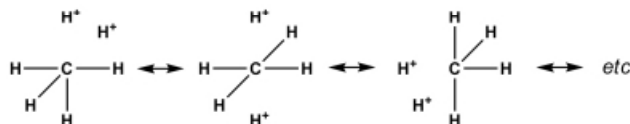
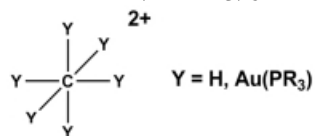


Figure: Some resonance forms for CH_6^{2+} that do conform to the octet rule

Just as for XeF_2 and SF_6 above, one can write down resonance structures that comply with the octet rule. Again such structures suggest a delocalised description of the bonding in MO theory, but now the terminal ligands carry a positive rather than negative charge. However, unlike the situation for XeF_2 and SF_6 we cannot invoke the participation of high energy d orbitals on carbon (the closest in energy would be the $3d$). Therefore we are compelled to seek only a hypervalent bonding description and this can be easily done using the basic MO scheme developed above for 12 valence electron AH_6 compounds. A qualitative MO diagram for CH_6^{2+} is given in the Figure below. This is also a model for $[C(AuPR_3)_6]^{2+}$ for the reasons outline above.

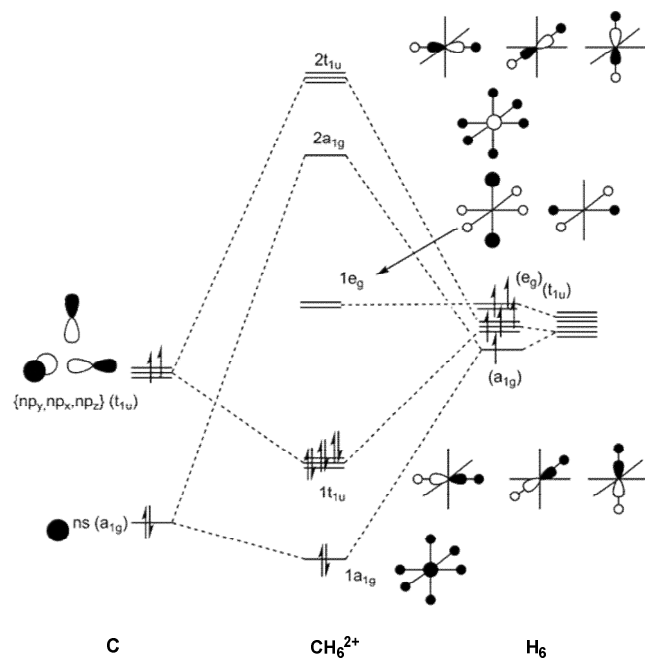


Figure: Qualitative fragment orbital interaction diagram for CH_6^{2+}

The bonding in CH_6^{2+} features a set of four filled σ -bonding MOs ($1a_{1g}$ and $1t_{1u}$) together with the corresponding vacant σ -anti-bonding MOs ($2a_{1g}$ and $2t_{1u}$) at high energy. Just as for 12 electron AH_6 compounds there are two non-bonding MOs located entirely on the peripheral atoms/ligands (*i.e.* the $1e_g$ set). However, the **key difference** in the 8 valence electron CH_6^{2+} (and $[\text{C}(\text{AuPR}_3)_6]^{2+}$) is that Au-C the **non-bonding e_g MO is vacant**.

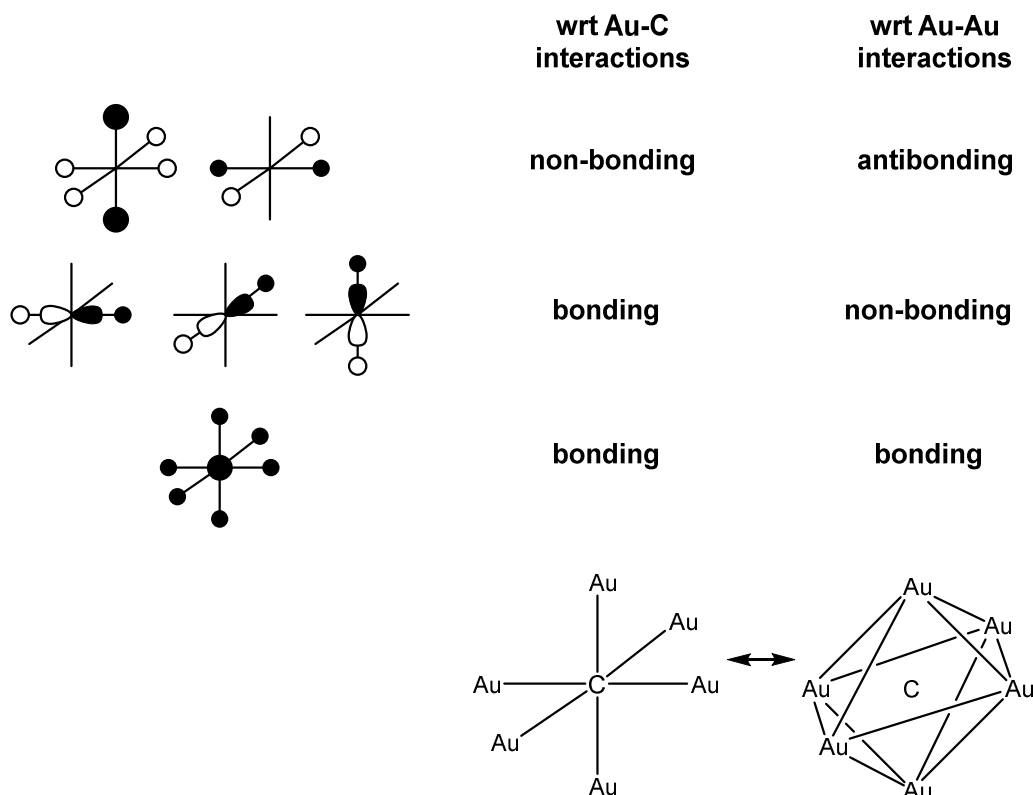
The fact that the e_g level is vacant for an 8 valence electron $\text{AH}_6 / \text{CY}_6^{2+}$ species has several **important consequences** for the **types of complex** that will form 8-electron AH_6 systems:

In the **12 electron species** the ligand-based $1e_g$ MOs of AH_6 are **occupied** so this is favoured by compounds with **electronegative** peripheral atoms and relatively electropositive central atoms (hence SF_6 is a good example). This will keep the $1e_g$ orbital **low** in energy. In the **8 electron species** the ligand-based $1e_g$ MOs of AH_6 are **vacant** and so they need to be high in energy if the molecule is to be stable. This requires the peripheral ligands to be **electropositive** relative to the central atom. This is one of the likely reasons why the gold complexes $[\text{C}(\text{AuPR}_3)_6]^{2+}$ in particular are so stable: here the $1e_g$ MO will be somewhat higher in energy than the carbon $2p$ AO manifold.

Different perspectives on the same thing: is $[\text{C}(\text{AuPR}_3)_6]^{2+}$?

(a) an octahedral coordination compound of C or

(b) a cluster of Au atoms with a carbon atom trapped in the middle?

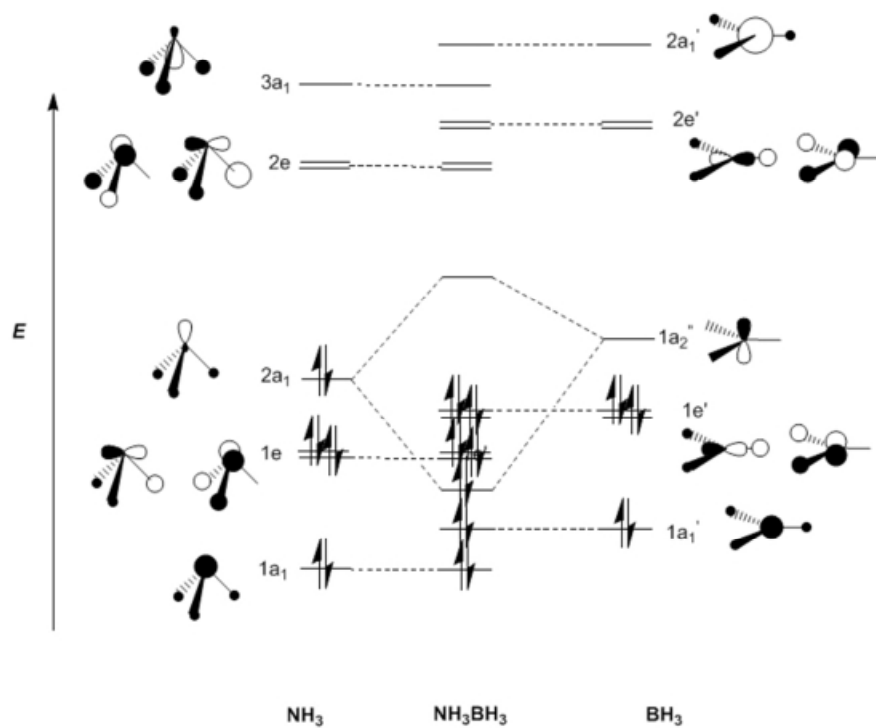


18. The fragment approach to building MO diagrams.

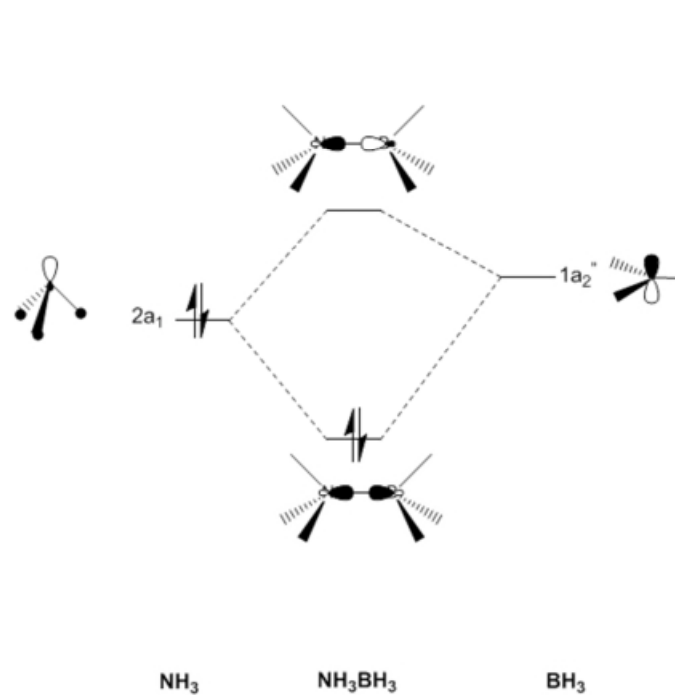
$\text{NH}_3 \cdot \text{BH}_3$

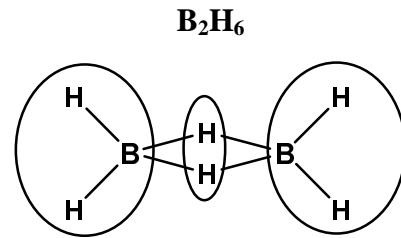
NH_3 : (see page 15) BH_3 : done as practice

Complete diagram

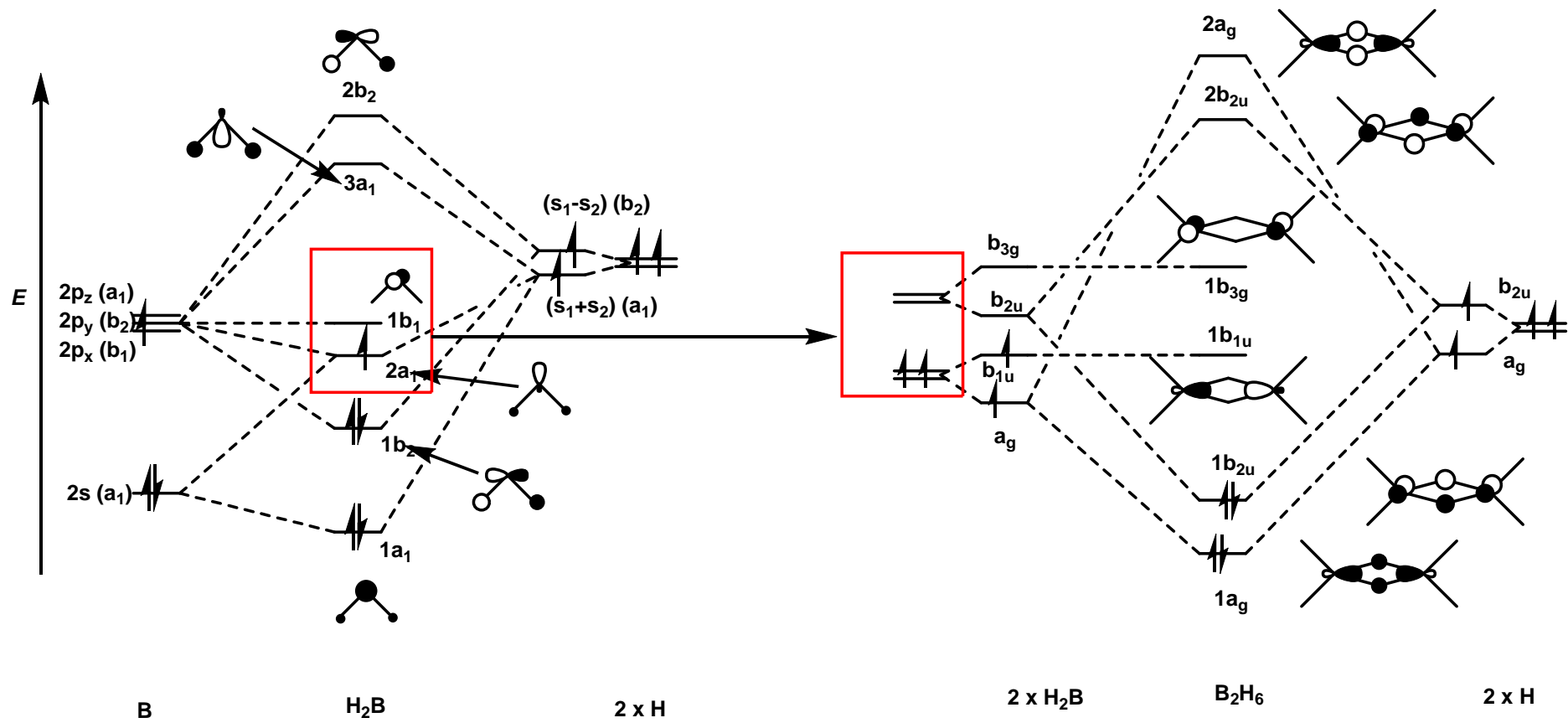


Simplified version

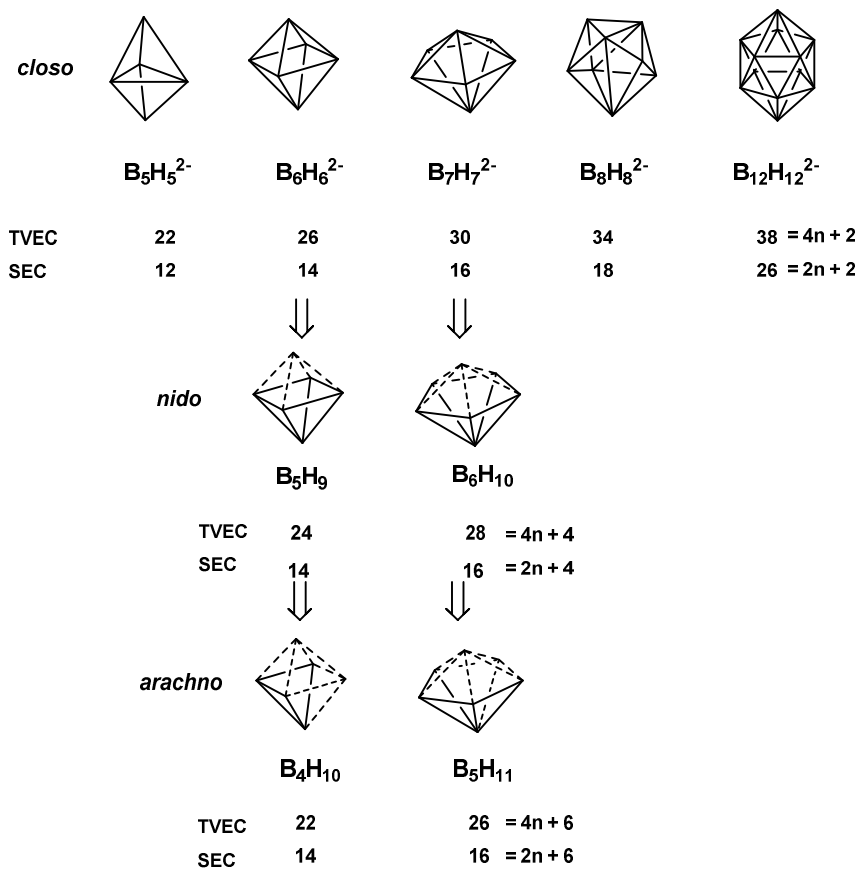
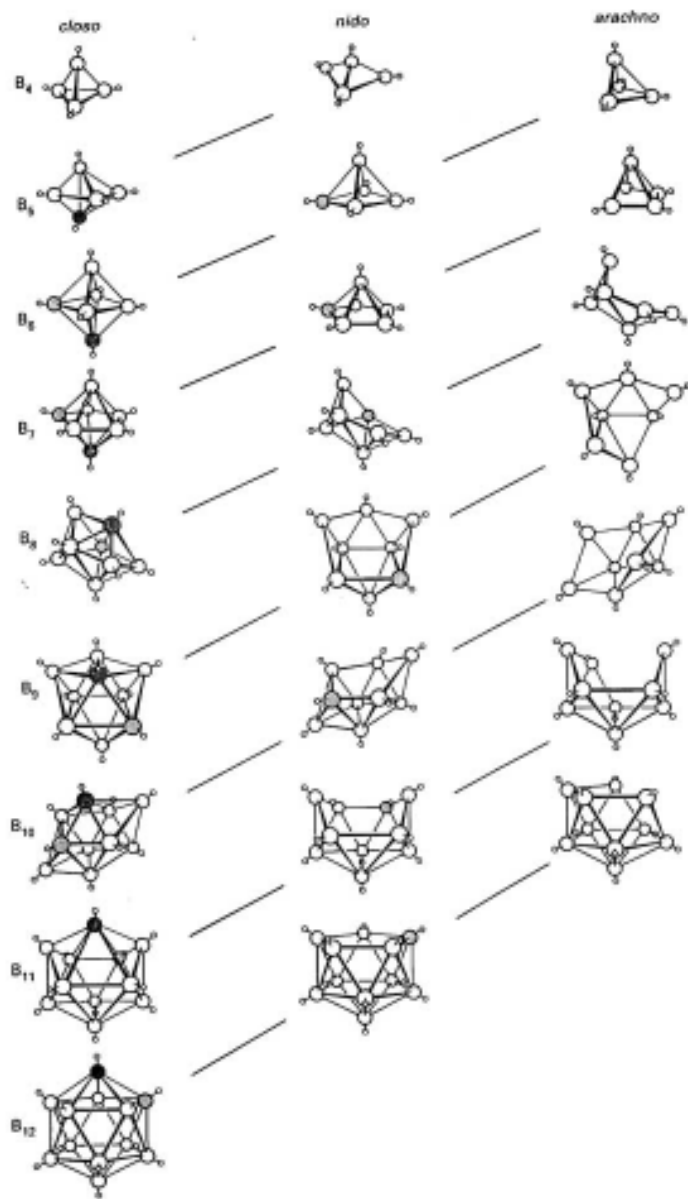




BH_2 : (c.f. H_2O , page 13, with 3 fewer electrons)



19. Bonding in electron-deficient clusters



Skeletal electron count:

$$\text{SEC} = \text{TVEC} - 2n \quad n = \text{number of vertex atoms}$$

2 electrons per vertex atom are involved in a bond or lone pair directed radially out from the cluster. These do not contribute to the bonding within the cluster skeleton, so delete 2 x no. of vertex atoms from the TVEC



Wade's rules

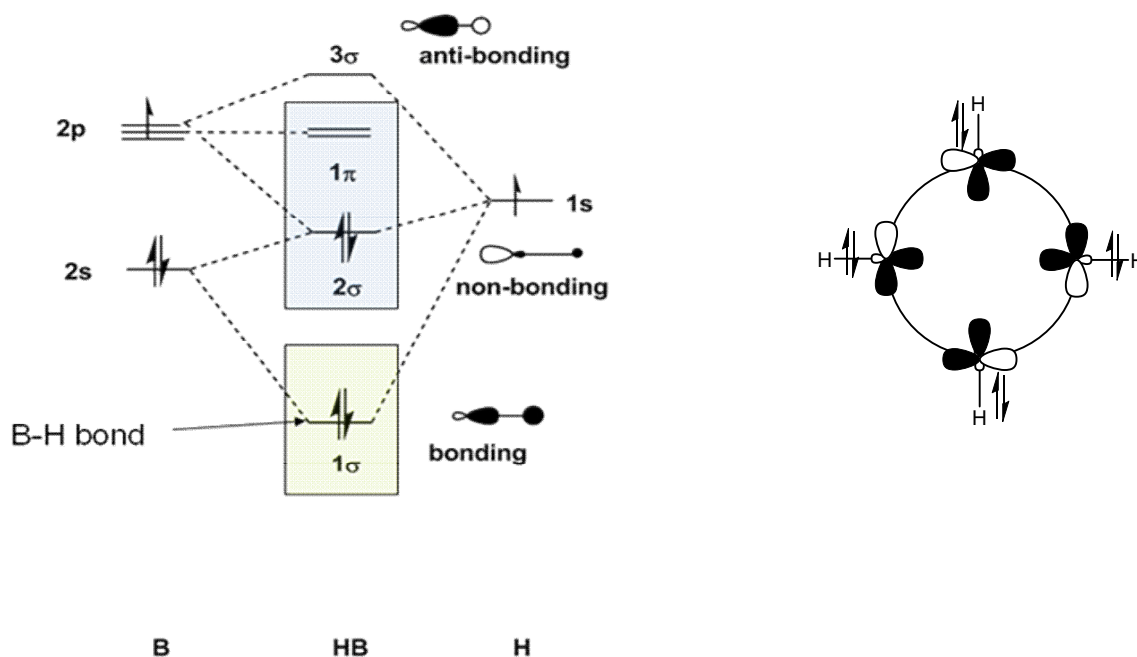
An n-vertex cluster with $2n+2$ skeletal electrons will adopt a *closo* structure based on a deltahedron with n vertices.

An n-vertex cluster with $2n+4$ skeletal electrons will adopt a *nido* structure based on a deltahedron with n+1 vertices, one of which has been removed

An n-vertex cluster with $2n+6$ skeletal electrons will adopt an *arachno* structure based on a deltahedron with n+2 vertices, two of which have been removed

Electronic basis of Wade's rules

Consider a B-H fragment: (page 9)



Bonding orbitals:

1 strongly bonding symmetric combination of σ orbitals + n less strongly bonding combinations of the π orbitals where n is the number of vertices

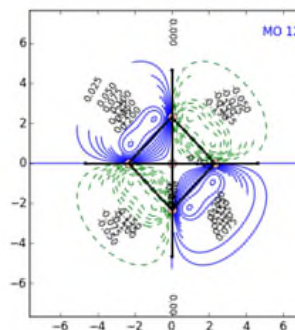
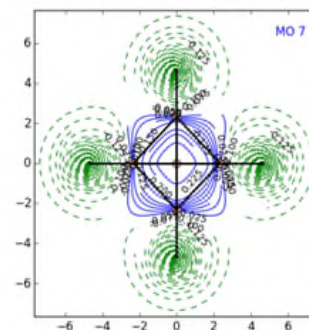
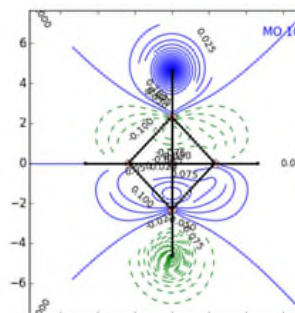
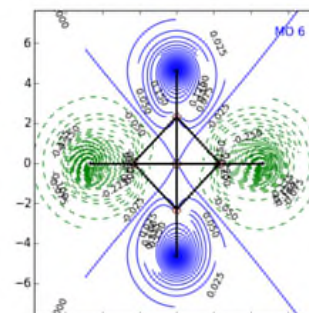
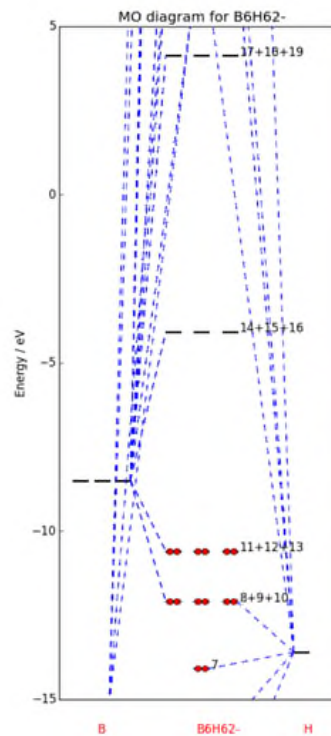
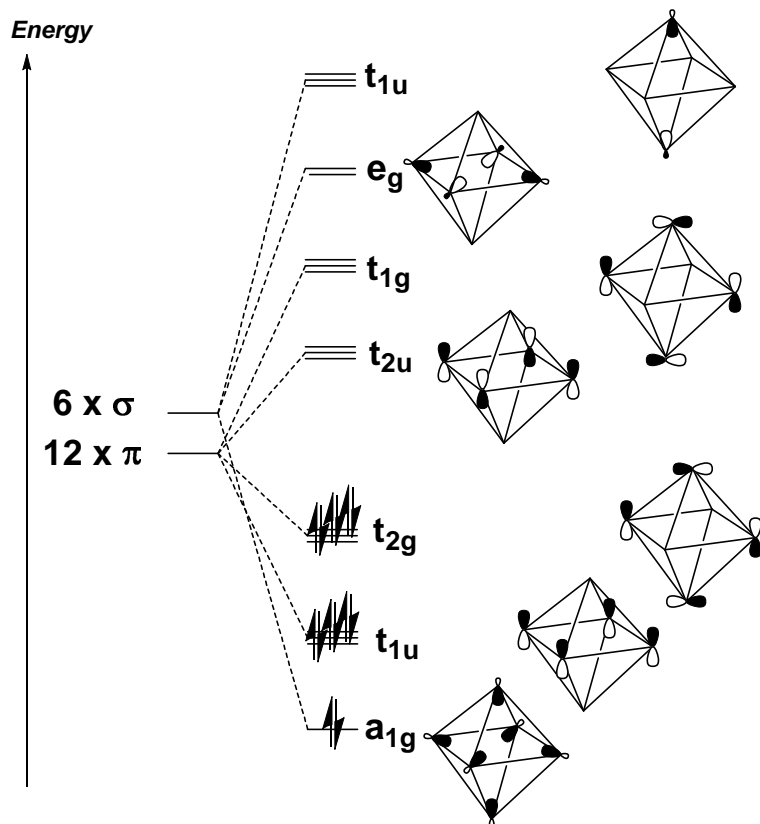
In general, for an n -vertex, *closo* polyhedron, there are $n + 1$ bonding orbitals in the cluster skeleton

$$\therefore \text{SEC} = 2n + 2$$

Each B-H fragment also has 2 electrons in a B-H bonding orbital

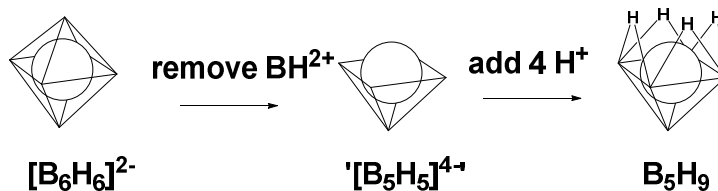
$$\therefore \text{TVEC} = 4n + 2$$

Example: interaction of 6 B-H fragments in $[\text{B}_6\text{H}_6]^{2-}$



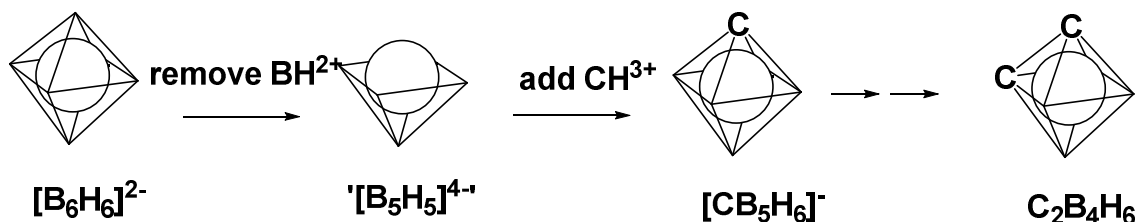
Extension to less electron-deficient clusters

Why are the structures of $[B_6H_6]^{2-}$, B_5H_9 and B_4H_{10} based on the same parent polyhedron?



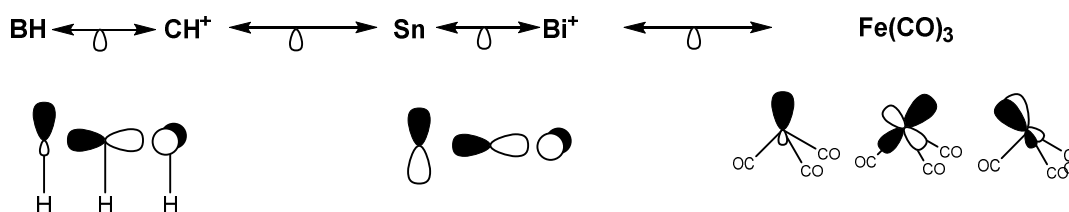
Isolobal analogies: used to rationalize structures of closely related species.

When we remove BH^{2+} , we remove 3 orbitals from the cluster framework. We can replace the missing BH^{2+} fragment with any other isoelectronic species, as long as it provides 3 orbitals with similar symmetry, for example CH^{3+} .



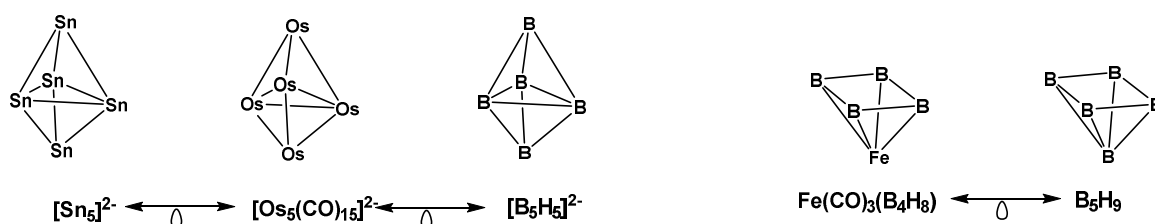
Two fragments are said to be *isolobal* if they have the following properties:

- 1) They have the same number of frontier orbitals
- 2) The frontier orbitals have the same symmetry
- 3) They have the same number of electrons in these frontier orbitals
- 4) The frontier orbitals are of *similar* energy



A lone pair on each atom, pointing out of the cluster, plays the same role as the terminal B-H or C-H bond in boranes or carboranes.

n.b. Fe, Ru, Os are d^8 : 6 electrons are in the ' t_{2g} ' orbitals, directed away from the ligands, leaving 2 to contribute to the bonding. Therefore $M(CO)_3$, $M = Fe, Ru, Os$ are *isolobal* with BH.



20. Octahedral transition metal complexes

You have already seen electrostatic (Crystal Field) approaches to the metal-ligand interactions in transition metal complexes. It is perhaps self-evident that such an electrostatic theory would not be appropriate for compounds such as $\text{Cr}(\text{CO})_6$ which has Cr in its zero oxidation state and neutral CO ligands. Moreover, small, anionic ligands like F^- produce only a small splitting of the d -orbital t_{2g} and e_g set energy levels while CO generally causes one of the largest. In addition there are electron spin resonance data for complexes such as $[\text{IrCl}_6]^{2-}$ [Ir(+4) which has a d^5 configuration with an unpaired electron] that reveal that the unpaired Ir $5d$ electron density is associated significantly with the 6 chloride ligands as well as the Ir centre. All of these observations are suggestive of a more covalent bonding model that we shall now develop using molecular orbital theory.

d -Orbital energies. You have already seen for AH_6 systems the effects of involving d -orbitals in post-transition metal compounds such as SF_6 . In these systems there is little participation of the nd orbitals in the bonding because they lie relatively high in energy above the valence ns and np AOs. This all changes for the transition metals. Now the valence AOs are the $(n+1)s$, $(n+1)p$ and nd ($n = 3, 4$ or 5). Within these three sets, the nd orbitals are the **most stable** of the valence orbitals in metal complexes as illustrated in the Figure below which shows a magnified view of the orbital order near $Z = 20$ where the $3d$ elements begin. The nd AOs are stabilised on crossing the transition series, and after the end of the series are best considered as being core-like and playing no further direct role in metal-ligand bonding.

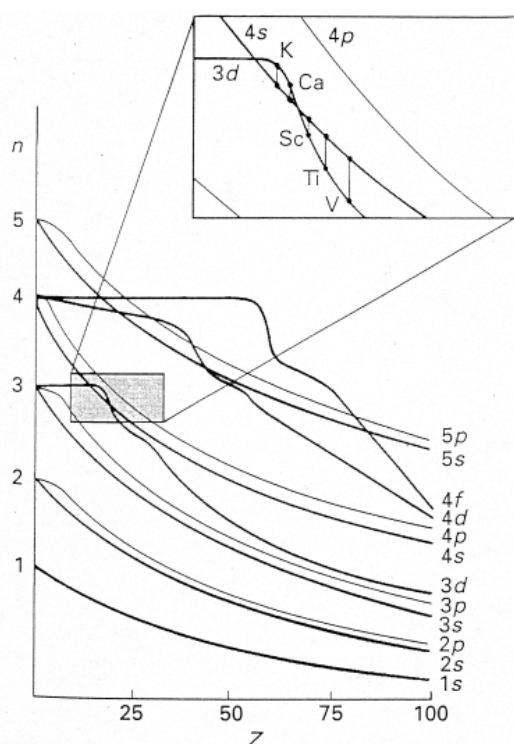


Figure: Energy levels of many-electron atoms. The inset shows a magnified view of the orbital order near $Z = 20$ where the $3d$ elements begin

***d* orbital overlaps.** The overlap of the *d* orbitals (and for 3*d* in particular) with ligand orbitals is small as they belong to the inner quantum shell and are not very radially extended. The overlap improves going down a group as the *d* orbitals acquire radial nodes and extend more into the interatomic region. This is the principal reason why transition metal-ligand bond strengths **increase** going down a group. This contrasts with the situation for main group metal-ligand bond strengths which tend to **decrease** with increasing principal quantum number.

The contracted nature of the 3*d* orbitals is made very apparent by the Figure below that shows the radial distribution functions for the valence orbitals of chromium. The maximum probability (r_{\max}) in the RDFs are $3d(r_{\max}) = 50$ pm; $4s(r_{\max}) = 150$ pm which may be compared to the metallic radius of chromium (128 pm). The semi-core like nature of the 3*d* has important bonding implications (see above); in contrast the very diffuse 4*s* orbitals overlap more effectively with the ligand donor orbitals.

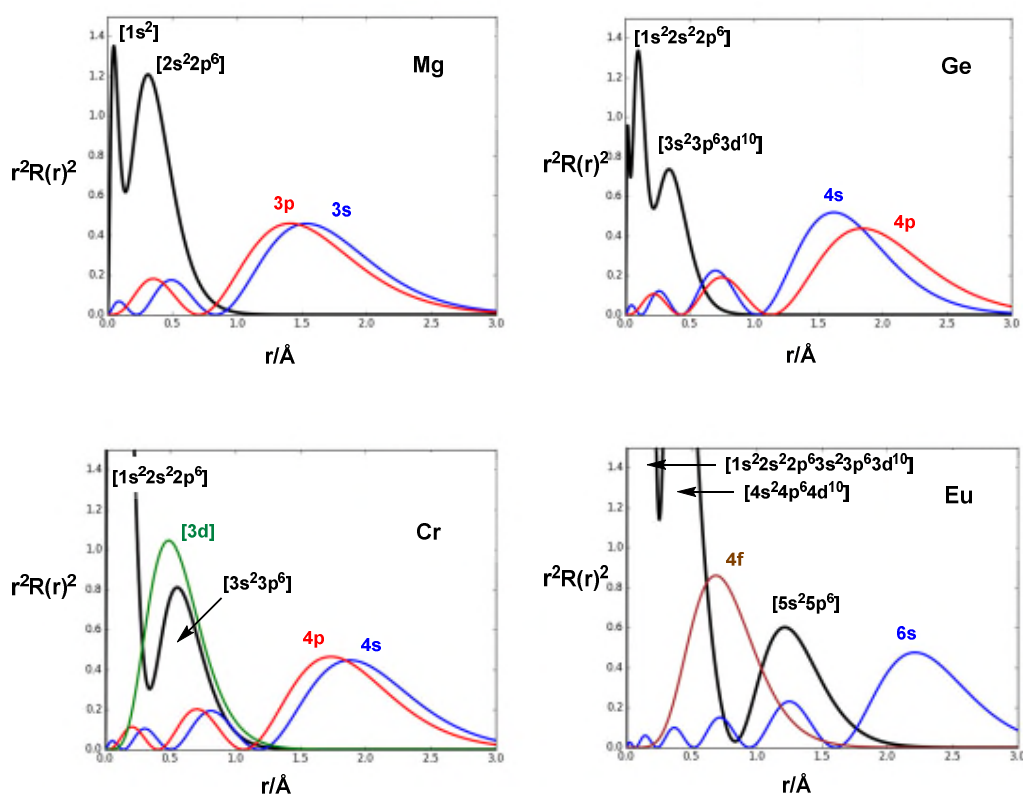


Figure: Radial distribution functions (RDFs) for the valence orbitals of main group, transition metal and lanthanide ions.

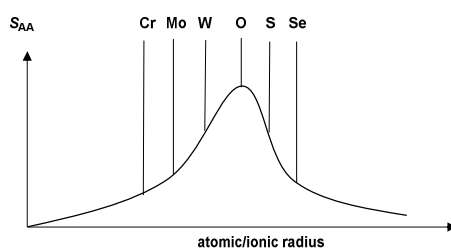


Figure: Diatomic orbital overlap *in the internuclear region*, as a function of orbital size (at fixed distance)

Octahedral transition metal complexes: σ -bonding

We shall look first at octahedral, O_h , transition metal systems with ligands that are capable of forming just σ bonds. Ligands such as NH_3 , H and CH_3 are examples of this.

Symmetry analysis: We will consider a hypothetical complex ML_6 with σ -only donor ligands (the symmetry properties of the donor orbitals will be the same as for H $1s$ orbitals). The symmetry analysis is the same as developed previously for the AH_6 system (page 37/38).

$$\begin{aligned}
 \text{M atom [1 x (n+1)s and 3 x (n+1)p AOs]: } & \Gamma(s) = a_{1g} & \Gamma(p_{x,y,z}) = t_{1u} \\
 \text{M atom (5 x nd AOs):} & \Gamma(d_{z^2}, d_{x^2-y^2}) = e_g & \Gamma(d_{xy}, d_{xz}, d_{yz}) = t_{2g} \\
 \text{For the L atoms (6 x } \sigma\text{-donor orbitals):} & \Gamma(6 \text{ x } \sigma\text{-donor}) = a_{1g} + t_{1u} + e_g \\
 \text{In total for the resulting } \text{ML}_6 \text{ molecule:} & \Gamma(15 \text{ MOs}) = 2a_{1g} + 2t_{1u} + 2e_g + t_{2g} \\
 \text{These are divided into } & \mathbf{12 \text{ } \sigma\text{-bonding/anti-bonding MOs:}} & 2a_{1g} + 2t_{1u} + 2e_g \\
 & \mathbf{3 \text{ } \sigma\text{-non-bonding MOs:}} & t_{2g}
 \end{aligned}$$

MO diagram for a model first row octahedral transition metal complex featuring only σ -interactions (the so-called **σ -only model**):

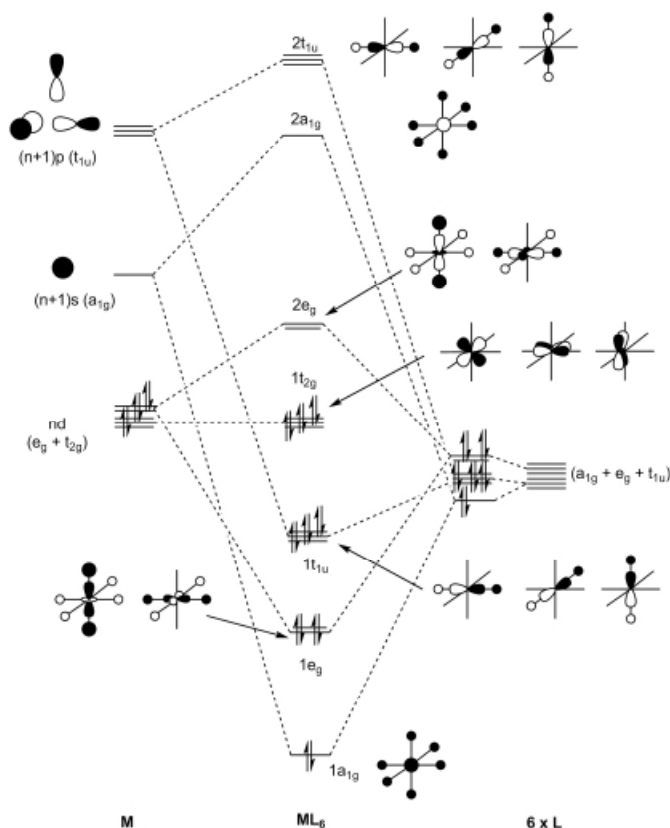


Figure: The σ -only LCAO MO diagram for a 1st row octahedral transition metal complex ML_6

A number of important points follow from this LCAO scheme:

The $1a_{1g}$, $1e_g$ and $1t_{1u}$ orbitals form a set of M-L σ -bonding orbitals. Because M is less electronegative than L they are **more localized on the ligands** than the metal. In other words, electrons in these MOs are ligand-based. We should expect the $1e_g$ orbitals to be more stable than the $1t_{1u}$ because nd AOs are more stable than $(n+1)p$ AOs. Indeed, the $(n+1)p$ AOs may be so high in energy, especially for early transition metals, that they contribute very little to the bonding. The $1a_{1g}$ MO is more stable than the $1e_g$ due to better overlap of the $(n+1)s$ AO with the $(L)_6$ SALCs as compared with that of the more contracted nd AOs.

The $2a_{1g}$, $2e_g$ and $2t_{1u}$ orbitals form a set of M-L σ^* anti-bonding orbitals. They are localized on the metal. Obviously populating these with d-electrons will lead to a reduced M-L bond strength.

The $1t_{2g}$ and $2e_g$ (σ^* anti-bonding) MOs have entirely (in the case of $1t_{2g}$) or predominantly (for $2e_g$) d orbital character. Any electrons in these orbitals are considered to be "***d*-electrons**".

It is therefore clear from the MO diagram that **no** metal complex ML_n can **ever** have electrons in the "s-orbitals" despite any corresponding gas-phase atomic configurations. **All metal-localized electrons in transition metal complexes are best considered as "*d*-electrons"**. For example, the valence electron configuration of Cr(g) is $3d^54s^1$ whereas for Cr(0) in $Cr(CO)_6$ the configuration is $3d^6$ [and in fact $t_{2g}^6 e_g^0$ for this O_h complex].

In the case of σ -only bonding ligands the $2e_g \rightarrow 1t_{2g}$ separation depends on the strength of the M-L σ interaction. This should:

increase on going down a group as M-L overlap increases;

increase with charge on the metal, as this will stabilize the d orbitals and decrease the energy gap between metal and ligand orbitals.

Comparison with the electrostatic model

An alternative way of treating transition metal complexes is to consider them as arrays of ions and dipoles. The metal ion is sitting in an electrostatic field generated by the ligands. These treatments are described as Crystal Field Theory, and Ligand Field Theory.

In crystal field theory the 12 electrons which occupy the $1a_{1g}$, $1e_g$ and $1t_{1u}$ bonding orbitals of MO theory are assumed to be localised entirely on the ligands. In MO theory these orbitals are *predominantly* localized on the ligands but have some metal character too.

In crystal field theory, the $2e_g$ orbitals are raised in energy with respect to the $1t_{2g}$ orbitals because of electrostatic interactions with the ligands while in ligand field theory they are raised in energy because

they are antibonding. The degeneracies remain the same as they are a consequence of the symmetry of the complex rather than the particular bonding model, so both models have their uses.

Ligand field theory is easy to parameterize and therefore to use to model spectral and magnetic properties. MO theory also gives a better qualitative understanding of the size of the d -orbital separations in various complexes.

MO occupations in octahedral complexes

Recall Hund's rules tell us that an atom or molecule achieves a lower energy if electrons are placed in separate degenerate orbitals with the same spin. This is because such a state keeps the electrons further apart, decreases electron-electron repulsion, and maximise exchange energy.

Even if the orbitals in question are not rigorously degenerate, it may still be advantageous to populate them separately with electrons of parallel spin rather than pairing electrons in the same orbital if they are close in energy (*c.f.* Cr ground state, $3d^5 4s^1$). This leads to the concept of "low-spin" and "high-spin" complexes.

High-spin and **low-spin** complexes: For octahedral complexes with between 4 and 7 d -electrons there are two alternative ways of filling the d orbitals. The complex may either maximize the spin putting electrons into the upper e_g orbitals, or fill the lower t_{2g} orbitals pairing the electrons. The two alternative configurations for a d^5 complex are thus: $t_{2g}^5 e_g^0$ (low spin) or $t_{2g}^3 e_g^2$.

The size of Δ_o relative to the pairing energy is critical in determining whether a complex is high or low spin. This is illustrated qualitatively for a d^5 ML_6 complex below.

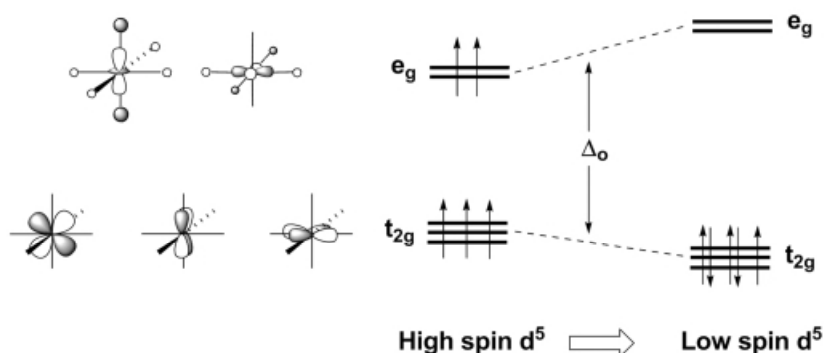


Figure: Qualitative spin-crossover for a d^5 ML_6 complex from high- to low-spin as Δ_o increases

For many first row transition metal complexes the energy required to pair two electrons is in the range 15,000 - 25,000 cm^{-1} . If $\Delta_o < 15,000$ cm^{-1} a high spin complex will result, if $\Delta_o > 25,000$ cm^{-1} a low spin complex will result.

For second and third row complexes the pairing energy is less due mainly to reduced electron-electron repulsion for the more diffuse $4d$ and $5d$ AOs.

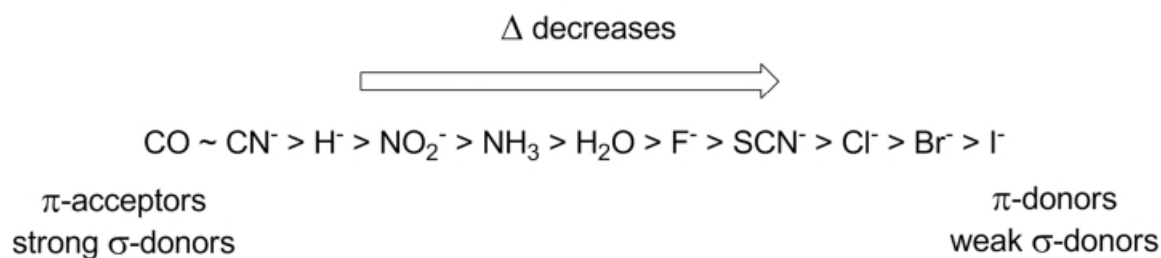
The number of unpaired electrons in a transition metal complex can be deduced from its magnetic properties. This is particularly useful for 1st row complexes where spin-orbit coupling is relatively small and the Russell-Saunders coupling scheme applies (see 3rd year lectures).

Table: Electronic configurations of octahedral complexes

Electron config ⁿ of metal ion		Electronic structure of complex	Number of unpaired e	Example
d^1		t_{2g}^1	1	$[\text{Ti}(\text{H}_2\text{O})_6]^{3+}$
d^2		t_{2g}^2	2	$[\text{V}(\text{H}_2\text{O})_6]^{3+}$
d^3		t_{2g}^3	3	$[\text{Cr}(\text{H}_2\text{O})_6]^{3+}$
d^4	low spin	t_{2g}^4	2	$[\text{Mn}(\text{CN})_6]^{3-}$
	high spin	$t_{2g}^3 e_g^1$	4	$[\text{Cr}(\text{H}_2\text{O})_6]^{2+}$
d^5	low spin	t_{2g}^5	1	$[\text{Fe}(\text{CN})_6]^{3-}$
	high spin	$t_{2g}^3 e_g^2$	5	$[\text{Mn}(\text{H}_2\text{O})_6]^{2+}$
d^6	low spin	t_{2g}^6	0	$[\text{Co}(\text{NH}_3)_6]^{3+}$
	high spin	$t_{2g}^4 e_g^2$	4	$[\text{CoF}_6]^{3-}$
d^7	low spin	$t_{2g}^6 e_g^1$	1	$[\text{Co}(\text{NO}_2)_6]^{4-}$
	high spin	$t_{2g}^5 e_g^2$	3	$[\text{Co}(\text{H}_2\text{O})_6]^{2+}$
d^8		$t_{2g}^6 e_g^2$	2	$[\text{Ni}(\text{NH}_3)_6]^{2+}$
d^9		$t_{2g}^6 e_g^3$	1	$[\text{Cu}(\text{H}_2\text{O})_6]^{2+}$

21 π -interactions and the spectrochemical series

Ligands are ordered according to the relative magnitude of Δ they produce. This order is known as the **spectrochemical series**. For the more common ligands:



The effect of the σ donor ability of the ligands is rationalised by noting that the metal e_g symmetry d orbitals ($2e_g$ in the MO scheme) are metal-ligand σ -anti-bonding. Ligands that are good σ donors (*i.e.* their σ donor orbitals have a good overlap and/or energy match with the metal d orbitals) form complexes in which the σ -bonding $1e_g$ MO is better stabilised. Consequently the metal-based $2e_g$ orbitals are more strongly anti-bonding and thus higher in energy. Pure σ -donors are rare (H^- and NH_3 are the only common examples) but H^- is a better σ -donor than NH_3 , so $\text{H}^- > \text{NH}_3$.

For a full picture of most complexes we also need to consider the π orbitals of the ligands. We will take the basic picture derived for the σ -only system and add on the π interaction. This is likely to be a small perturbation on the σ system as π overlap is smaller than σ overlap.

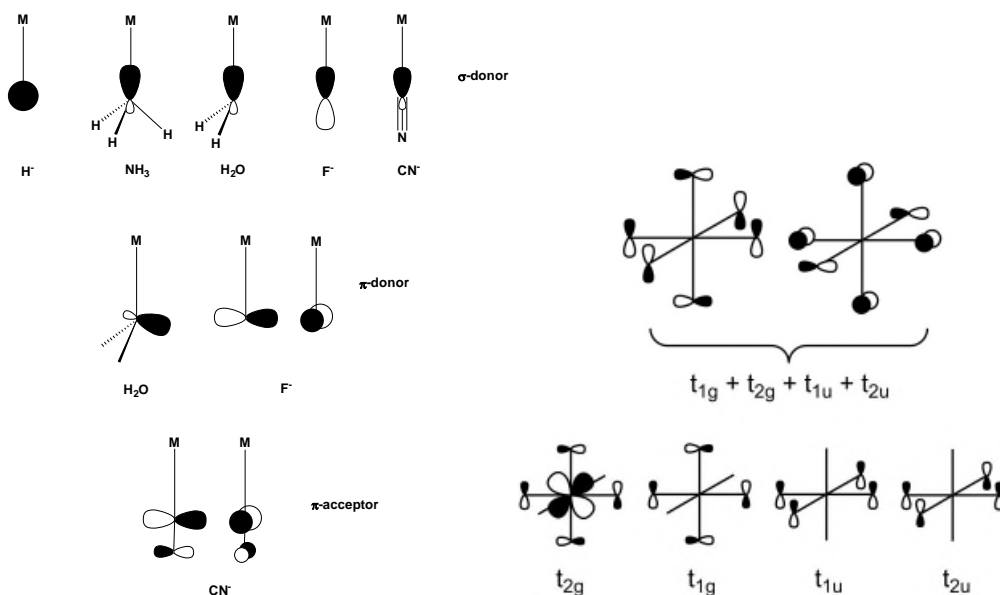


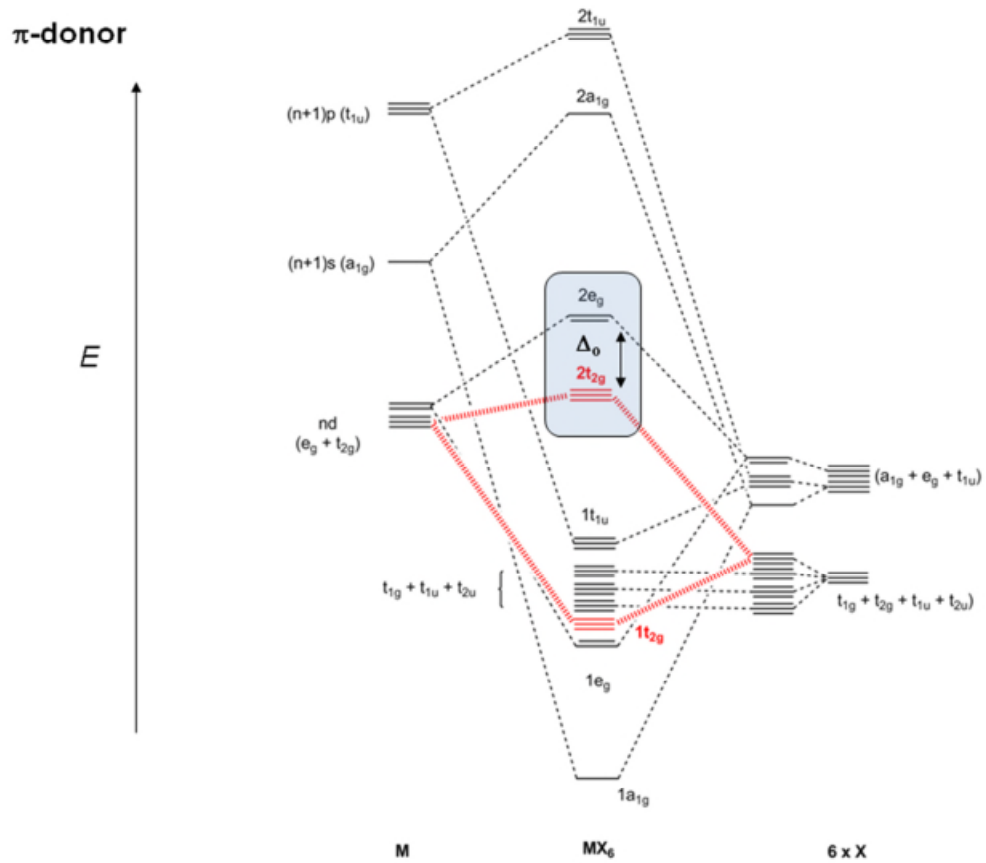
Figure: π orbitals and their SALCs (one of the triply degenerate set in each case).

Symmetry analysis: Each of the ligands in a complex ML_6 can offer up one or two π -type orbitals for M-L π bonding. The possible SALCs of ligand π donor orbitals are shown below using for convenience ligand p orbitals as the generating π donor function (in reality they could be p orbitals on e.g. F^- or π^* orbitals on e.g. CO – only the symmetry matters for now). The twelve p orbitals (two on each L) give four SALCs of t_{1g} , t_{2g} , t_{1u} and t_{2u} symmetry. Only the one with t_{2g} symmetry can find a match with the metal d orbitals. The other three sets of π donor SALCs will be π -non-bonding in the metal complexes. **Only one** of each set of triply degenerate SALCs is shown:

Ligands tend either to have low lying π orbitals that are occupied (e.g. F^- , Cl^- , NR_2^-) or higher lying π orbitals that are unoccupied (e.g. CO , CN^-). The effect on the largely metal t_{2g} orbitals will differ in the two cases. The nature and extent of the π interaction is very important in determining the size of Δ .

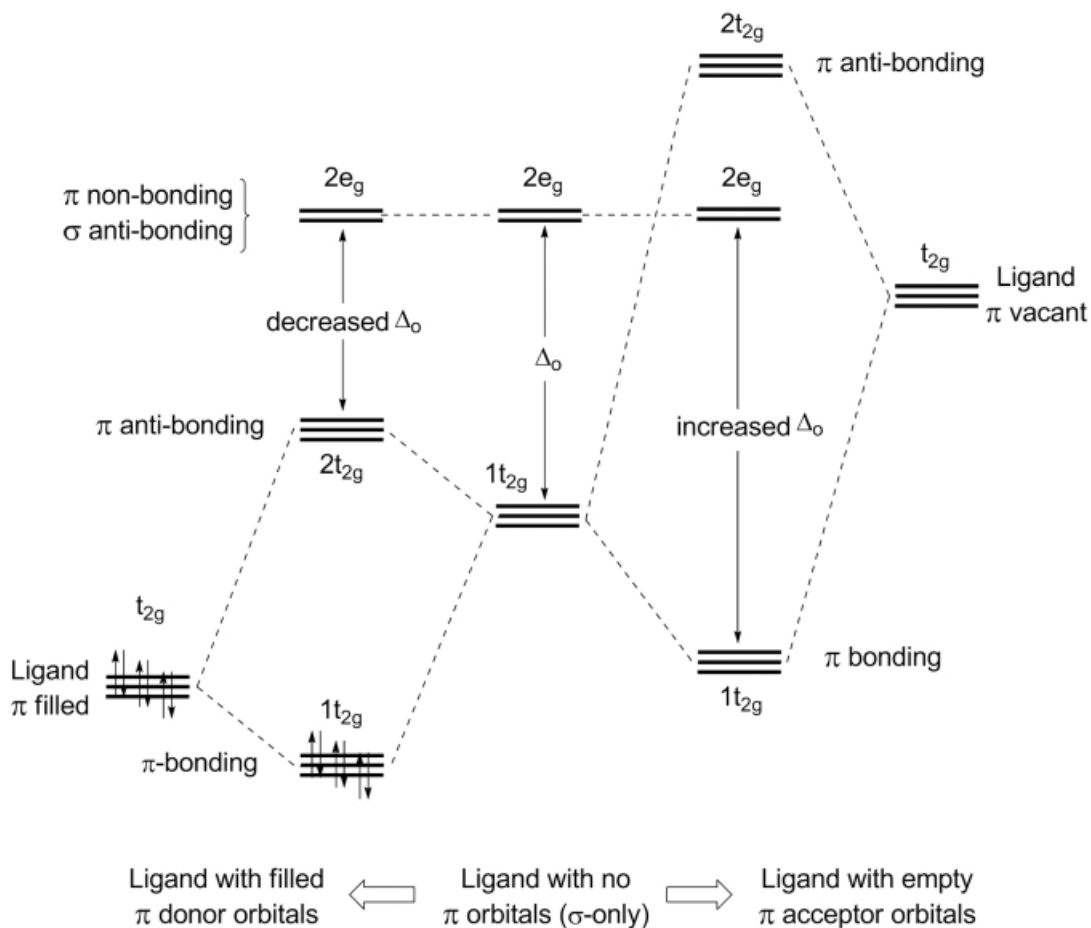
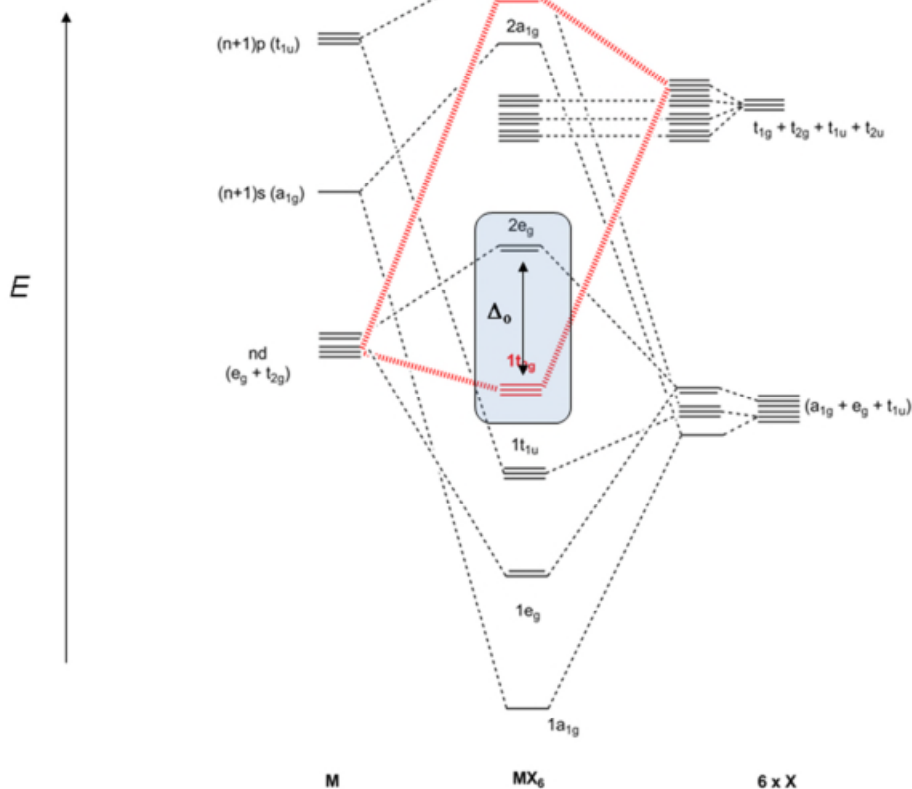
π -donor ligands destabilise the metal t_{2g} d orbitals. These metal-localized MOs become M-L π -anti-bonding. The magnitude of Δ decreases. A consequence of these effects is that π -donor ligands tend to stabilise high oxidation states (*i.e.* low d electron counts).

π -acceptor ligands stabilise the metal t_{2g} d orbitals. These metal-localized MOs become M-L π -bonding. The magnitude of Δ increases. A consequence of these effects is that π -acceptor ligands tend to stabilise low oxidation states (*i.e.* higher d electron counts).



An aside: why is the second t_{1u} non-bonding?

π -acceptor



Summary figure: The two alternative effects of M-L π -bonding as a perturbation of a ML_6 σ -only model

The spectrochemical series can therefore be rationalized in terms of the σ / π donor / acceptor properties of the ligands. π ligands can stabilise or destabilise the t_{2g} d orbitals, therefore increasing or decreasing, respectively, Δ .

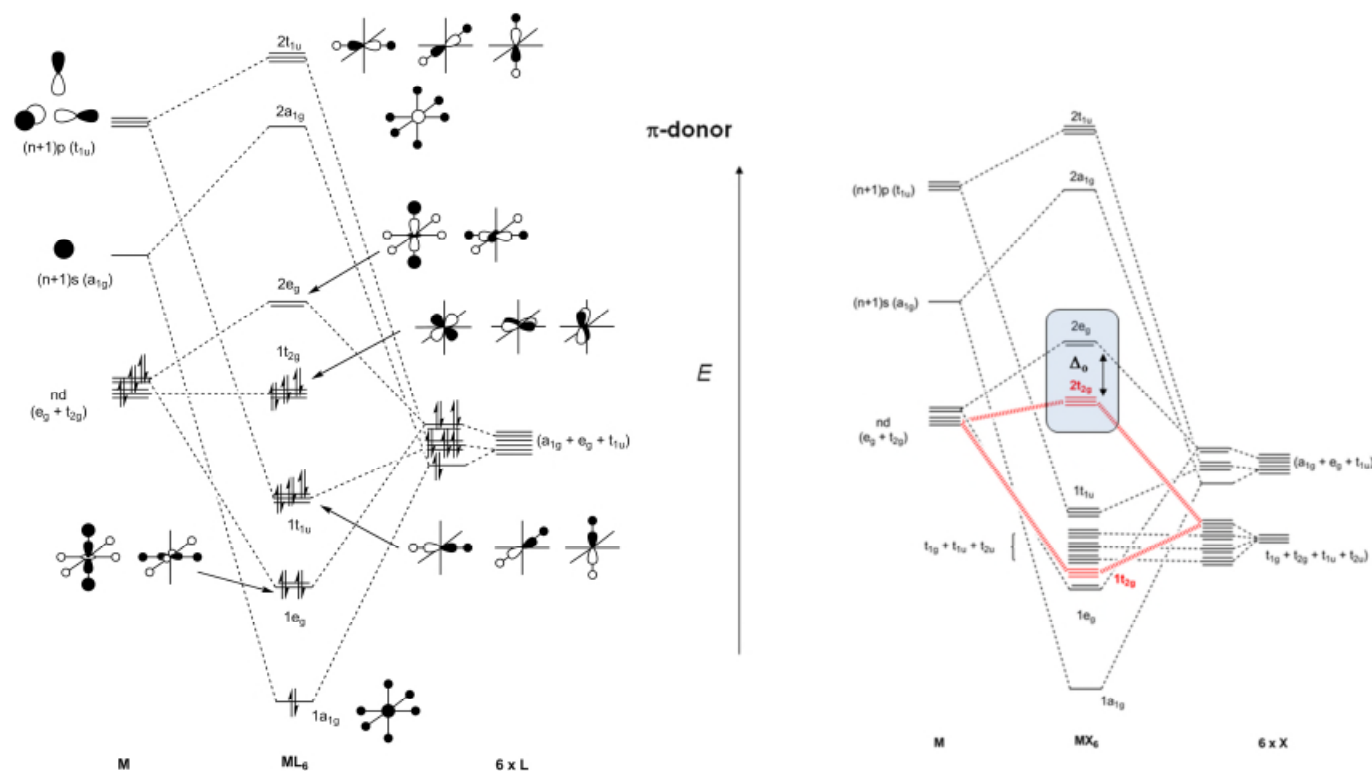
Top tip: When dealing with spectrochemical series problems, always look for the σ -only ligand as your reference point. This will almost always be NH_3 as it is the only common example.

σ/π ligands and the 18-electron rule

The 18-electron rule arises (in an octahedral complex) from complete filling of the orbitals up to t_{2g} . More generally, it can be traced to the use of the ns , np and $(n-1)d$ valence orbitals (9 in total). It is the analogue of the octet rule in main-group complexes. There is an important difference though:

For the octet rule, the ns and np orbitals have the same principal quantum number, and therefore the radial maxima occur at approximately the same distance from the nucleus.

For the 18-electron rule, the radial maxima of $\{ns, np\}$ and $(n-1)d$ are at very different distances (see rdfs on page 48), and so it is very difficult to simultaneously optimise overlap with all 9 orbitals. The end result is that there are many more exceptions to the 18-electron rule than there are to the octet rule.



σ -only	12 σ bonding + 6 non-bonding	$[\text{Co}(\text{NH}_3)_6]^{3+}$
π -donor	12 σ bonding + 6 π anti-bonding	$[\text{RuCl}_6]^{4-}$
π -acceptor	12 σ bonding + 6 π bonding	$(\text{Cr}(\text{CO})_6)$

Electron counts < 18 are most common for π donors, where the t_{2g} orbital becomes slightly antibonding.

Other factors in determining Δ . The principal quantum number of the metal. The overlap between the metal d orbitals and the ligand orbitals increases going down a transition metal group. This results in an increase in Δ as the metal e_g orbitals become more strongly anti-bonding.

complex	$[\text{Co}(\text{NH}_3)_6]^{3+}$	$[\text{Rh}(\text{NH}_3)_6]^{3+}$	$[\text{Ir}(\text{NH}_3)_6]^{3+}$
$\Delta_o =$	22,900 cm^{-1}	34,000 cm^{-1}	40,000 cm^{-1}

The charge on the metal. The $t_{2g} \rightarrow e_g$ d orbital splitting tends to increase with charge when M-L σ interactions are the most important feature in the bonding. This is because charge stabilises the metal orbitals and brings them closer in energy to the ligand orbitals. For example, in $[\text{V}(\text{H}_2\text{O})_6]^{2+}$ $\Delta_o = 12,400 \text{ cm}^{-1}$, whereas in $[\text{V}(\text{H}_2\text{O})_6]^{3+}$ $\Delta_o = 17,850 \text{ cm}^{-1}$:

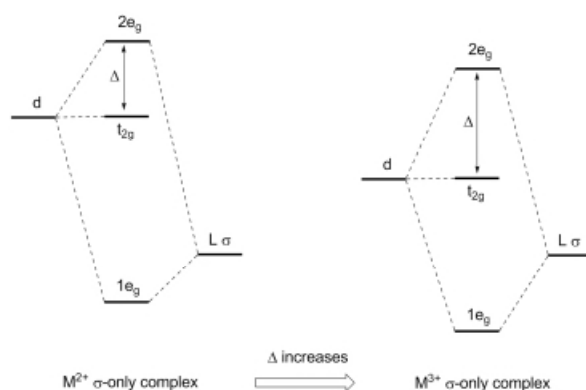


Figure: The increase in Δ as charge on the metal increases (σ -only effects considered)

However, we need also to consider the balance between any improved σ interactions as the d orbitals are stabilised and any decreased π -bonding as the metal t_{2g} orbitals move further away in energy from any ligand π acceptor SALCs. Thus for *both* $[\text{Fe}(\text{CN})_6]^{4-}$ and $[\text{Fe}(\text{CN})_6]^{3-}$ the value of $\Delta \sim 34,000 \text{ cm}^{-1}$. This is because as the $3d$ orbitals get closer in energy to the σ donor orbital they get further away from the π acceptor orbital of CN^- :

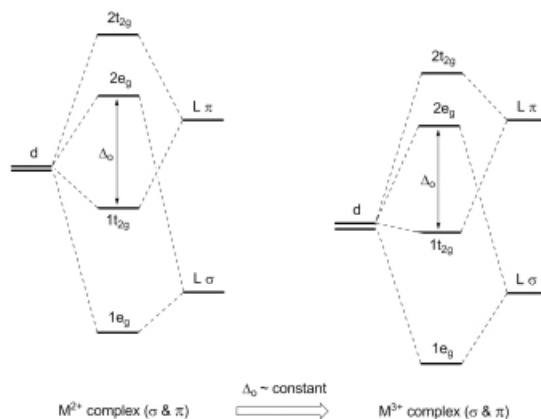


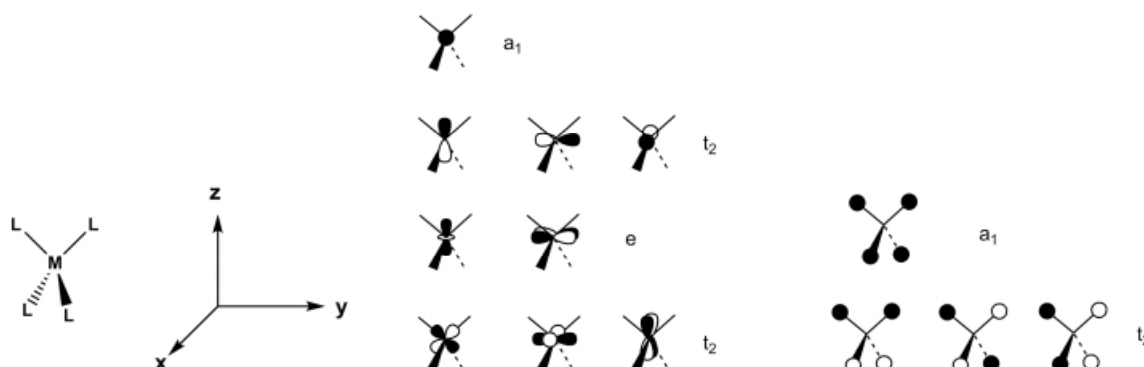
Figure: Opposing effects on the σ - and π -interactions as the metal charge increase

22. Molecular orbitals for 4-coordinate geometries: ML_4 (T_d and D_{4h})

Apart from octahedral, the most common shape for a transition metal complex is tetrahedral ML_4 . Another four coordinate geometry is square planar (D_{4h}) ML_4 although this is typically found only for complexes with a d^8 (and occasionally d^4 and Jahn-Teller distorted d^9) configuration. We shall briefly analyse σ bonded T_d and D_{4h} ML_4 complexes.

Tetrahedral ML_4 complexes

Symmetry analysis: The coordinate system chosen here has one of the C_2 (S_4) axes lying along the molecular z axis.



The $(n+1)s$, $(n+1)p$ and nd AOs of M and the SALCs of T_d (L)₄ σ donor orbitals span the irreducible representations:

$$\text{M atom [1 x } (n+1)s \text{ and 3 x } (n+1)p \text{ AOs]: } \quad \Gamma(s) = a_1 \quad \Gamma(p_{x,y,z}) = t_2$$

$$\text{M atom (5 x } nd \text{ AOs):} \quad \Gamma(d) = e + t_2$$

$$\text{For the L atoms (4 x } \sigma\text{-donor orbitals):} \quad \Gamma(4 \text{ x } \sigma\text{-donor}) = a_1 + t_2$$

$$\text{In total for the resulting } ML_4 \text{ molecule:} \quad \Gamma(13 \text{ MOs}) = 2a_1 + 3t_2 + e$$

Overall there will be a set of M-L bonding ($a_1 + t_2$) and anti-bonding (also a_1 and t_2) MOs. The nd e orbital set ($d_{z^2}, d_{x^2-y^2}$) are strictly non-bonding by symmetry. There will be a further t_2 set of orbitals that are only slightly σ^* anti-bonding (because the metal has two t_2 sets of valence AOs but the (L)₄ σ donor SALCs offer up only one t_2 set).

An LCAO MO diagram for ML_4 is illustrated below. The a_1 ligand combinations form the strongly bonding and anti-bonding MOs $1a_1$ and $2a_1$ respectively. The metal e symmetry orbitals are non-bonding. Both of the metal t_2 sets (from $p_{x,y,z}$ and d_{xy}, d_{xz}, d_{yz}) can, as illustrated above, find a correct match with the ligand t_2 SALCs. However, the greater overlap with the metal $(n+1)p$ orbitals results in strongly bonding $1t_2$ and anti-bonding $3t_2$ MOs derived mainly from these. The smaller

overlap with the metal nd orbitals yields weakly σ -anti-bonding MOs (the $2t_2$ set) localised mainly on the metal and forming part of the "d orbital" manifold.

Thus, just as the t_{2g} and e_g MOs in O_h ML_6 complexes are considered to be mainly d orbital in character, so the $1e$ and $2t_2$ MOs in a T_d ML_4 complex are regarded in a similar way.

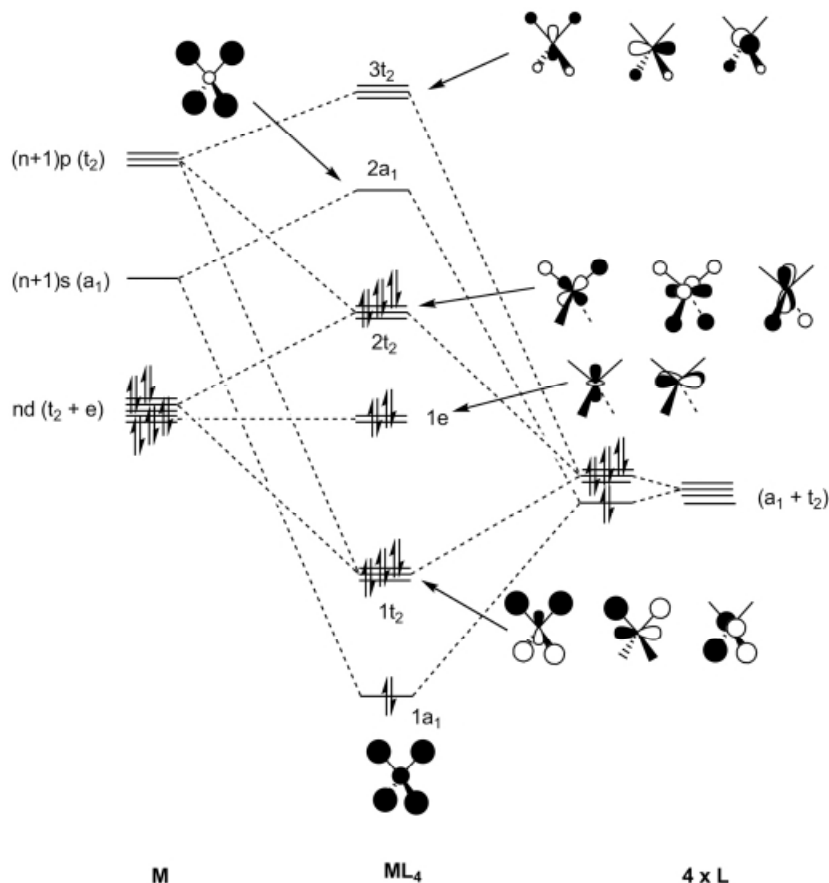


Figure: A σ -only LCAO MO diagram for a tetrahedral transition metal complex ML_4

Note: each orbital of t_2 symmetry is a linear combination of the form

$$\phi(nt_2) = c_1 nd(M) + c_2(n + 1)p(M) + c_3 L_4$$

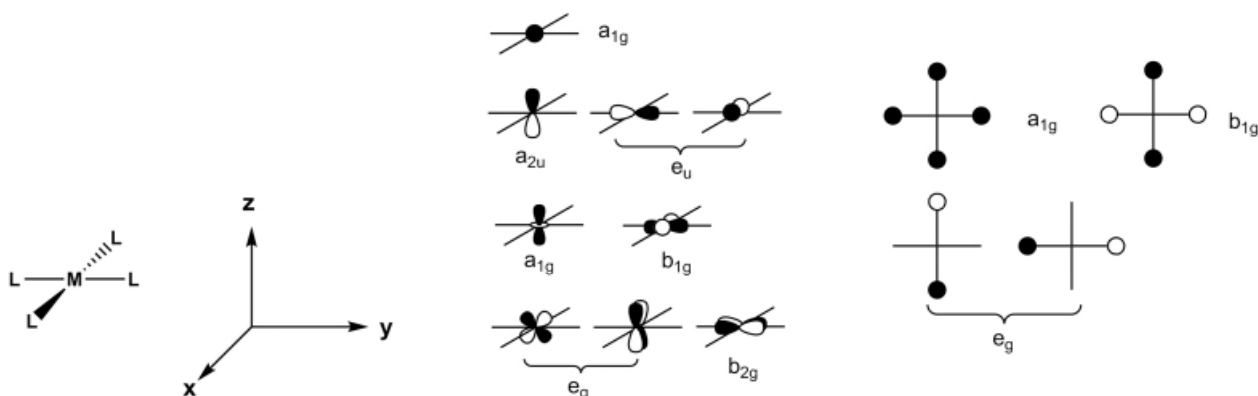
The separation between the $1e$ and $2t_2$ MOs in a T_d ML_4 complex is often referred to a Δ_t . The value of Δ_t is $\sim 4/9$ of Δ_o for an otherwise equivalent ML_6 complex (*i.e.* for the same ligands, same metal, same oxidation state). This can be attributed to the presence of fewer ligands in an ML_4 complex versus an analogous ML_6 . The consequence of the comparatively small Δ_t value is that virtually all T_d ML_4 complexes of the 1st row transition metals are high spin ($\Delta_t < \text{spin pairing energy}$ even for strong field ligands). Watch out for an exception - $\text{Co}(\text{norbornyl})_4$, a low-spin tetrahedral d^5 complex.

Square planar ML_4 complexes

Symmetry analysis: Consider a hypothetical complex ML_4 with σ -only donor ligands (the symmetry properties of the donor orbitals will be the same as for H 1s orbitals).

The coordinate system chosen has the M-L vectors of ML_4 arranged along Cartesian x and y axes.

The point group of square planar ML_4 is D_{4h} .



The $(n+1)s$, $(n+1)p$ and nd AOs of atom M and the SALCs of D_{4h} $(L)_4$ span the irreducible representations shown below.

$$\text{M atom } [(n+1)s \text{ and } (n+1)p \text{ AOs}]: \quad \Gamma(s) = a_{1g} \quad \Gamma(p_z) = a_{2u} \quad \Gamma(p_{x,y}) = e_u$$

$$\text{M atom } (5 \times nd \text{ AOs}): \quad \Gamma(d_{z^2}) = a_{1g} \quad \Gamma(d_{x^2-y^2}) = b_{1g} \quad \Gamma(d_{xy}) = b_{2g} \quad \Gamma(d_{xz}, d_{yz}) = e_g$$

$$\text{For the L atoms } (4 \times \sigma\text{-donor orbitals}): \quad \Gamma(4 \times \sigma\text{-donor}) = a_{1g} + b_{1g} + e_u$$

$$\text{In total for the resulting } ML_4 \text{ molecule:} \quad \Gamma(13 \text{ MOs}) = 3a_{1g} + 2b_{1g} + 2e_u + a_{2u} + b_{2g} + e_g$$

A general MO diagram for a square planar transition metal complex featuring only σ -interactions is shown on the following page.

There are four strongly σ -bonding ($1a_{1g}$, $1e_u$ and $1b_{1g}$) and strongly σ -anti-bonding ($3a_{1g}$, $2e_u$ and $2b_{1g}$) levels. The former set accommodate the four pairs of electrons required to form the four M-L σ bonds. Another a_{1g} symmetry MO is found at intermediate energy (*i.e.* the $2a_{1g}$ orbital). This is because there are two AOs [the $(n+1)s$ and nd_{z^2}] on the metal than can interact with the $(L)_4$ a_{1g} SALC. As usual, it is the $(n+1)s$ metal orbital that overlaps best with the ligand donors. Hence the only weakly anti-bonding "middle" level, namely $2a_1$, has predominantly nd_{z^2} character.

There are four strictly (by symmetry) σ -non-bonding MOs. These are the $1a_{2u}$, $1e_g$ and $1b_{2g}$ orbitals. The $1a_{2u}$ lies relatively high in energy because it is pure $(n+1)p_z$ AO in character (remember that the $(n+1)p$ orbitals are the least stable of the transition metal valence orbitals). The $1e_g$ and $1b_{2g}$ orbitals are equivalent to the triply degenerate t_{2g} d orbital manifold in octahedral ML_6 complexes. For a σ -only complex, the $1e_g$ and $1b_{2g}$ orbitals are isoenergetic (have the same energy) but are not all degenerate by symmetry - only the nd_{xz} and nd_{yz} AOs form a strictly degenerate pair ($1e_g$). This is known as ‘accidental degeneracy’ and will be removed in a more sophisticated treatment (*i.e.* including π effects).

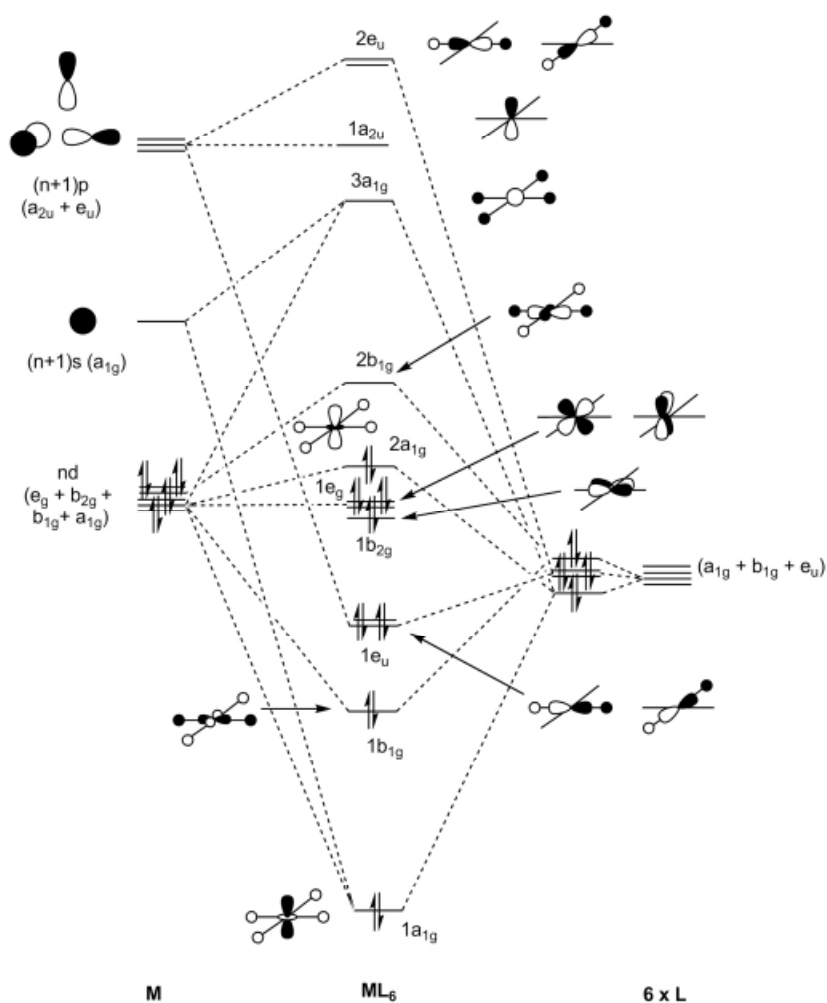


Figure: A σ -only LCAO MO diagram for a square planar transition metal complex ML_4

The ‘16-electron rule’

The 18-electron rule is based on the idea that all 9 valence orbitals on the metal ($5 \times d$, $3 \times p$, $1 \times s$) are being ‘used’. ‘Used’ can either mean ‘used’ to form a bonding combination ($1a_{1g}$, $1t_{1u}$, $1e_g$ in the octahedron) or ‘used’ to hold approximately non-bonding electrons ($1t_{2g}$ in the σ -only octahedron). So in a stable 16-electron complex, one of the 9 valence orbitals is not being ‘used’ in the same way. The orbital in question is the p_z orbital: there is no symmetry match to a ligand SALC, so it is not ‘used’ to form a bond, and it is empty, so is not ‘used’ to hold non-bonding electrons.

Square planar *versus* tetrahedral coordination and 16 VE systems

The figure below shows a Walsh diagram for the conversion of a square planar (D_{4h}) ML_4 complex to the tetrahedral form. We focus only on the nd orbital energies. The relative energies of the key orbital energies in terms of Δ_o are also shown.

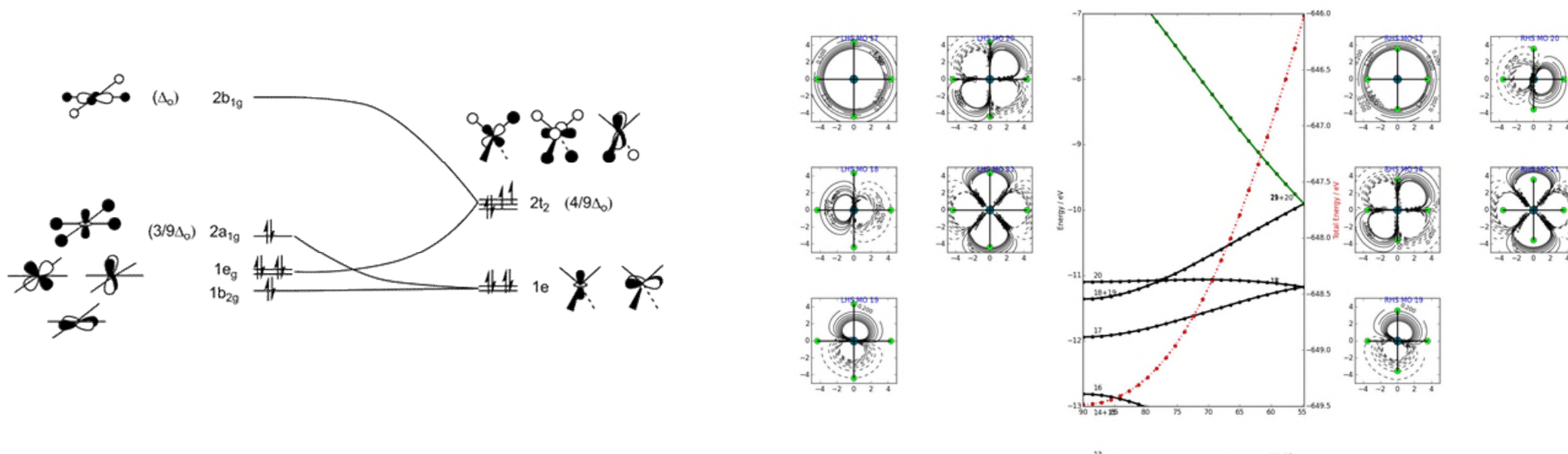


Figure: A σ -only Walsh diagram relating square planar and tetrahedral complexes ML_4 (cartoon and “real” for $[PdCl_4]^{2-}$ – note Cl is not a pure σ -only ligand, so the real picture isn’t quite as simple as implied in the cartoon!

In deciding between tetrahedral and square planar coordination we should consider:

Steric factors which will favour T_d (larger L-M-L angles).

The nd electron count – i.e. the population of the various nd orbitals. This should be done in terms of the actual orbital energies (in terms of Δ_o values) and the effects on M-L bonding.

The diagram shows that:

The t_2 orbitals in T_d - ML_4 are somewhat antibonding (as is the $2a_{1g}$ MO of D_{4h} - ML_4). However in T_d - ML_4 there are four M-L antibonding electrons whereas in low spin D_{4h} - ML_4 there are only two. This weakening effect is shown in the average M-L bond lengths listed below for d^8 nickel complexes:

Bond	Square planar	Tetrahedral
Ni–N	1.68 Å	1.96 Å
Ni–P	2.14 Å	2.28 Å
Ni–S	2.15 Å	2.28 Å
Ni–Br	2.30 Å	2.36 Å

$d^8 ML_4$ complexes will favour a square planar structure in the case of a large Δ_o value (i.e. such that $\frac{6}{9} \Delta_o$ exceeds the spin pairing energy). In this case the *two* electrons in the D_{4h} - ML_4 HOMO ($2a_{1g}$) destabilise the compound by $2 \times \frac{3}{9} \Delta_o = \frac{6}{9} \Delta_o$, whereas the *four* electrons in the HOMO (t_2) of T_d - ML_4 destabilise the compound by $4 \times \frac{4}{9} \Delta_o = \frac{16}{9} \Delta_o$.

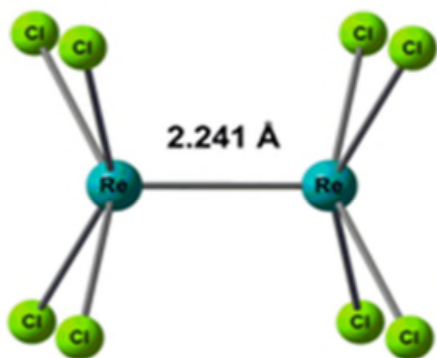
However, if the Δ_o value is small (i.e. with a weak field ligand) the energetic preferences in terms of nd orbital occupation are insufficient to overcome the steric disadvantages of forcing the ligands closer together and the T_d - ML_4 isomer is more stable.

Larger ligands imply greater steric repulsions, so a larger Δ_o is required to impose a square-planar geometry.

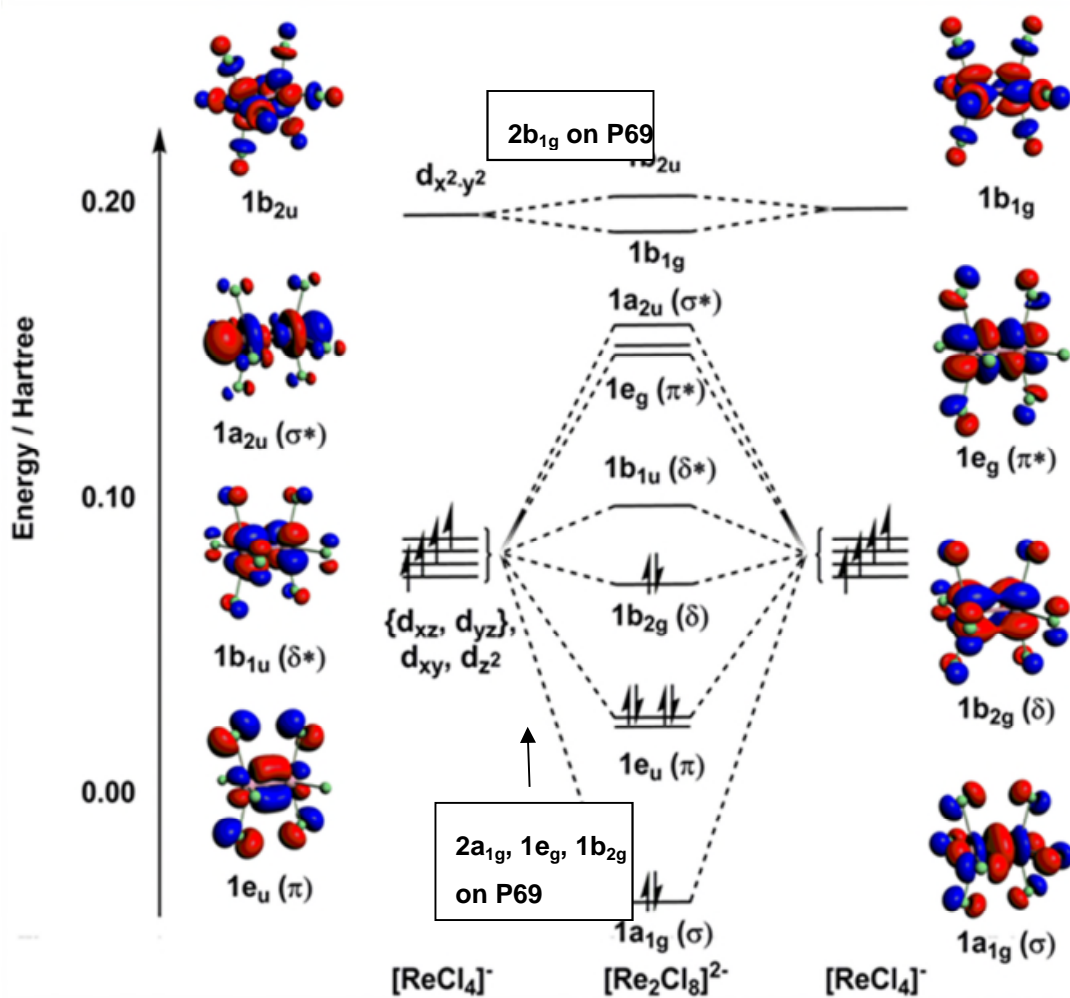
Thus we find $[Ni(CN)_4]^{2-}$ is square planar whereas $[NiCl_4]^{2-}$ is tetrahedral. Note that $[PdCl_4]^{2-}$ and $[PtCl_4]^{2-}$ are also square planar due to the larger Δ values associated with the 4d and 5d elements.

23. A miscellany of bonds

$[\text{Re}_2\text{Cl}_8]^{2-}$ and the quadruple bond (Cotton, 1964).

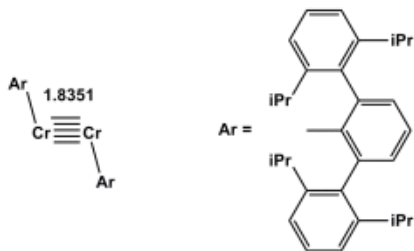


$= \{ \text{ReCl}_4^{1-} \}_2$ so use square planar fragment orbitals as a starting point (from page 67)

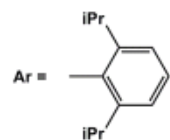
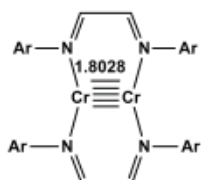


n.b. same diagram for $\text{Cr}_2(\text{CH}_3\text{COO})_4(\text{H}_2\text{O})_2$ (ICL lab course, Schlenk line expt)

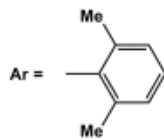
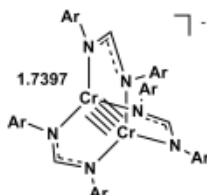
Cr₂Ar₂ and the quintuple bond (Power, 2005).



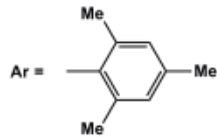
Power 2005



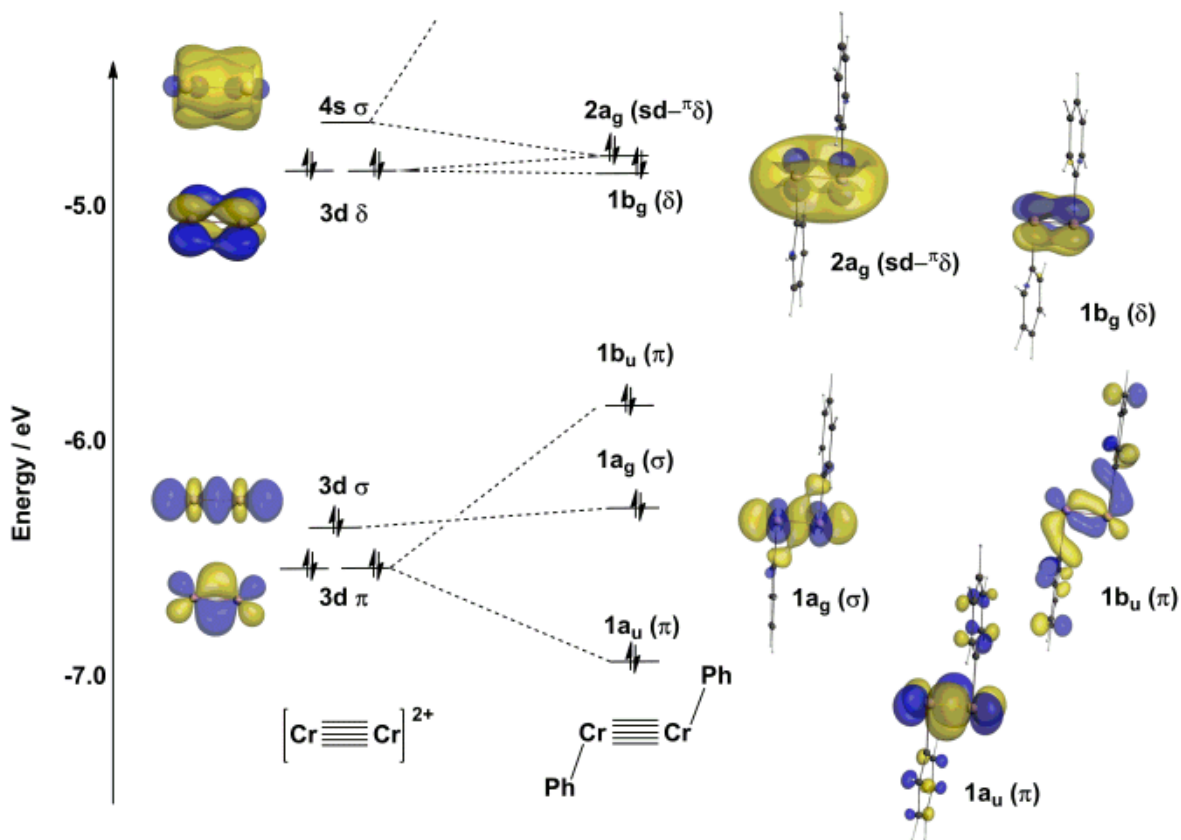
Theopold 2007



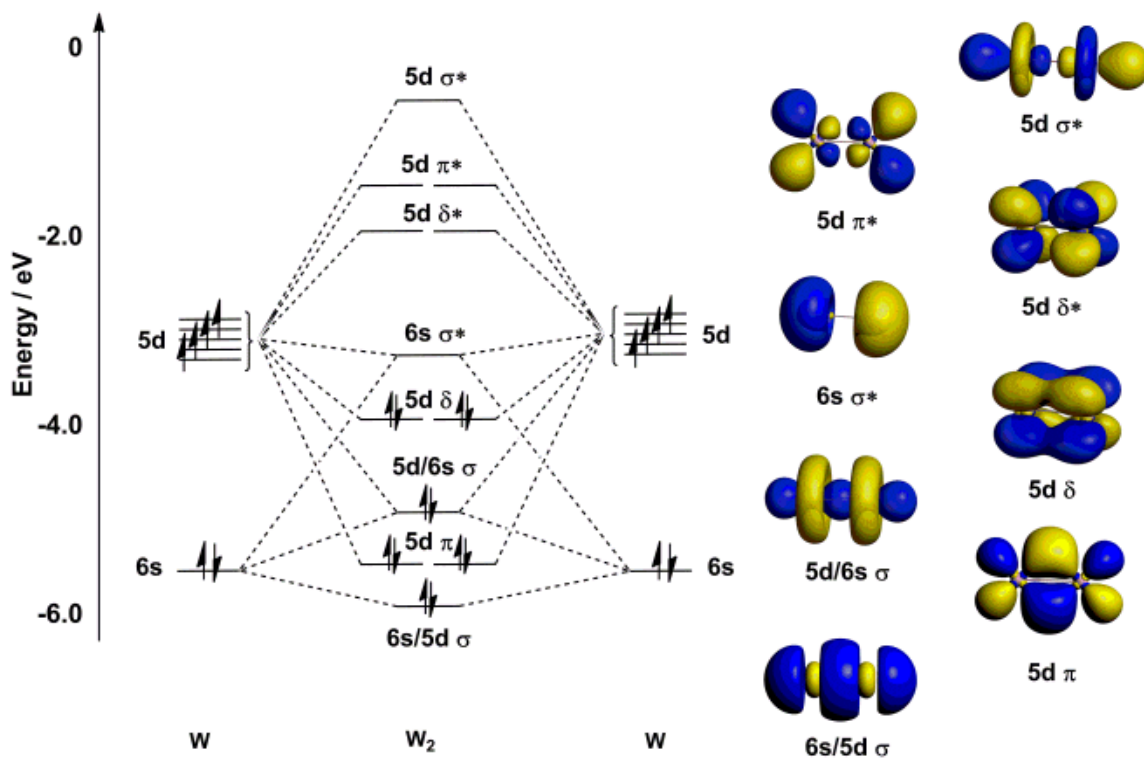
Tsai 2008



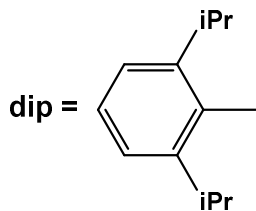
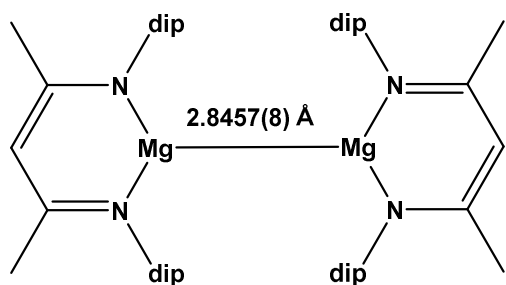
Tsai 2008



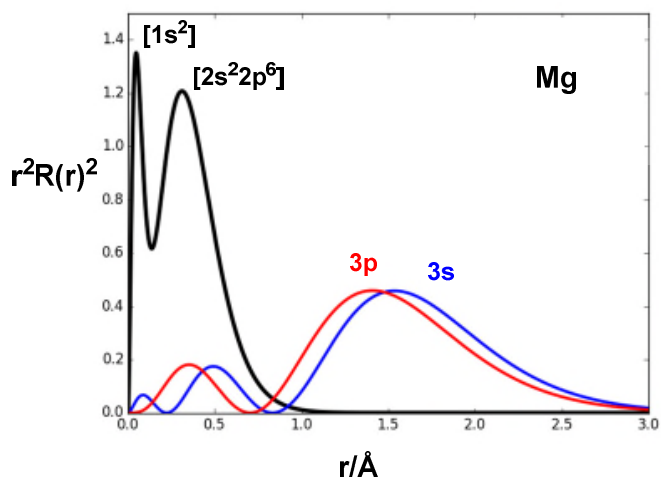
W_2 : a sextuple bond .



A stable compound of Mg(I)!!



Jones, 2005



Appendix Character tables and linear combinations of orbitals.

<http://global.oup.com/uk/orc/chemistry/qchem2e/student/tables/>

The Groups C_{nv} ($n = 2, 3, 4, 5, 6$)

C_{2v} ($2mm$)	E	C_2	$\sigma_v(xz)$	$\sigma'_v(yz)$		
A_1	1	1	1	1	z	x^2, y^2, z^2
A_2	1	1	-1	-1	R_z	xy
B_1	1	-1	1	-1	x, R_y	xz
B_2	1	-1	-1	1	y, R_x	yz

C_{3v} ($3m$)	E	$2C_3$	$3\sigma_v$			
A_1	1	1	1	z		$x^2 + y^2, z^2$
A_2	1	1	-1	R_z		
E	2	-1	0	$(x, y)(R_x, R_y)$		$(x^2 - y^2, 2xy)(xz, yz)$

D_{3h} ($\bar{6}$) $m2$	E	$2C_3$	$3C_2$	σ_h	$2S_3$	$3\sigma_v$		
A'_1	1	1	1	1	1	1		$x^2 + y^2, z^2$
A'_2	1	1	-1	1	1	-1	R_z	
E'	2	-1	0	2	-1	0	(x, y)	$(x^2 - y^2, xy)$
A''_1	1	1	1	-1	-1	-1		
A''_2	1	1	-1	-1	-1	1	z	
E''	2	-1	0	-2	1	0	(R_x, R_y)	(xz, yz)

D_{4h} ($4/mmm$)	E	$2C_4$	C_2	$2C'_2$	$2C''_2$	i	$2S_4$	σ_h	$2\sigma_v$	$2\sigma_d$		
A_{1g}	1	1	1	1	1	1	1	1	1	1		$x^2 + y^2, z^2$
A_{2g}	1	1	1	-1	-1	1	1	1	-1	-1	R_z	
B_{1g}	1	-1	1	1	-1	1	-1	1	1	-1		$x^2 - y^2$
B_{2g}	1	-1	1	-1	1	1	-1	1	-1	1		xy
E_g	2	0	-2	0	0	2	0	-2	0	0	(R_x, R_y)	(xz, yz)
A_{1u}	1	1	1	1	1	-1	-1	-1	-1	-1		
A_{2u}	1	1	1	-1	-1	-1	-1	-1	1	1	z	
B_{1u}	1	-1	1	1	-1	-1	1	-1	-1	1		
B_{2u}	1	-1	1	-1	1	-1	1	-1	1	-1		
E_u	2	0	-2	0	0	-2	0	2	0	0	(x, y)	

O_h ($m3m$)	E	$8C_3$	$6C_2$	$6C_4$	$3C_2$ ($=C_4^2$)	i	$6S_4$	$8S_6$	$3\sigma_h$	$6\sigma_d$	
A_{1g}	1	1	1	1	1	1	1	1	1	1	$x^2 + y^2 + z^2$
A_{2g}	1	1	-1	-1	1	1	-1	1	1	-1	
E_g	2	-1	0	0	2	2	0	-1	2	0	$(2z^2 - x^2 - y^2, \sqrt{3}(x^2 - y^2))$
T_{1g}	3	0	-1	1	-1	3	1	0	-1	-1	(R_x, R_y, R_z)
T_{2g}	3	0	1	-1	-1	3	-1	0	-1	1	(xy, xz, yz)
A_{1u}	1	1	1	1	1	-1	-1	-1	-1	-1	
A_{2u}	1	1	-1	-1	1	-1	1	-1	-1	1	
E_u	2	-1	0	0	2	-2	0	1	-2	0	
T_{1u}	3	0	-1	1	-1	-3	-1	0	1	1	(x, y, z)
T_{2u}	3	0	1	-1	-1	-3	1	0	1	-1	

T_d ($43m$)	E	$8C_3$	$3C_2$	$6S_4$	$6\sigma_d$	
A_1	1	1	1	1	1	$x^2 + y^2 + z^2$
A_2	1	1	1	-1	-1	
E	2	-1	2	0	0	$(2z^2 - x^2 - y^2, \sqrt{3}(x^2 - y^2))$
T_1	3	0	-1	1	-1	(R_x, R_y, R_z)
T_2	3	0	-1	-1	1	(x, y, z) (xy, xz, yz)

$C_{\infty v}$	E	$2C_\infty^\phi$...	$\infty\sigma_v$	
$A_1 \equiv \Sigma^+$	1	1	...	1	z $x^2 + y^2, z^2$
$A_2 \equiv \Sigma^-$	1	1	...	-1	R_z
$E_1 \equiv \Pi$	2	$2 \cos \phi$...	0	(x, y) (R_x, R_y) (xz, yz)
$E_2 \equiv \Delta$	2	$2 \cos 2\phi$...	0	$(x^2 - y^2, 2xy)$
$E_3 \equiv \Phi$	2	$2 \cos 3\phi$...	0	
...	
...	

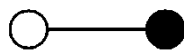
$D_{\infty h}$	E	$2C_\infty^\phi$...	$\infty\sigma_v$	i	$2S_\infty^\phi$...	∞C_2	
Σ_g^+	1	1	...	1	1	1	...	1	$x^2 + y^2, z^2$
Σ_g^-	1	1	...	-1	1	1	...	-1	R_z
Π_g	2	$2 \cos \phi$...	0	2	$-2 \cos \phi$...	0	(R_x, R_y) (xz, yz)
Δ_g	2	$2 \cos 2\phi$...	0	2	$2 \cos 2\phi$...	0	$(x^2 - y^2, 2xy)$
...	
Σ_u^+	1	1	...	1	-1	-1	...	-1	z
Σ_u^-	1	1	...	-1	-1	-1	...	1	
Π_u	2	$2 \cos \phi$...	0	-2	$2 \cos \phi$...	0	(x, y)
Δ_u	2	$2 \cos 2\phi$...	0	-2	$-2 \cos 2\phi$...	0	
...	

n = 2 (C_{2v})

A₁ (1/2)^{1/2} (φ₁ + φ₂)

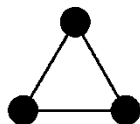


B₂ (1/2)^{1/2} (φ₁ - φ₂)



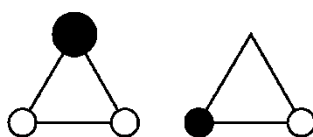
n = 3 (C_{3v})

A₁ (1/3)^{1/2} (φ₁ + φ₂ + φ₃)



E (1/6)^{1/2} (2φ₁ - φ₂ - φ₃)

(1/2)^{1/2} (φ₂ - φ₃)



n = 4 (T_d)

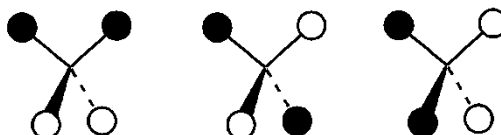
A₁ (1/4)^{1/2} (φ₁ + φ₂ + φ₃ + φ₄)



T₂ (1/4)^{1/2} (φ₁ + φ₂ - φ₃ - φ₄)

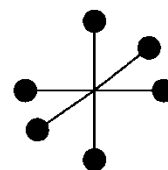
(1/4)^{1/2} (φ₁ - φ₂ - φ₃ + φ₄)

(1/4)^{1/2} (φ₁ - φ₂ + φ₃ - φ₄)



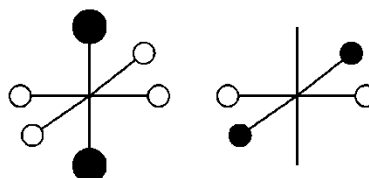
n = 6 (O_h)

A_{1g} (1/6)^{1/2} (φ₁ + φ₂ + φ₃ + φ₄ + φ₅ + φ₆)



E_g (1/2)^{1/2} (φ₃ - φ₄ + φ₅ - φ₆)

(1/12)^{1/2} (2φ₁ + 2φ₂ - φ₃ - φ₄ - φ₅ - φ₆)



T_{1u} (1/2)^{1/2} (φ₁ - φ₂)

(1/2)^{1/2} (φ₃ - φ₄)

(1/2)^{1/2} (φ₅ - φ₆)

